Investigation of Agricultural Biomass Ashes as Supplementary Cementitious Materials.

Thesis

Presented in Partial Fulfillment of the Requirements for the Degree Master of Science in the Graduate School of The Ohio State University

By

Jarron Mark Mihoci, B.S.

Graduate Program in Civil Engineering

The Ohio State University

2023

Thesis Committee:

Dr. Lisa E. Burris, Advisor

Dr. Anthony Massari

Dr. Halil Sezen

Abstract

The objective of this study is to analyze the effects of using agricultural biomass ash as a sustainable supplementary cementitious material. The potential for these waste materials to be used effectively in cementitious systems would promote global sustainability in both agriculture and construction. Three agricultural materials are explored in this study: hemp hurd, corn stover, and wheat straw. Corn stover and wheat straw have historically strong markets in the Midwest, and can generate significant waste. Hemp farming is a newer and strictly regulated enterprise in the United States, but the market has potential for growth due to the material's versatility. The chemical variability of each of these materials are contrasted among three sources mostly across the Midwest United States. The results can be assessed to inform future building code recommendations for alternative supplementary cementitious materials. The practicality of using these materials in cementitious systems is explored in this study by assessing the reactivity and performance of agricultural ashes at 10% and 20% replacement of ash for cement volume.

The results of this study indicate that wheat straw ash and corn stover ash make naturally good pozzolans, assessed by their reactivity and contribution to improved long term hardened properties. These materials are viable for up to 20% volumetric replacement of cement for durability improvements, and up to 10% volumetric

replacement for benefits to compressive strength. Hemp hurd ash showed lower reactivity in its natural state and did not perform like a traditional SCM. However, many chemical treatment techniques can be applied to optimize the properties of these materials by removing impurities, standardizing ash chemistry, and thereby improving the ash performance in cementitious systems. Additionally, variability in material chemistry and performance is significant in some results including reactivity.

Dedication

"For from him and through him and to him are all things. To him be glory forever. Amen."-Romans 11:36

Acknowledgments

I am grateful and thankful to my advisor, Dr. Lisa Burris, for her support of my academic goals and research over the last two years. Her knowledge and kindness have encouraged me to be confident in my abilities and curious to explore the depths of what graduate studies have to offer. I am incredibly thankful for her mentorship.

I would like to thank Dr. Anthony Massari and Dr. Halil Sezen for their support during my studies and for being a part of my committee. In the same way I am very grateful to Dr. Daniel Pradel for his mentorship and for the opportunity to serve as a graduate teaching assistant in his lab classes.

My friends in the cement laboratory have been incredibly helpful and have created a meaningful and enjoyable environment for learning. I am thankful for Erin Stewartson, Cansu Acarturk, Yujia Min, Garrett Tatum, Madiha Ammari, Gaurab Shrestha, Anna Tenhagen, Kamilla Wieckowski, Brendan Mastro, and Mahmod Yahya for their help and friendship. I am additionally thankful to the American Concrete Institute and Anderson Concrete for the opportunity to work on this project, and for their guidance in doing so. Additional thanks to Dr. Kyle Riding and Dr. Prannoy Suraneni for their advice and help in research, and to Dr. Tyler Ley and Dr. Shinhyu Kang for fly ash information.

I would especially like to thank my fiancée, CaseyAnna Harmon, for her generous support of my academic endeavors and growth. Finally, I am eternally grateful to my loving parents, John and Janeen, for their constant dedication to my growth in every dimension, as I seek to live out my calling. Their endless support and encouragement made graduate school an easy choice, and an enjoyable experience. Thanks be to God.

Vita

May 2021……B.S., Engineering

B.S., Applied Mathematics

Geneva College

Beaver Falls, PA

August 2021 to present……Graduate Teaching/Research Assistant

Department of Civil, Environmental, and

Geodetic Engineering

The Ohio State University,

Columbus, OH

Fields of Study

Major Field: Civil Engineering

Table of Contents

List of Tables

List of Figures

Chapter 1. Introduction

1.1 Research Problem Statement

Sustainability is a concern in engineering and construction, and the use of alternative materials in concrete construction is being reimagined. Ordinary portland cement is commonly used in concrete construction, but its production and use have a significant carbon footprint. Additionally, agriculture is one of the oldest and most essential industries in the world. The harvesting and processing of agricultural crops produces large amounts of material waste regardless of cultivation efficiency. Both industries have negative contributions to sustainability that can be reduced.

The objective of this study is to analyze the effects and variability of using agricultural material waste as a sustainable supplement to ordinary portland cement. The pozzolanic potential of various agricultural materials including hemp hurd, corn stover, and wheat straw is assessed in this study by exploring the raw material treatment techniques and using the treated ash as a volumetric substitute in cement pastes and mortar specimens. Additionally, the variability of the chemistry and mechanical properties of these materials are contrasted among various locations across the Midwest United States. The results can be assessed to inform future building code recommendations for alternative supplementary cementitious materials.

1.2 Thesis Organization

The body of this thesis is organized into seven chapters. Chapter one provides a general introduction to the work through a specific research problem statement. This provides a foundation and justification for the work done. Chapter two provides an in-depth literature review of relevant information that is explored in later sections of the report. Chapter three conveys details about the materials used for this study. Information about the cements, agricultural products, acids, and other testing materials are provided in this section. Chapter four outlines testing methods associated with the work performed. This section is organized to show how raw material was treated and prepared for testing firstly, and proceeds to describe testing methods for characterization and performance of the ashes in cementitious systems. Chapter five provides selected results from testing, organized by relevant topic. Chapter six discusses the results presented in chapter five with reference to the problem statement. Chapter seven is a conclusion to the research body, and a recommendation for future investigation.

Chapter 2. Background

2.1 Cement Systems

Concrete is a widely used building material that has been used for thousands of years. It is the most abundant man-made material on earth, and over four billion tons of concrete are produced each year globally (Jonathan Hilburg, 2019). In its simplest form, concrete consists of sand, aggregate, water, and cement. Cement is a unique manufactured material that reacts with water and hardens. In 2022, the United States produced 95 metric tons of cement (CemNet.com, 2023).

Cement manufacturing has great construction and economic value, but it comes with environmental cost in the form of carbon dioxide generation as well as a significant energy cost. For every one kilogram of concrete produced, approximately one kilogram of CO_2 is released from the cement clinkering and concrete mixing processes (Tait & Cheung, 2016) and cement manufacturing in 2021 was estimated to have contributed 5% to total global CO_2 emissions (Friedlingstein et al., 2022).

2.1.1 Composition

The most common form of cement is ordinary portland cement, which was first patented by Joseph Aspdin in 1824. Portland cement is produced primarily from lime (CaO), alumina (Al_2O_3), iron (Fe_2O_3), and silica (SiO_2). Raw materials including

limestone, clay, and sand are blended and then added to a kiln and heated to 1450 °C to produce clinker. The clinker is then cooled, and gypsum (~5%) is interground to prevent premature or false setting of concrete before the silicate reactions can provide strength ($CaSO_4$ $2H_20$). It also slows the C_3A reaction during early hydration. The reactions that take place can be complex, therefore shorthand abbreviations are used in this report for the compounds mentioned, shown in Table 2-1. The finished cement clinker is chemically composed of various phases listed in Table 2-2.

Table 2-1: Cement chemistry notations.

Compound	**Formula**	**Shorthand**
Calcium Oxide (Lime)	CaO	C
Aluminum Oxide (Alumina)	Al_2O_3	A
Silicon Dioxide (Silica)	SiO_2	S
Ferric Oxide	Fe_2O_3	F
Sulfur trioxide (Sulfate)	SO_3	$
Water	H_2O	H

Table 2-2: Cement compound notations and composition

Compound	**Shorthand Formula**	**Percent by Weight** (depends on cement type)
Tricalcium silicate (Alite)	C_3S	50-70
Dicalcium silicate (Belite)	C_2S	10-30
Tricalcium aluminate	C_3A	3-13
Tetracalcium aluminoferrite (Ferrite)	C_4AF	5-15
Calcium sulfate dihydrate (Gypsum)	C$$H_2$	3-7

The functions of cement compounds include:

- Tricalcium silicate (C_3S): Hydrates quickly and is responsible for early strength gain and hardening.
- Dicalcium silicate (C_2S): Dicalcium silicate hydrates slowly and is responsible for long-term strength gain.
- Tricalcium aluminate (C_3A): Hydrates extremely quickly, reacting almost immediately after dissolution. C_3A will release high amounts of heat and result in a rapid early set, however, it provides little strength. Gypsum is used to slow down the C_3A reaction, so that strength can develop properly.
- Tetracalcium aluminoferrite (C_4AF): This compound is used as a flux in the manufacturing process, as it is able to lower the melting temperature of silica from 1650 °C to 1427 °C. It hydrates quickly and provides the gray color to

cement, however its major contribution is not to providing strength (Mindess et al., 2003).

- Calcium sulfate dihydrate (gypsum): Gypsum is used to control the C_3A hydration reaction so that a the cement does not begin to harden shortly after water is introduced. It is interground with clinker in the manufacturing process.

Recently, much of U.S. cement production, including in Ohio, has shifted to portland limestone cement due to growing needs to reduce the carbon footprint. Portland limestone cement (PLC) is a blended cement (Type IL) that consists of ~12% limestone, but has no reduction in performance when compared to ordinary portland cement (OPC) (Sharma et al., 2021). Due to reduced availability of Type I portland cement, this research primarily utilizes PLC for testing.

2.1.2 Cement Hydration

The process of hydration begins when water mixes with anhydrous cement clinker. When water is added to the clinker minerals, an exothermic reaction begins. This reaction can be seen in the initial peak on a calorimetry curve. The water present quickly dissolves sulfates and gypsum to produce an alkaline solution. This description will focus on the hydration products and their role in the concrete matrix. Once the solution has reached saturation, compounds precipitate out as solids.

The main hydration reaction that takes place occurs when C_3S reacts with water to create calcium silicate hydrate (C-S-H) and calcium hydroxide (C-H). C-S-H has a highly variable structure which can be amorphous or crystalline and it forms 50%-60% of the

hydrated cement paste volume. It is the primary strength giving phase in hydrated cement, and it gains strength internally through production of long calcium silicate chains, held together by covalent, ionic, and Van der Waals bonding. Calcium hydroxide (C-H) also has a variable structure which forms 20%-25% of the hydrated cement paste volume. This product does not contribute as much to strength development, but it has an important role in keeping the pore solution alkaline.

Cement hydration is often tracked through isothermal calorimetry, which measures the rate of heat produced by cement hydration, over time. There are five main stages of the portland cement hydration process. As indicated in Figure 2-1, stage I is known as the initial dissolution stage, in which cement contacts water. Stage II is known as the induction stage, during which dissolution is slowly occurring. Stage III and IV include the major C_3S and C_3A reactions, both showing up as exothermic peaks. Stage V is the steady state continuation of the hydration process, with slow reactions that never fully come to completion as long as water is available to continue to drive hydration reactions.

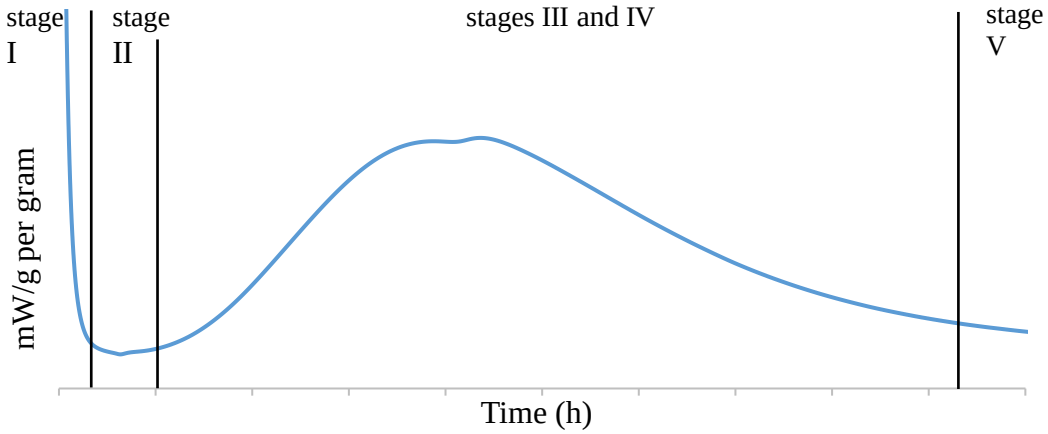

Figure 2-1: Typical isothermal calorimetry curve reflecting hydration of portland cement.

2.1.3 Cement Sustainability

During the cement manufacturing process, carbon dioxide is released from calcination. Calcination involves the decomposition of limestone (calcium carbonate) to lime (calcium oxide), producing carbon dioxide as a biproduct.

$$CaCO_3 + HEAT \rightarrow CaO + CO_2$$

This equation only describe the calcination process, and do not consider the amount of combustion fuel required to heat the kilns, quarry materials, or transport materials. Clinker making is estimated to require 1.75 ± 0.1 MJ per kg, however, inefficient processes raise the energy requirement (Hendriks et al., 2004).

The concrete production industry faces an increasing challenge to balance environmental risk with economic production. Environmental concern comes from carbon dioxide emissions from three sources: fossil fuel oxidation, and carbonation (Andrew, 2019). With global cement production accelerating rapidly in the last 50 years, the industry has been trying to reduce the severity of environmental concerns. In recent years, attempts have been made to identify materials with pozzolanic properties to partially replace cement to decrease its use. Portland cement has been identified for causing 74% - 81% of total CO_2 emissions from commercially produced concrete (Flower & Sanjayan, 2007). Because of this, alternative cements and supplementary cementitious materials have been developed and blended to reduce the amount of portland cement used. However, performance and quality must be sustained to maintain

economic and social contributions through a life cycle assessment (García-Segura et al., 2014). Since concrete production is not slowing down, sustainability must be paramount.

2.1.4 Supplementary Cementitious Materials (SCMs)

Supplementary cementitious materials (SCMs) are materials that can be used as partial replacements of cement in concrete mixes and pastes. Materials with high amounts of accessible calcium, alumina, and/or silica will allow the hydration reaction to continue through those materials interacting with hydrated C-H to produce more C-S-H and/or C-A-S-H. These gels are amorphous, strength providing reaction products that will further densify concrete, reducing permeability, and increasing strength. Calcium hydroxide is easily dissolved, and the pozzolanic reaction will use it to produce more C-S-H which improves pore structure and strength development.

It is advantageous to use SCMs in concrete mixtures for several reasons. Firstly, it reduces the amount of cement required for a mixture, reducing associated carbon footprint and cost, as most of these materials are cheaper than portland cement. Additionally, these materials are often the trash of industrial processes, meaning they would otherwise be wasted. This includes fly ashes and silica fume. In addition, SCMs have been shown to improve concrete performance and durability, if used correctly.

2.2 Agricultural Materials used as SCMs

With shortages of common SCMs such as fly ash occurring throughout the U.S., other sources of pozzolanic materials are needed to support production of sustainable

concrete. One material source that has been identified, but not yet produced at commercial scale, is ash created from agricultural biomass (Aprianti et al., 2015; B. et al., 2023; Lim et al., 2012).

2.2.1 Chemical Composition of organic materials

Plant matter consists of substances with unique chemical compositions and contributions to the plant's maturation and survival. Additionally, as a plant matures, its composition will change significantly (Weaver et al., 1978). One of the major components of agricultural materials are the major lignocellulosic materials (cellulose, hemicellulose, and lignin). In agricultural residues, the quantities of these components are estimated to be 35%-50% cellulose, 20%-35% hemicellulose, and 10%-25% lignin (Wei et al., 2017). Other lignocellulosic materials are present in the forms of waxes, pectins, and other compounds (Peng et al., 2010). The three major lignocellulosic materials mentioned previously have the largest contribution to weight of these materials, particularly in the stems. These compounds will be discussed individually.

2.2.1.1 Cellulose

Cellulose is a polysaccharide containing thousands of glucose units. Being the most abundant biopolymer on Earth, it serves as the main structural component in plants. In stems and woody materials, there exists a matrix of lignin in which cellulose fibers serve a structural purpose. Cellulose forms bonds at the first and fourth carbon atoms on the glucan molecule in a glycosidic bond that repeats between D-glucose units. Because

the hydroxyl groups form hydrogen bonds with oxygen, the chain is held in place in a straight-chain polymer form. These bonds form fibrils, which give cellulose a crystalline structure with high tensile strength. Microfibrils contain several crystalline cellulose chains, alternating with amorphous regions. Cellulose content of plant materials can be estimated with a variety of methods, including strong acid hydrolysis (A. Sluiter, n.d.). Thermogravimetric analysis has been used to determine that cellulose pyrolysis occurs between 315 °C and 400 °C, and that its pyrolysis is the only endothermic reaction among the three major constituents (Yang et al., 2007a). Cellulose decomposition is important to the material's use as an SCM due to the negative effect of crystalline sugars on cement hydration.

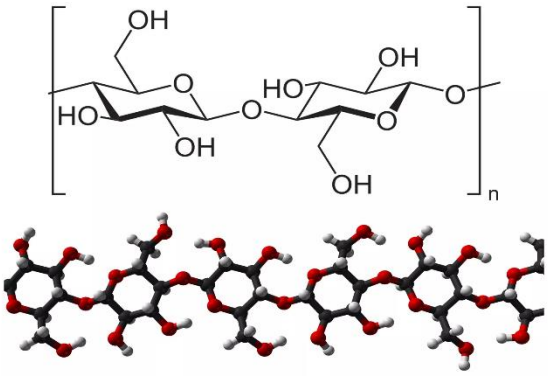

Figure 2-2: Cellulose forms by linking glucose subunits. NEUROtiker, Ben Mills / Public Domain

2.2.1.2 Hemicellulose

Hemicelluloses are polysaccharides that work alongside lignin to hold together long cellulose fiber chains. Hemicellulose makes up less of the biomass portion than

cellulose, but is important to the function of both cellulose and lignin. Hemicelluloses are completely amorphous and are classified by the main sugar product in the backbone of the molecule. The most common sugar residues are xylans, mannans, xyloglucans, and glucans (Wyman et al., n.d.). Because hemicellulose is a broad classification for noncellulose, nonpectin cell wall molecules, their structural composition and functionality can vary greatly. These polysaccharides do not bond directly to cellulose but are attracted via hydrogen bonds and van der Waals forces (Wyman et al., n.d.). Hemicellulose serves to strengthen cell walls by interacting with cellulose and lignin, forming a highly cohesive product (Scheller & Ulvskov, 2010). Hemicellulose pyrolysis occurs between 220 °C and 315 °C (Yang et al., 2007a). Hemicelluloses are the largest concern for removal for concrete systems (Vo & Navard, 2016). Pretreatments like field retting or thermochemical soaking can decompose the hemicellulose cell wall structure (Gusovius et al., 2019). Hemicellulose has a low thermal stability and therefore can also be easily hydrolyzed by dilute acid (Vo & Navard, 2016).

2.2.1.3 Lignin

Lignin is a group of complex polymers that work alongside hemicellulose to provide structural support to cell walls. The name “lignin” came from a scientist named Schultze in 1865 to describe the decomposed portion of wood when soaked in nitric acid (K.V. Sarkanen, 1971). It is an amorphous, heterogenous collection of three-dimensional polymers. Its biological function is to fill spaces in the cell wall layers through rigid covalent bonds to hemicellulose that contribute to compressive strength. It is also

considered an important defense against disease and water intrusion leading to decay. It is the second most abundant natural polymer on Earth, behind cellulose (A. Nair et al., 2017). Lignins are made from phenylpropanoid building blocks like hydroxycinnamoyl alcohols and monolignols (Lu & Ralph, 2010). Because lignin is so complex, there are still academic controversies over its structural regularity (Sederoff et al., 1999). Lignin is far less hydrophilic than the other cellulosic materials, and it has natural stiffness, therefore it is difficult to degrade. It degrades over a large temperature range, from 160 °C to 900 °C (Yang et al., 2007a).

Industrial Lignins

Around 100 million tons of technical lignins are produced per year, mostly from the pulp and paper industries (FAO, 2019). This type of lignin is often produced from the bioethanol industry as a byproduct during the hydrolysis process. It can be produced as a result of solid pretreatment (delignification). These pretreatment procedures are often quite costly, and the use of these methods for energy production have slowed in the United States after a few years of experimentation in the early 2010's. The sustainable part of these processes is that they are designed to produce zero waste, as the wastes can be easily processed for other purposes (Falah et al., 2020). As part of the waste recycling process, this solid waste has been used in concrete and cement research as a mortar additive. Industrial lignin, often referred to as high lignin residue, has a comparable effect on hydration as a water reducer (Ataie & Riding, 2014a; Falah et al., 2020). Studies on

industrial lignin reactivity in cement systems are limited, as material is relatively difficult to find from active bioethanol producers.

2.2.1.4 Metal Contamination from Soils

One of the major factors in variability of plant material chemistry comes from absorption of minerals and contaminants from the soil. Being that most agricultural materials are grown primarily as a food source, they are often treated with synthetic pesticides which contaminate the soil. Similarly, if a field is in an industrially polluted region, heavy metals can enter the crops and accumulate in the plant's vegetative and reproductive organs (Angelova et al., 2004). The genotype of the plant provides the largest variability of the plant to absorb and distribute heavy metals, and this often can be connected to the filtration ability of the root system (Hocking & McLaughlin, 2000).

Some heavy metals are beneficial for plant growth, like copper and zinc which serve as activators for enzymatic reactions (Kiran et al., 2022). Some are beneficial to organisms in minute quantities, such as iron, nickel, copper, cobalt, manganese, vanadium, and molybdenum (Kiran et al., 2022). Then, there are some metals that have largely harmful effects on living organisms in any quantity if consumed, like lead, cadmium, uranium, and mercury (Wallace & Buha Djordjevic, 2020). Because metals cannot be broken down, if concentrations increase above a specific threshold, it can cause damage to internal cellular structures, cause chlorosis, induce oxidative stress, stop growth, and reduce enzymatic and metabolic activity of the plant. It is important to remember that the label "heavy metal," does not imply that the presence of the metal is

necessarily bad for the plant. Plants need certain metals at a proper quantity to achieve optimal metabolic function.

Inorganic fertilizers are ubiquitous sources of heavy metal concentrations in plants. Fertilizers are used to promote plant growth and yield by providing additional sources of phosphorous, nitrogen, and potassium. However, trace elements of B, Cu, Co, Fe, Mn, Mo, Ni, and Zn are often introduced through fertilization and fungicide application (Alloway, 2013; Wallace & Buha Djordjevic, 2020). In the urban soil, concentrations of heavy metals are often significantly higher than in the rural soil. This is due to the deposition of dust from industrial processes and air pollutants, corrosion of metal structures, paint application, solid and liquid wastes, and fertilizer use (Alloway, 2013; Kaiser et al., 2015). The presence of containments in either setting promotes serious risks to human health from consuming toxins, and potential risks for the use of these materials in cementitious systems. (Bermudez et al., 2011; Custodio et al., 2021; Wallace & Buha Djordjevic, 2020). Hydration retardation can be caused by heavy metals like lead and zinc (Weeks et al., 2008). This leads to reductions in early age compressive strength, although some elements like copper and lead are predominantly absorbed by the CSH gel (Gineys et al., 2010).

Elemental composition in soils near the agricultural material sources are shown in Table 2-3. This data was accumulated from a 2007 study in the United States performed by the United States Geological Survey (USGS) using data from 4,857 sites over six years (Smith et al., 2013). Color-scaled maps from this survey are presented in Figure 2-3, to show relative trends across all sampling locations. These maps and data are intended

to display the large amount of general variability in soils across the country, which may affect the growth, composition, and performance of ashes created from agricultural products.

Table 2-3: Composition in the horizon A layer of soils near agricultural material sources. (Smith et al., 2013)

US soil geochemical landscape site	#3088	#11260	#9296	#10300	#6104	
Location	Wooster, OH	Clark County, OH	LaPorte County, IN	Christian County, KY	Sedgwick County, KS	
Element or mineral	A horizon	A horizon	A horizon	A horizon	A horizon	Units
Depth	0-20	0-13	0-23	0-4	0-10	cm
Aluminum	4.64	4.83	3.36	2.02	4.36	wt. %
Arsenic	14.2	7.4	7.6	4.7	4.8	mg/kg
Calcium	0.23	0.66	0.25	0.19	2.91	wt. %
Chromium	37	38	29	33	30	mg/kg
Copper	15.5	15.7	26	6.8	11.9	mg/kg
Iron	2.44	2.37	1.75	1.07	1.41	wt. %
Potassium	1.58	1.71	1.21	0.53	1.78	wt. %
Magnesium	0.35	0.45	0.21	0.15	0.36	wt. %
Manganese	733	681	396	507	294	mg/kg
Sodium	0.52	0.71	0.36	0.12	0.72	wt. %
Phosphorus	660	550	1160	350	270	mg/kg
Lead	30.1	23.7	80.6	28.8	30.4	mg/kg
Rubidium	72.5	76.2	51.9	30.6	76.4	mg/kg
Sulfur	0.03	0.02	0.03	0.03	0.02	wt. %
Uranium	3.2	3.4	1.8	1.3	2.1	mg/kg
Zinc	81	53	120	45	129	mg/kg

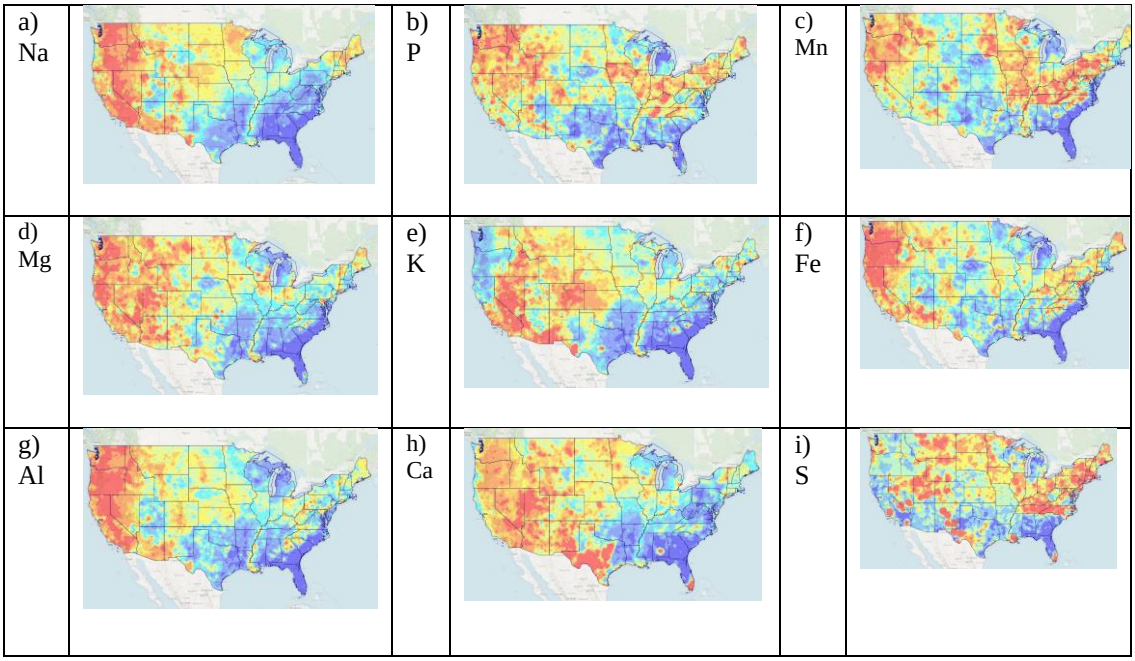

Figure 2-3: Maps of elemental concentrations in the soil A layer across the United States. Relative scale. a) sodium, b) phosphorous, c) manganese, d) magnesium, e) potassium, f) iron, g) aluminum, h) calcium, i) sulfur (Smith et al., 2013).

2.2.2 Availability and Variability of Agricultural Materials

2.2.2.1 Hemp Hurd

The cultivation of hemp has begun to accelerate in western countries in the last decade as the plant has gained popularity for use in CBD products, and the use of its fibers in products like rope, fabrics, and paper. The hemp plant is occasionally referred to by its scientific name, *Cannabis sativa*. From a global perspective, hemp is one of the

world's oldest annual crops, and it has been known to adjust well to many climates and environments (Salentijn et al., 2015). Legality of the plant differs in each country, but it is slowly being legalized in the United States with governmental regulation. According to a global research study, the global hemp market is estimated to be valued at USD 6.8 billion in 2022, with projected growth up to USD 18.1 billion by 2027 (Research and Markets, 2022). In the United States, the hemp growing market is young and new. In 2021, 48% of industrial hemp producers did not claim farming as their primary occupation, and 58% of all farmers have not been in the business for over five years (USDA, 2021b). Industrial applications for the hemp plant involve the leaves and the fibers, which are internal to the stem. Of the 54,152 acres of hemp planted in the United States in 2021: 19.7 million pounds were cultivated for floral hemp, 4.37 million pounds for grains, 33.2 million pounds for fibers, and 1.86 million pounds for seeds (USDA, 2021b). Most of these farmers are harvesting to a specific category of use, leaving most of the hemp hurd and biomass wasted, which is a major problem for cultivators. Hemp has a dry matter yield of 10 tons per hectare in some cases, which is significant, especially when considering that the growth of a hemp plant in 4 months produces over 4 times more biomass than a forest of the same size (Pargar et al., 2021; Vassilev et al., 2015; Zampori et al., 2013). Currently, the waste of the hemp plant is deposited in landfills, so availability of the biomass is large and growing. Pargar et al. reports the ash content of hemp hurd to be between 4% and 8% by weight (Pargar et al., 2021). Assuming an average ash content of 6%, and a useable percentage of harvested dry

material is 50% across the 54,152 acres planted, 6,334 tons of hemp hurd ash could have been generated in 2021.

Mechanical properties of the hemp plant can vary greatly based on location, soil conditions, climate, processing limitations, and stem diameter, which is a concern for its use in cementitious systems(M. Liu et al., 2015). In general, hemp is known to have significant amounts of calcium, phosphorous, and magnesium (Pargar et al., 2021). The hemp stem and fiber can vary due to harvest time and field retting as well, but it is known that the major constituents of hemp are cellulose, hemicellulose, and lignin, which compose up to 90% of their dry weight (M. Liu et al., 2015),. The hemp hurd (woody core fibers) consists of 40% - 48% cellulose, 18% - 24% hemicellulose, and 21-24% lignin. The hemp blast fibers consist of 57% - 77% cellulose, 9% - 14% hemicellulose, and 5% - 9% lignin (Gümüşkaya et al., 2007).

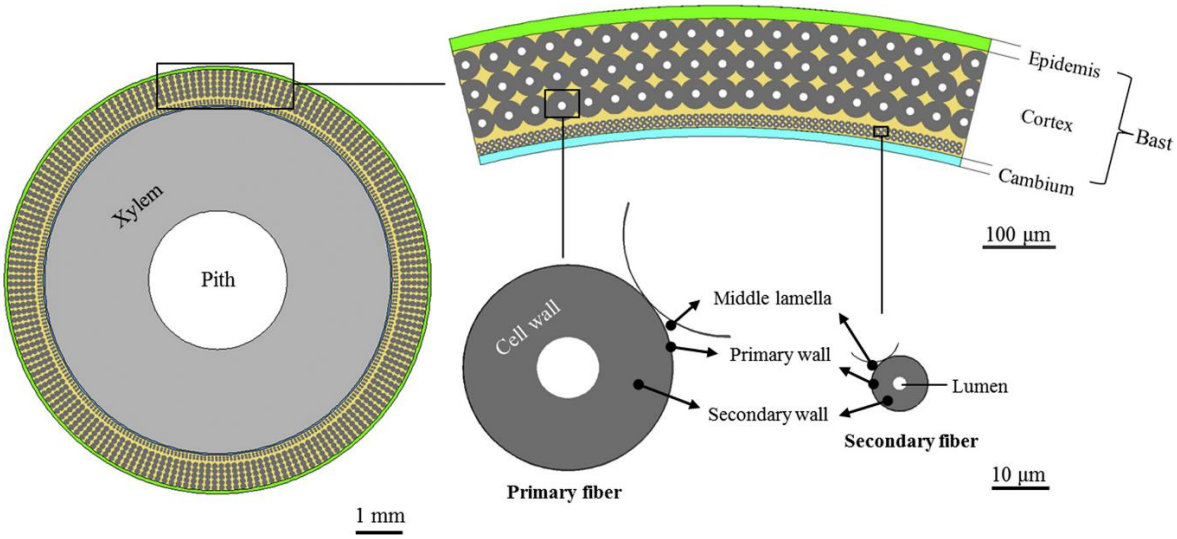

Figure 2-4: Hemp stem and fibers. (Liu et al., 2015)

2.2.2.2 Corn Stover

In the 2021-2022 production year, the United States produced 382.9 metric tons of corn, with a world production of 1,214.9 metric tons in the same year (USDA, 2023a). Corn is an annual crop with a large production in the United States, particularly in the midwestern states. Corn is mostly harvested for its grain, leaving the stalk and leaves as waste products. Corn stover is composed of 50% stalks, 22% leaves, 15% cobs, and 13% husks (Morissette et al., 2011). A 2018 study from Thailand reports that 41% of corn farmers burn their waste in the field out of necessity (Arunrat et al., 2018). Available research demonstrates that the ash content of corn stover can range from 3% - 8% for untreated material (Lizotte et al., 2015). Assuming an ash content of 5%, and a useable percentage of harvested dry material is 50%, the United States could create 6.3 million metric tons (6.9 tons) of corn stover ash per year (Shakouri et al., 2020).

Corn stover mechanical properties can vary for the same reasons as hemp. Additionally, conditions during storage can begin to degrade and change the moisture content of the material (Ray et al., 2020). Corn stover is known to have particularly high concentrations of phosphorous, which could lead to slagging, alkali-silica reaction, and retardation of cement hydration (Niu et al., 2016; Shakouri et al., 2020). Corn stover composition is dependent on part of the plant, but in bulk, its composition includes 35% cellulose, 20% hemicellulose, and 12% lignin (Pan et al., 2019).

2.2.2.3 Wheat Straw

In the 2021-2022 production year, the United States produced 44.8 of the world's 779.3 metric tons of wheat straw (USDA, 2023a). Wheat is an abundant and inexpensive annual crop that can grow in various climates on flat ground as well as steep slopes. Its production is vital to food, pharmaceutical, and cosmetic industries. Wheat has 5 major morphological parts including leaves, grain, grain axis, nodes, and internodes. It consists mainly of cellulose (28% - 39%), hemicellulose (23% - 24%), and lignin (16% - 25%) (Álvarez et al., 2021).

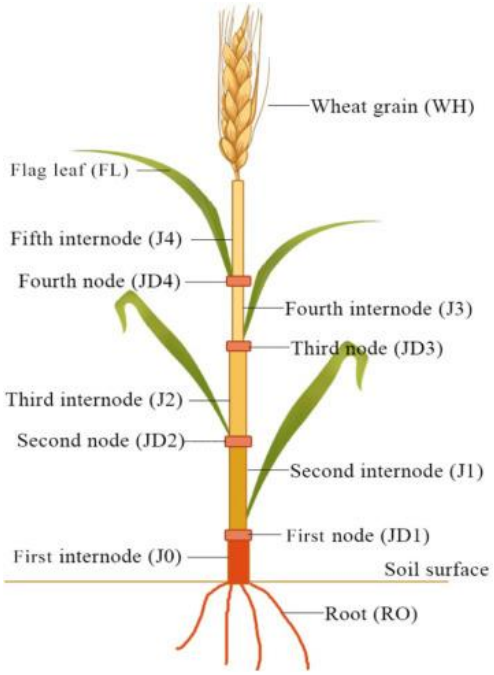

Figure 2-5: Wheat straw parts. (Zhang et al., 2020)

Wheat straw is known for having high amounts of silica in the cutile parts, which make it advantageous for use in cementitious systems (Biricik et al., 1999). Relatively

few agricultural biomass materials have more amorphous silica naturally (75% - 90%) than wheat (Martirena & Monzó, 2018). Variation in wheat straw chemistry mainly comes from soil content and environmental conditions, as wheat straw is notably susceptible to absorption of heavy metals from the soil (Bermudez et al., 2011; Biricik et al., 1999; Zhang et al., 2020).

Wheat straw cultivation also results in much waste. Historically, wheat straw that was not used for its grains has been used for building materials, feed, bedding, substrates for growing mushrooms, and pulp/paper making (Smil, 1999). Wheat straw is an abundant resource with many uses, and its waste could provide valuable material to the cement industry. The ash content of wheat straw is estimated to be between 4-7% ((Bruun et al., 2010)). Between 2020 and 2022, an average of 51.3 million tons of wheat straw were produced in the United States per year ((USDA, 2023b)). Assuming a usable crop yield of 50% and an ash content of 6%, over 1.5 million tons of wheat straw ash could be generated in the United States per year.

2.2.2.4 Rice Husk

Rice is the one of the most important cereal grain crops in the world, particularly in Asia, which outputs 90% of the global rice production (Lim et al., 2012). The global production of rice is projected to reach 516.1 million tons in the 2022-2023 harvesting year (USDA, 2023b). In the United States, rice is grown in large quantities in Arkansas, Alabama, Louisiana, Texas, and California (USDA, 2021a).

Rice husk is potentially the most used agricultural SCM. Rice husk is the hard shell that protects the rice grain on the plant which is estimated to be 20% - 33% of the paddy weight (Lim et al., 2012). It is the only organic material distinctly mentioned in ACI committee 232's report on natural pozzolans (American Concrete Institute & ACI Committee 232., n.d.). Rice husk is known for having high amounts of natural silica when burnt (90% - 96%), making it known as an active pozzolan. Its composition is mainly cellulosic sugars, but it also contains about 20% lignin and 20% hemicellulose (Park et al., 2004). For much of history, the rice husk was wasted material, but today it is being used successfully as an SCM, and as an energy/fuel source (Lim et al., 2012).

Rice husk variability mainly comes from differences in thicknesses of various layers of the fibers and walls of the husk. These differences can cause severe changes in material structure, evident in tensile strengths varying between 19 and 135 MPa depending solely on rice husk variety (Chen et al., 2018). The upper range of tensile strength reported is similar to that of nylon, making the material very flexible due to high amounts of cellulose (Chen et al., 2018). In a similar manner to other materials, mechanical properties can change as a result of cultivation practice as much as regional variability.

2.2.3 Processing Agricultural Materials

2.2.3.1 Pretreatment

Agricultural biomass can contain many impurities that may inhibit cement hydration, or may not have reactive silica easily accessible. Thermochemical

pretreatment techniques have been explored to improve pozzolanic reactivity of biomass ashes by increasing the available surface area, increasing the amount of amorphous silica, and by decreasing the carbon content of the material (Ataie et al., 2013; Chandrasekhar et al., 2006; Feng et al., 2004).

As described previously, several challenges are present in the lignocellulosic biomass including crystallinity of the cellulose, hydrophobicity of the lignin, and the lignin-hemicellulose matrix trapping cellulose and impurities (Fatma et al., 2018). The bioethanol industry has developed ways to break the covalent and ionic bonds between these polymers to access and isolate them for treatment. These processes can be expensive and energy intensive. For use as a pozzolan, it is beneficial to remove surface impurities, increase the surface area of the particle, disrupt the lignin structure, and hydrolyze the hemicellulose (Bokhari et al., 2021).

There are four main categories of pretreatment for biomass materials: physical, chemical, solvent, and biological. Aside from milling, which is a physical treatment, this study will focus only on chemical treatments. Chemical treatments generally use diluted acid or alkaline solution soaks with the goal of disrupting lignin-carbohydrate complexes to hydrolyze hemicellulose and cellulose (Balat et al., 2008). The presence of lignin is not necessarily a problem, as it does not interfere with setting and it is known to protect the biomass against water intake (Vo & Navard, 2016). These treatments help provide a homogenous surface of glucose, which allows the bond between the biomass surface and surrounding matrix to require less energy in formation. The hydroxyl groups in lignocellulosic materials in cellulose's crystalline region are inaccessible, however the

amorphous region has hydroxyl groups that are able to react with the outside medium. In addition to increasing the surface area for reaction, pretreatments of this nature can also be vital in removing large amounts of impurities like K_2O and P_2O_5 from the material (Shakouri et al., 2020).

The simplest and cheapest pretreatment is a water soak. This helps remove impurities and some low molar mass hemicellulose, and can often be done in the field in the form of field retting (Shakouri et al., 2020; Vo & Navard, 2016). Another common method is an alkali treatment, which is known to be effective at removing impurities and low molar mass hemicellulose, as well as improving fiber-matrix adhesion (Bokhari et al., 2021; Pacheco-Torgal & Jalali, 2011; Sedan et al., 2008; Zhao et al., 2020). Sodium hydroxide is the most common alkali treatment, although titanium alkoxide, copper-chromium-arsenate, sodium alginate, and others have been used. Sodium hydroxide treatment not only will dissolve cellulose, hemicellulose, and lignin, but it will alter the surface morphology of the plant biomass at higher concentrations (Kabir et al., 2013). In concrete, alkali-treated fibers have exhibited a reduction in water absorption, improved tensile strength, and a stronger bond. However, if an alkaline condition is applied, there is a risk of strength decrease (Gu, 2009). Sodium hydroxide treatment must also be followed with a long rinse, or salt contamination is possible.

Acid treatments must also be followed with a long rinse, or the ash could introduce a low pH substance to the cement matrix (Shakouri et al., 2020). Studies show inconsistent results when using acid-washed organic matter, but most suggest it is effective at removing impurities through leaching. Common acid pretreatments include

nitric, hydrochloric, and sulfuric acids with strengths between 0.1M and 1M. Acid soaking is more effective at leaching impurities from the biomass with longer duration (Shakouri et al., 2020). Acid treatment has been shown to make particles less porous, contributing to better densification in the cement matrix and better removal of cellulose during burning (Ataie & Riding, 2014a, 2014b). The biggest advantage of using this type of treatment is the removal of impurities like sugars, chlorine, phosphorous, and potassium, which can greatly slow cement hydration (Jorge et al., 2004; Shakouri et al., 2020). It also can remove metals like calcium and magnesium, which do not negatively impact hydration (Ataie et al., 2013). For some materials, it is worth the energy and material cost to remove a large amount of phosphorous from the structure (Shakouri et al., 2020). Since acid treatment can be costly and time consuming however, and many studies have shown that simply water rinsing greatly improves the material performance and chemistry (Ataie et al., 2013; Ataie & Riding, 2014b; Eggeman & Elander, 2005; Feng et al., 2004; Galbe & Zacchi, 2012; Shakouri et al., 2020; Sun & Cheng, 2005).

2.2.3.2 Calcination

Outside of hemp-crete construction, which uses raw material, agricultural product usage as an SCM must be in ash form. There are several ways to burn agricultural biomass, the most common being open burning and muffle furnace calcination. Agricultural burning is a common disposal method, but an undesirable practice from an environmental perspective. An estimated 108.6 kilotons of emissions were generated in the United Sates in 2020 from burning agricultural waste (FAO Stat, 2020). The Rice

Straw Burning Reduction Act of 1991 in California attempted to ban biomass burning, however the reduction in burning was not significant or sustained because it is simply the easiest way to dispose waste material (Air Resources Board 1998., 1999).

Figure 2-6: Agricultural waste burning: a) in Madagascar. (Tiy Chung, 2021). b) Open air burning of corn cob ash. (Jimoh & Apampa, 2013).

The primary concerns in selecting a calcination regime are energy consumption, and time required for processing. If this is to be a sustainable procedure, it should minimize energy consumption while being an efficient processing regime. In a controlled test burning corn cob ash, it was estimated that open air burning energy consumption was 4.3 MJ/kg ash whereas muffle furnace burning consumed 216,166 MJ/kg of ash. In this open-air burning environment, it was estimated that 0.27 kg of CO_2 were omitted per kilogram of ash (Jimoh & Apampa, 2013). This is favorable when considering portland cement clinker production consumes 5.16 MJ of energy and emits 0.97 kg CO_2 per kilogram (William T. Choate, 2003). Open-air burning of agricultural materials can be done sustainably, but care must be taken to limit temperatures that could cause crystallization of silica and other compounds. Increasing crystallization has been seen via

x-ray diffraction at temperatures as low as 600 °C – 700 °C (Bonifacio & Archbold, 2022). Open air agricultural burning is not a new technology, and research shows that keeping fires small and monitoring them can keep crystalline silica from being formed .(Deshmukh et al., 2012; D. G. Nair et al., 2008)

Uniformity in ash produced can be increased through finishing in or solely using an electric muffle furnace. Considerations for calcination procedure depend on pretreatment, material LOI, amount of material to process, and size of furnace. One of largest factors in muffle furnace burning is the amount of oxygen availability for the material to burn evenly and quickly. One study used one-inch-thick layers of material in ceramic bowls (S. A. Memon & Khan, 2018). Some research has been published using large ovens and racks set up vertically to catch falling ash as it burns (Ataie & Riding, 2014a). Other researchers opt for two step processes, one in a larger oven with a lower temperature to reduce volume significantly, before finishing the burning in a smaller oven with a higher temperature (Kevern & Wang, 2010; Ribeiro & Morelli, 2014). This process can be done in several ways, and a unique process can be formed to maximize the efficiency of the equipment available to the researcher.

Another consideration is selecting an optimal calcination temperature. On one hand, there is the concern about crystalline silica if calcination is pushed to too high of temperatures. A 2004 study on silica crystallization with rice husk ash showed that cristobalite did not appear via X-ray diffraction until 700 °C (SHINOHARA & KOHYAMA, 2004). On the other hand, ASTM C618-22 requires that for a calcined material to be considered a natural pozzolan, the LOI must be below 10% (ASTM, 2022),

requiring temperatures at least as high as 500 °C for most agricultural products. Biricik et al. determined ash content and SiO_2 content by burning wheat straw at 575 °C for 5 hours, which revealed an ash content of 8.6% and a SiO_2 content of 73% (Biricik et al., 1999). Other tests on wheat straw show ash contents between 8% - 11% and SiO_2 contents between 88% - 91% and there is evidence that the soil content and environmental conditions will cause variations in the wheat straw's chemical properties (Biricik et al., 1999). Biricik et al. tested 8 calcination temperatures between 300 °C and 1000 °C and 7 hold times between 1 hour and 30 hours and found that a 5 hour burn between 570 °C and 670 °C was ideal for reactivity, the best being at 670 °C (Biricik et al., 1999). They concluded that ash content depends both on calcination temperature and silica crystallization because at a temperature of 800 °C, a more complete burning occurred, but this temperature caused some of the amorphous silica to crystalize. The results of similar studies are compared in Table 2-3.

Table 2-4: Selected LOI & silicon oxide results from literature.

Source	Material	Calcination Time/Temp	Pretreatment	LOI (%)	SiO_2 Content (%)
(Ataie & Riding, 2014a)	Corn stover	2h @ 500 °C 1h @ 650 °C 1h @ 650 °C 1h @ 650 °C	HCl HCl Water none	6.1 3.8 10.6 22.8	76.5 77.9 47.4 28.4
(Ataie & Riding, 2014b)	Wheat straw Rice straw	1h @ 650 °C 2h @ 500 °C	HCl HCl	1.2 2.2	86.5 85.7
(Aprianti et al., 2015) (review)	Corn cob ash	Varies	Varies	0.9-1.5	65.4-67.3
(Biricik et al., 1999)	Wheat straw	5h @ 575 °C	none	8.6	73.0-74.0
(Pargar et al., 2021)	Hemp	4h @ 500 °C 4h @ 600 °C 6h @ 600 °C 4h @ 800 °C 6h @ 800 °C	none	No direct data, but max ash content of 8%	1.2 0.8 0.7 1.0 0.8
(Shakouri et al., 2020)	Corn stover	2 steps: min @ 550 °C	HNO_3 Water none	0.2 4.0 9.0	85.7 64.8 49.0
(Kevern & Wang, 2010)	High silica corn ash Corn ash	4 steps: 500 °C - 700 °C	None None	5.3 11.4	35.6 38.3

A higher LOI is generally an indicator of higher unburnt carbon content. High LOI can be problematic for use of ashes in cementitious mixtures as unburnt carbon will

adsorb admixtures, especially air entraining admixtures, from solution. High LOI has been linked to delayed hydration, and slower compressive strength development in a study using ground bagasse ash (Chusilp et al., 2009). However, if the balance between amorphous silica and unburnt carbon is maximized, reactivity can raise later age strengths. In Pargar et al.'s 2021 study, they show that as cement replacement by agricultural SCM increases from 5% to 25%, 28-day compressive strength decreases by a factor of 8% to 42% (Pargar et al., 2021). They point out that this is also due to the increased carbon absorption, which affected compaction and hydration at higher replacement levels. (Ataie & Riding, 2014a, 2016; Bonifacio & Archbold, 2022; Shakouri et al., 2020).

2.2.4 Agricultural Materials in Cementitious Systems

There are numerous advantages to using agricultural or organic materials in cementitious systems, aside from reducing a quantity of the cement in a mixture. Many biomasses have good thermal insulation properties, low cost, and low density. Additionally, compared to fly ash and silica fume, agricultural biomass is renewable and not supplied from an industrial process, so it may be possible to optimize their production for maximized cementitious mixture properties. Use of agricultural materials in the concrete industry can also reduce disposal of agricultural-waste solids that fill landfills or lay in fields to be burned (Vo & Navard, 2016). Currently these materials are being studied for use as cement replacement materials and as aggregate replacement materials. Durability of biomass materials is an area where research is currently lacking, but

proposed solutions to durability concerns include coating of materials to reduce absorption, chemical treatments to adjust the amount of reactive material in the ash, and physical treatments to improve the physical and mechanical performance of these materials (Mwaikambo & Ansell, 2002; Sousa Coutinho, 2003). Biomass is gaining interest globally as a solution to environmental concerns in the concrete industry, and waste concerns in the agriculture industry.

2.2.4.1 Hemp Ash

The hemp plant has many unique features that make it versatile. Hemp fibers have long been used for their thermal insultation properties in non-structural hempcrete technology (Charai et al., 2021). However, this study will focus on the use of hemp hurd (the woody stem portion) in cementitious systems. The usage of the material in structural and high-performance systems is not well researched currently.

Research involving hemp biomass ash has often cited workability as a potential problem, and have used superplasticizer for this reason (Pargar et al., 2021). Production of the ash can also present difficulty, because of the low ash content of portions of the plant. Research generally shows poor workability and compressive strength, as well as increased water demand at substitution rates above 15% due to the high absorption capacity of the material (B. et al., 2023; Pargar et al., 2021). Lower percentages of untreated hemp ash substitution indicate hemp ash can be used as a filler for economic reasons. The reported low reactivity of untreated hemp ash results from the relatively low

silica content of the ash, while being high in potassium and calcium (Stevulova et al., 2014).

Pretreatment may be the best way to improve the quality of hemp ash for reactivity. Pretreatments like water rinsing and saturated lime water soaking have somewhat improved the delaying of cement hydration (Guo et al., 2020). More complex methods like vapothermal curing of hemp shives have been effective at depolymerizing hemicellulose and cellulose for easier degradation, but it is unclear whether this improves mechanical properties of concrete (Karam et al., 2021). Currently, research is limited in the use of hemp as an SCM due to its low silica content and relatively new legal presence in the United States. Research should be done to explore ways to pretreat this material to increase its reactivity, as well as study its long-term performance in cementitious systems.

2.2.4.2 Corn Stover Ash

Corn stover has potential as an SCM due to its availability, ash content, and chemistry. This material is relatively new to consideration as an SCM, but published research shows potential for this to be a significant resource to the cement industry.

Pretreatment has been shown to effectively improve the reactivity of corn stover, due to the removal of potassium, calcium, magnesium, and phosphorous (Ataie & Riding, 2014a). Corn stover commonly contains these impurities in high amounts of sylvite (KCl), $KCaPO_4$, and crystalline quartz (Ataie et al., 2013; Shakouri et al., 2020). The LOI of the ash decreases with acid or water pretreatment, which is ideal for reactivity

(Teymouri & Shakouri, 2023). Among these factors, the removal of phosphorous and reduction in carbon content could greatly improve the hydration of these systems. In some cases, compressive strength is improved using a substitution of 20% pretreated corn stover ash (Ataie & Riding, 2014a; Shakouri et al., 2020). Shakouri et al. showed that long term chloride intrusion can be improved with the use of corn stover as an SCM, especially when the ash has been pretreated (Shakouri et al., 2022).

Currently, studies show that mechanical properties of corn stover concretes can be improved using simple pretreatment measures. However, due to the high amount of alkaline matter in corn stover, more research should be done to ensure that alkali-silica reaction will not be promoted with its use. Studies on durability of corn stover ash containing concretes are few and recent, so this is an area of growing research and interest in the industry.

2.2.4.3 Wheat Straw Ash

Wheat straw has a longer and more documented history for use as an SCM. It is naturally high in amorphous silica, (88 – 91%) making it effective at achieving pozzolanic reactivity (H.C. Visvesvaraya, 1986). Calcination temperature and fineness contribute to changes in pozzolanic reactivity of this material, with disagreement regarding optimal calcination temperature (M. Amin et al., 2019). Some studies show more effective reactivity with calcination near 500 °C, whereas some show the best reactivity near 670 °C (Ataie et al., 2013; Biricik et al., 1999). In some studies, crystalline

silica begins forming beyond 600 °C, which leaves the silica ineffective for reaction (M. Amin et al., 2019; S. Memon et al., 2018).

Wheat straw ash has effectively been used to increase the amount of hydration products and improve mechanical properties up to a replacement percentage of 20% by mass (Al-Akhras & Abu-Alfoul, 2002; M. Amin et al., 2019; Ataie et al., 2013; Katman et al., 2022). Wheat straw ash notably changes heat of hydration observations, in many cases accelerating the time of peak heat flow and resulting in a higher total heat of hydration (Ataie et al., 2013). Porosity has been studied through N_2 adsorption testing which indicates refinement of the pore structure due to an increase in BET surface area when finely ground wheat straw ash is used (M. N. Amin et al., 2022). It is suggested that fine particles of wheat straw ash effectively provide nucleation sites for hydration products to form. Furthermore, the densification of wheat straw ash notably produces a significant (75%) decrease in water absorption at 90 days as well as a drop in water penetration depth (Bheel et al., 2021; S. Memon et al., 2018). Memon et al. (2021) observed a strength loss in wheat straw ash concrete when the concrete underwent 5% sulfuric acid immersion, but that weight loss due to acid exposure decreased with increasing amounts of wheat straw ash, indicating that this material may provide additional resistance to acid attack (S. A. Memon et al., 2021). Wheat straw has also been shown to prevent damage from sulfate attack and chloride penetration (Binici et al., 2008; Qudoos et al., 2019). In summary, wheat straw ash has performed well as a supplementary cementitious material in durability tests and mechanical tests due to the

densification of the pore structure from reactive, fine particles with significant available surface area and high silica content.

2.2.4.4 Rice Husk Ash

Rice husk ash also has documented use as an SCM. Rice husk ash was first identified for use in concrete with two German patents in 1924 Click or tap here to enter text.. It has been used successfully since then in proportions of the cement binder up to 30% by mass. The ACI's recommendation for use of rice husk ash is to use it as a 5%-15% substitution by mass to generate lower-permeability concrete (American Concrete Institute & ACI Committee 232., n.d.).

Due to the high porosity of rice husk ash, the system rheology can change dramatically with high amounts of this material, therefore its use is limited because of the high water demand (Martirena & Monzó, 2018). This material, however, is highly reactive, with studies showing pozzolanic activity indexes near and above 140% at 28 days (Nehdi et al., 2003). Pretreatments and calcination optimization have been shown to further enhance the reactivity of rice husk ash (Feng et al., 2004; Kaleli et al., 2020). At 12.5% substitution, the 28-day compressive strength of a rice husk sample increased 40% over a control test, and other tests have confirmed the benefit to compressive strength development (Ismail & Waliuddin, 1996; Nehdi et al., 2003; Shaaban, 2021). There is significant densification that occurs in these systems that leads to improved chloride resistance and surface scaling performance, with proper material grinding (Nehdi et al., 2003; Sousa Coutinho, 2003). Rice husk ash has also been effective at reducing damage

from alkali-silica reaction and sulfate attack (Abbas et al., 2017; Chindaprasirt et al., 2007; Hasparyk et al., 2000). However, despite the improvements observed with use of rice husk ash in concrete, a recent study reported that the use of rice husk ash in concrete can lead to concerns of carbonation (Pandey & Kumar, 2020). Marangu et al. showed that a 15% substitution of rice husk caused a carbonation depth of 2.36 mm, compared to a depth of 1.10 mm for a control sample (Marangu et al., 2020).

2.2.5 Current Codes for Agricultural Materials

Use of supplementary cementitious materials in concrete systems can greatly affect performance characteristics of the material. As a result, understanding the variability of using agricultural materials as SCMs is important for industry comfort and large-scale implementation. Currently the specification most relevant to SCMs like fly ash is ASTM C618-22 (ASTM, 2022). Agricultural ash would be considered a *Class N* pozzolan, and current ASTM guidelines require it to meet certain chemical and physical standards. The chemical standards notably include a 70% minimum combined content of silicon dioxide, aluminum oxide, and iron oxide (ASTM, 2022) and limits on the loss on ignition of 10%. If pozzolans are to be used in blended cements, the relevant specifications are ASTM C595 and ASTM C1157.

The American Concrete Institute (ACI) committee 232.1R-12 published a report titled, “Report On The Use Of Raw Or Processed Natural Pozzolans In Concrete.” This report outlines specifications, test methods, and handling techniques for natural pozzolans based on product used, for example mass concrete, structural concrete, and concrete

masonry. It explicitly mentions rice husk ash, which is known to have 90% - 96% silica content after burning, making it extremely reactive ((American Concrete Institute & ACI Committee 232., n.d.)). The recommendation from ACI is to use it as a 5% - 15% replacement by mass and meet the chemical composition and physical requirements of ASTM C618.

The adoption of new materials to codes takes time, and agricultural materials need more long-term studies to prove adequate and consistent performance. Currently, agricultural ashes can be used as natural pozzolans, but technical guidelines are lacking for proportions and use of these materials other than the one mentioned by ACI.

The goals of this study are therefore to provide better understanding of the consistency in performance of ashes produced to be used as SCMs in concrete mixtures, from agricultural materials. Three sources of hemp hurd, corn stover, and wheat straw were each collected mostly from across the midwestern United States to assess variability among the materials, an area in which research is currently lacking. Ash preparation techniques are explored using chemical pretreatments, calcination, and ball milling with the goal of understanding and optimizing the chemistry of each material. This is assessed through analysis of material density, crystallinity, oxide composition, and absorption. A second phase of this study uses an optimized agricultural ash to assess the performance and reactivity of the ash in cementitious systems. Performance analysis includes studying both fresh and hardened properties of cementitious systems with partial replacement of agricultural ash for cement, as well as assessments of reactivity.

Chapter 3: Experimental Materials

Two cement types were utilized for this research due to material availability. The first was an ASTM Class 1 ordinary portland cement meeting ASTM C150 standards, used only in particle size distribution results (ASTM, 2019a). The second type was a blended Type IL portland limestone cement meeting ASTM C595 standards (ASTM, 2019b). The oxide contents of these materials were tested through x-ray fluorescence.

Table 3-1: Oxide composition of cements and fly ashes.

	OPC	PLC	Class F Fly Ash	Class C Fly Ash
SiO_2	19.73	18.09	48.81	40.11
Al_2O_3	4.66	4.41	26.62	26.61
Fe_2O_3	3.93	3.41	6.65	4.54
CaO	63.93	62.16	9.3	19.45
MgO	2.05	2.29	1.95	5.72
K_2O	0.55	0.61	1.93	0.91
Na_2O	0.10	0.10	1.75	3.74
SO_3	2.74	2.56	0.28	0.76
TiO_2	0.00	0.00	1.46	0.64
P_2O_5	0.00	0.00	0.14	1.42
SrO	0.00	0.00	1.10	0.10
LOI	1.64	5.55	-	-

Table 3-2: Phase compositions of cements.

	C_3S	C_2S	C_3A	C_4AF
OPC	65.55	7.11	5.72	11.95
PLC	72.95	3.18	5.92	10.37

A Quikcrete premium play sand, which was sieved to meet the requirements for particle size distribution specified in ASTM C778 for graded sand (ASTM, 2017), was used as a fine aggregate in all mortar cubes. The particle size distribution of the sand is shown in Figure 3-1. Specific gravity of the sand was determined to be 2.62 according to ASTM C128, and its absorption capacity was calculated to be 2.5% (ASTM, 2015).

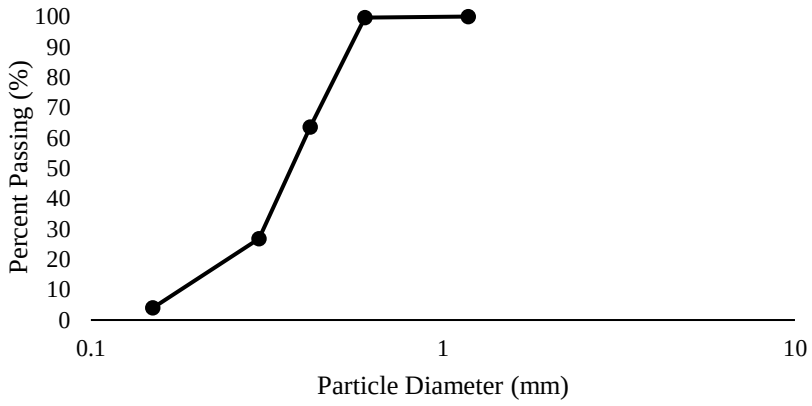

Figure 3-1: Sand particle size distribution.

The water used for all pretreatment soaking, mortar mixes, specific gravity testing, and pastes was deionized 18 kOhm water. Acids were used in diluted amounts for

pretreatment of agricultural materials before calcination. Acids used for pretreatments were obtained from Fisher Scientific and included hydrochloric acid (reagent grade), sulfuric acid (technical grade), and nitric acid (certified ACS plus). Woeber's brand distilled white vinegar (5% acidity) was also used to create an acetic acid solution. Sodium hydroxide was obtained from Acros (analysis grade), in the form of extra pure micropearls. Chemicals used for R^3 calorimetry testing included calcium hydroxide (certified powder), and potassium hydroxide (technical grade flakes) both from Fisher Chemical. Calcium Carbonate powder (99% extra pure) was obtained from Acros Organics. Quartz powder, finer than the number 325 mesh, was used as an inert filler. All X-ray diffraction (XRD) tests used an internal standard of zincite (ZnO). This zincite came from Alfa Aesar and has a 99.9% purity, metals basis, and is finer than the number 200 mesh. Sika ViscoCrete 2100 superplasticizer was employed for use in one mortar mix. MasterAir AE200 air entraining admixture was used for foam index testing.

Agricultural products were obtained from various locations across the American Midwest for testing. Table 3-3 summarizes the location of each product, and its abbreviation for the rest of the report. The locations are identified on a map in Figure 3-2. The specific gravity of each material's ash, tested according to the pycnometer method described in chapter 4.2.2, is shown in Table 3-4. For reference, the typical specific gravity of a fly ash ranges from 2.1-3.0 (FWHA, n.d.).

Table 3-3: Agricultural material sources and description.

Sample	Agricultural Material	Source	Biomass Description
H-F	Hemp	Bar-sur-Aube, France	hurd
H-KY	Hemp	Pembroke, Kentucky	hurd and fibers
H-KS	Hemp	Independence, Kansas	hurd and fibers
C-OH	Corn Stover	Wooster, Ohio	stalks, leaves, cobs
C-IN	Corn Stover	Chesterton, Indiana	Stalks, leaves, cobs
C-KS	Corn Stover	Cunningham, Kansas	stalks, leaves, cobs
W-OH	Wheat Straw	Xenia, Ohio	baled wheat
W-IN	Wheat Straw	Chesterton, Indiana	baled wheat
W-KS	Wheat Straw	Lehigh, Kansas	baled wheat

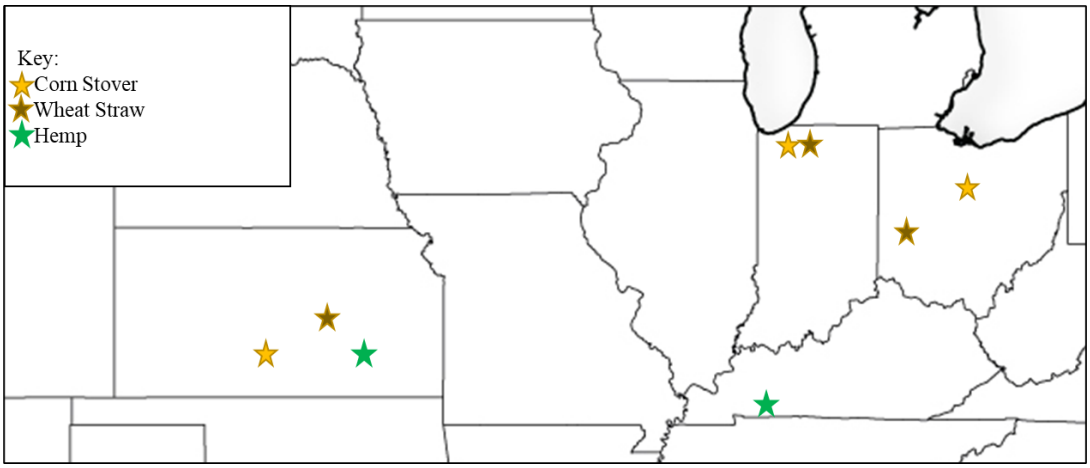

Figure 3-2: Map of agricultural material sources.

Table 3-4: Agricultural ash specific gravities.

Sample	Specific Gravity
Quartz	2.59
H-F	2.54
H-KY	2.86
H-KS	2.82
C-OH	2.60
C-IN	2.56
C-KS	2.69
W-OH	2.44
W-IN	2.51
W-KS	2.32
Lignin	1.25

After a preparation process including calcination to 500°C and a five-hour ball milling procedure, each ash was analyzed by x-ray diffraction (XRD) and x-ray fluorescence (XRF) to determine the mineral and elemental compositions of the ashes shown in Figure 3-3. These ashes were produced for use in further characterization and performance testing. Figure 3-4 shows XRD scans of each final ash, and the mineral phases present are quantified in Table 3-5. Table 3-6 provides oxide composition of each agricultural ash from XRF testing.

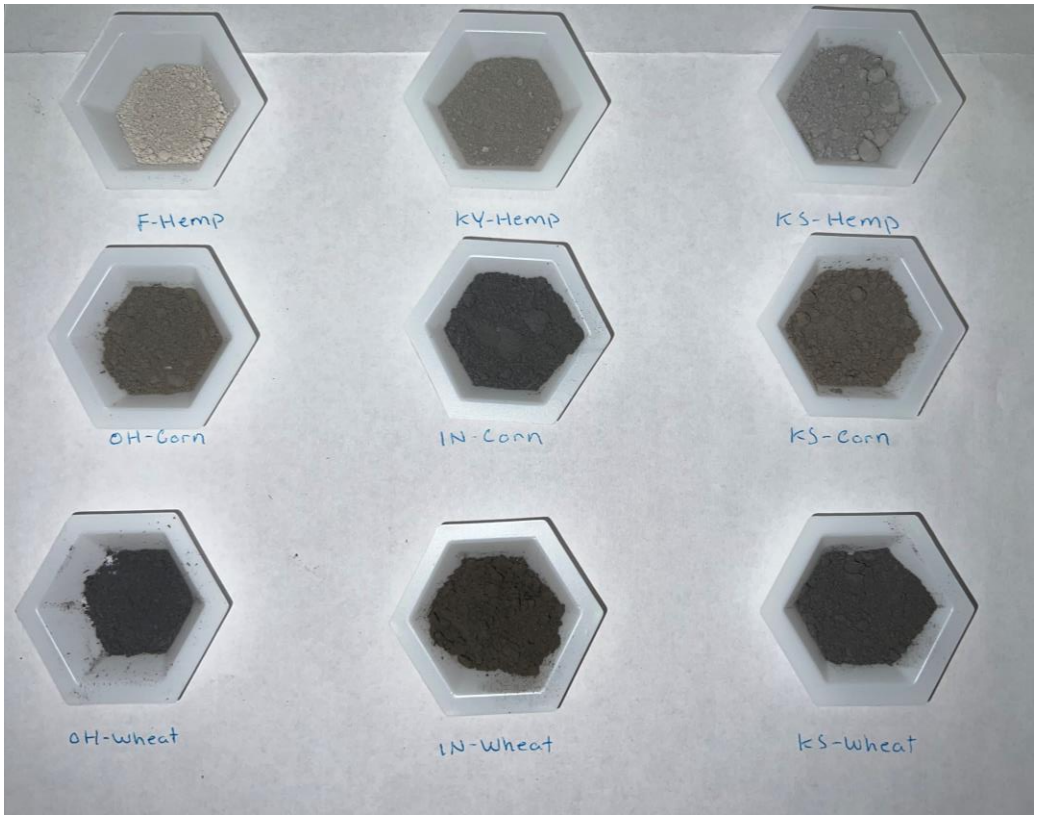

Figure 3-3: Agricultural ashes used for testing.

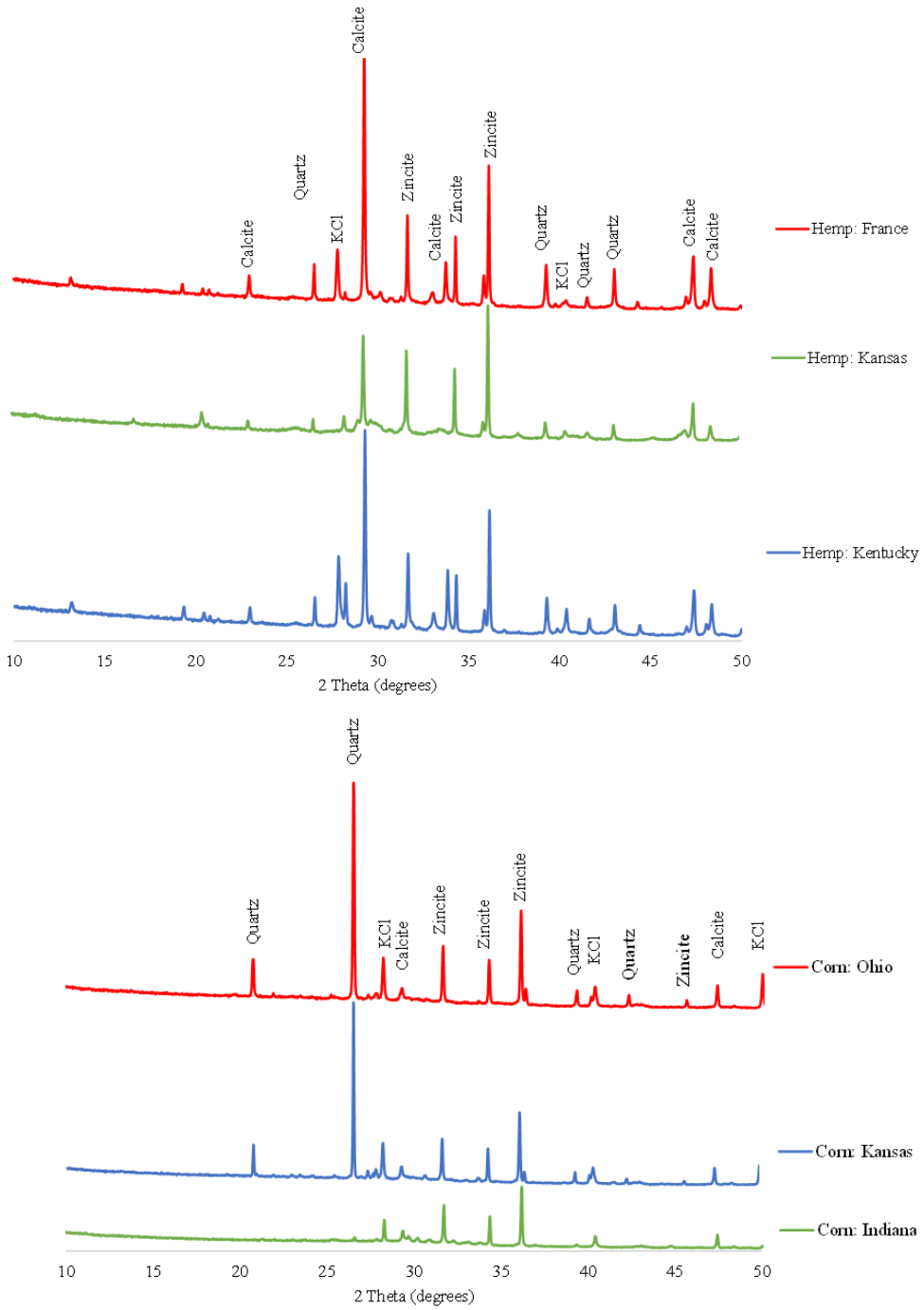

Continued

Figure 3-4: XRD scans of agricultural ashes, sorted by material type.

Figure 3-4 Continued

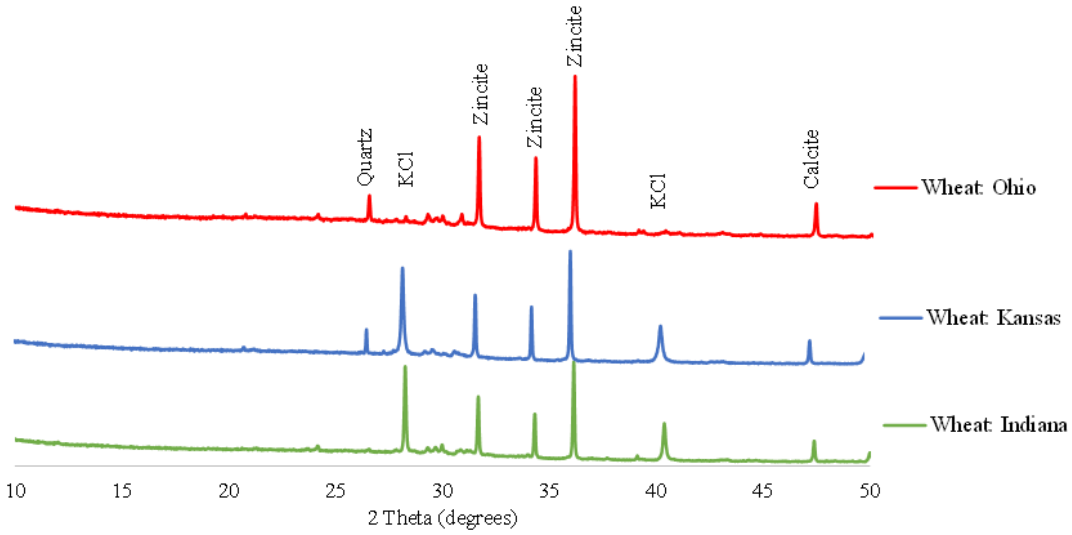

Table 3-5: XRD refinement results, given in percent.

Name	H-F	H-KY	H-KS	C-OH	C-IN	C-KS	W-OH	W-IN	W-KS
Amorphous	47.7	46.7	82.2	61.7	84.7	58.9	87.7	94.3	76.4
Calcite ($CaCO_3$)	36	31.4	15.4	4.3	5.4	4.7	2.5	2.5	2.6
Sylvite (KCl)	0.2	3.1	1.3	3.8	3.1	4.7	7.7	0.3	9.9
Quartz (SiO_2)	2	5.7	0.7	25.6	1	23.8	0	1.7	2.2
Portlandite ($Ca(OH)_2$)	0	0	0	0.2	0.6	0.5	0	0	0.1
Albite ($NaAlSi_3O_8$)	9	7.4	0.4	3.8	2.7	7	0	0	7.8
Sodium Phosphate (NaH_2PO_4)	5.1	5.7	0	0.7	2.6	0.4	0	0	0
Magnesium Phosphate Hydrate ($H_2Mg_3O_9P_2$)	0	0	0	0	0	0	2	1.2	1.1

Table 3-6: Final ash oxide content per XRF, given in percent.

	H-F	H-KY	H-KS	C-OH	C-IN	C-KS	W-OH	W-IN	W-KS
Al_2O_3	32.4	35.8	49.5	7.5	18.9	10.1	16.0	3.3	9.1
SiO_2	24.4	23.3	24.1	60.9	63.8	46.7	68.0	67.1	74.3
P_2O_5	5.3	7.6	0.0	0.0	5.8	0.0	5.7	0.0	0.9
SO_3	20.3	14.5	9.0	1.8	5.2	2.8	7.7	1.8	6.8
TiO_2	0.6	1.0	0.8	2.8	0.0	1.7	0.0	1.8	0.6
Cr_2O_3	0.8	0.8	0.9	0.4	0.4	0.3	0.3	0.3	0.3
MnO	1.0	3.9	1.3	1.6	0.6	0.4	0.5	2.4	0.2
Fe_2O_3	15.0	11.8	14.0	24.1	4.7	37.8	1.5	23.0	7.7
ZnO	0.4	0.8	0.3	0.7	0.5	0.1	0.2	0.3	0.1
CuO	0.0	0.5	0.0	0.3	0.1	0.1	0.1	0.1	0.0
LOI	33.3	32.7	14.1	9.2	11.8	6.4	15.5	1.9	8.6
$SiO_2 + Al_2O_3 + Fe_2O_3$	71.8	70.9	87.7	92.4	87.5	94.6	85.5	93.4	91.1

For evaluating the performance of agricultural materials against typical SCMs, a class F fly ash and a class C fly ash were chosen. Class C fly ashes are defined by ASTM C618-22 by having a calcium oxide (CaO) content above 18%, while class F fly ashes consist of less than 18% CaO (ASTM, 2022). The fly ash material, oxide analysis presented in Table 3-7, and the particle size distribution provided in Figure 3-4 were provided by Tyler Ley and Shinhyu Kang from Oklahoma State University. An industrial hydrolysis lignin, produced from agricultural residue feedstock was tested in small amounts. The fractionation process was supercritical water. This material was donated by National Renewable Energy Laboratory (NREL) in Golden, Colorado.

Chapter 4: Methods

4.1 Ash Preparation

4.1.1 Pretreatment

Thermochemical pretreatments were performed on some of the raw materials in order to remove hemicellulose or lignin from the materials, as well as other impurities. Practically, this is one of the costliest portions of material preparation. Chemical pretreatments were primarily tested with the French hemp material. Four acid pretreatments were tested: 0.1 M hydrochloric acid (HCl), 0.1 M sulfuric acid (H_2SO_4), 0.1 M Nitric acid (HNO_3), and acetic acid with 5% acidity. Each soak solution was prepared using DI water, and a 1.0-liter total volume. Each 1.0-liter soak contained 100 grams of agricultural material. The biomass was immersed for a length of 24 hours, at a temperature of 70 °C, maintained through use of a hot plate. After 24 hours, the leachate was collected and filtered through 0.11 μm filters for Inductively Coupled Plasma (ICP) testing. The remaining material was rinsed with DI water until the pH returned to neutral.

ICP testing quantified the elements that leached into the liquid from the material using an Agilent 5100 ICP-OES using prepurified Argon (99.998% purity). Calibration standards from Supelco of Al, Ca, Fe, K, Mg, and Na in 2% nitric acid were used. All samples were diluted in 2% nitric acid (v/v).

4.1.2 Ash Production

Calcination is imperative to removing impurities of organic material, reducing LOI, as well as producing a material that can be milled to a fine size. Two Thermo Fisher Scientific muffle furnaces were used. A smaller furnace with a 112 in^3 volume was used in conjunction with a larger oven with a volume of 1008 in^3. It was determined through thermogravimetric analysis that for these materials, the mass change after calcination at 500 °C is between 0.4% and 4.1%. At temperatures between 600 °C – 800 °C, silica and phosphates have been shown to begin crystalizing, which would negatively impact their performance in cementitious systems (Bonifacio & Archbold, 2022; H.C. Visvesvaraya, 1986; Ribeiro & Morelli, 2014). Final calcination was done at 500 °C for two and a half hours for all materials.

In order to process the large volumes of materials required for production of cementitious samples some materials were pre-calcined in a 30-gallon metal drum. All corn and wheat samples were burnt in part using this procedure. Temperature was monitored throughout processing using an Etekcity infrared thermometer capable of a maximum temperature of 610 °C. Loading of the drum filled nearly half of the available volume. Burning was completed for most materials in the first five minutes, but the materials were cooled completely for nearly one hour before transferring into smaller buckets. Due to the heat of initial ignition, recorded temperatures were around 550 °C - 600 °C for the first minute of burning. After that short time, temperatures remained below 500 °C and slowly cooled completely.

Figure 4-1: Open burning process

A Shimpo PTA-01 ball mill with ¼ - ½” ceramic grinding media in a 1-liter ceramic jar loaded with a consistent 30-gram mass was used to create a uniform particle size ash. The mill operates at a constant speed of 84 revolutions per minute. Each milling sequence lasted 5 hours.

4.2 Characterization

4.2.1 Particle Size Analysis

Particle size analysis of ashes were analyzed using dry-dispersion laser diffraction (Malvern Mastersizer MSS). One gram of dry powder was loaded into a 50 mL plastic graduated cylinder and was scanned using laser light scattering through an air medium in nearly ten seconds. The device was capable of measurements in the range of 0.01µm-3500µm using Mie and Fraunhofer scattering analysis. The detector was in a log-spaced array arrangement with an angular range of 0.015-144 degrees.

4.2.2 Specific Gravity

The specific gravity of the final ashes was measured using a pycnometer method. A 100-milliliter pycnometer was first weighed while filled to the line with DI water. Most of the water was then removed, and the pycnometer was loaded with 50-gram samples and mechanically agitated for a 20-minute period to remove air bubbles from the sample before refilling the pycnometer to the line and recording the final weight. Specific gravity was calculated using the following equation:

$$Gs = \frac{dry\ material\ weight}{dry\ material\ weight + water\ filled\ pycnometer\ weight - final\ pycnometer\ weight}$$

4.2.3 Thermogravimetric Analysis

Thermogravimetric analysis was used to determine appropriate calcination temperatures for organic materials, and to assess major changes in structural changes through thermal degradation from pretreatments. The thermal decomposition of all samples was monitored from 25 to 1000 °C, heating at 10 °C/minute using alumina DSC/TG pans in a Mettler-Toledo DSC/TGA instrument. For organic samples, a testing atmosphere of air was used with sample sizes between 5 mg and 10 mg. A flow rate of 80 ml/min was used to prevent damage to the temperature sensors with organic matter combustion.

For cementitious systems, thermogravimetric analysis was also used to estimate calcium hydroxide (CH) consumption over time. Mass loss between 400 °C and 500 °C is

known to be associated with calcium hydroxide dehydration (K. Scrivener et al., 2016). After mixing, cement pastes were stored in one ounce plastic cups for 24 hours after mixing in a 100% relative humidity environment. After 24 hours, the pastes were submerged in lime water and tested at 7, 28, 56, 90, and 135 days. At each testing point, a sample was removed from the lime water and surface dried. Then, using a pestle, it was hit until interior fragments of roughly 100 mg size broke off. It was important not to use edge pieces because these portions have higher $Ca(OH)_2$ content. For 15 minutes, the interior pieces were submerged in isopropanol to stop hydration. After this period, the sample was dried in an oven at 40 °C for 2 hours. When dry, the sample was ground into noticeably finer than sand powder form until approximately 100 mg was obtained and stored under vacuum until TGA testing took place. For cement paste TGA samples, an inert nitrogen atmosphere was used with 30 – 50 mg samples. The calculations for calcium hydroxide consumption involve basic stoichiometry, and equation 5.3 mentioned in the thermogravimetric analysis chapter of, "A Practical Guide to Microstructural Analysis of Cementitious Materials" (K. Scrivener et al., 2016).

$$Ca(OH)_{2,paste} = \frac{Ca(OH)_{2,measured}}{weight\ at\ 600^\circ\ C * (1 + \frac{W}{C})}$$

4.2.4 Foam Index Testing

The foam index test for cementitious systems was used to determine the air entraining admixture (AEA) absorption of SCMs (Tyler Ley et al., 2008). The AEA solution was diluted to 7.5%. A covered 4 fluid ounce circular plastic container with a

2.5-inch diameter was partially filled with 25 grams of water, 8 grams of PLC, and 2 grams of SCM. The test was conducted according to ASTM C1827-20 using manual agitation at 4 shakes per second (ASTM, 2020b). Drops of AEA were added after the 30 second initial agitation, and subsequent agitations lasted 10 seconds. This process was repeated until a stable foam layer was visible at the surface of the water. If the foam layer was visible, that volume of AEA was recorded as the foam index.

4.2.5 Quantitative X-ray diffraction

The crystalline phases in agricultural samples were studied using X-ray diffraction scans performed using a BRUKER D8 XRD device in flat plate reflection mode using a copper x-ray source producing CuKα radiation. The scans ranged from 5 to 70° 2θ with a 0.2° 2θ step size and a 2 second step time. Prior to scanning, specimens were ground to pass a number 325 sieve and mixed with a 10% zincite (ZnO) internal standard. Powders were backloaded into the XRD sample holder to prevent preferential orientation errors and were grazed with a razor blade to ensure a flat scan surface (Bish & Reynolds, 1989). QXRD analyses were conducted using Profex Open Source XRD (Profex) and Rietveld Refinement software(Bish & Howard, 1988; Doebelin & Kleeberg, 2015). Profex was used to identify phase contents of ash samples including amorphous contents, which are expected to be high in organic samples.

4.2.6 X-ray fluorescence

X-ray fluorescence was performed on all agricultural samples to provide oxide data using a Bruker CTX portable countertop XRF analyzer. Its excitation source is a Rh target x-ray tube with a 4-watt max output. This unit is designed to be used in the field for geochemical exploration, limestone detection, and heavy metal detection in soils and organic material. This device is capable of detecting elements from magnesium to uranium, and is calibrated internally before each test. Each 3-gram sample was tested three times and averaged.

4.2.7 Scanning Electron Microscopy

Imaging of agricultural materials was performed on a Thermo Scientific Apreo FEG SEM device using a traditional Everhart-Thornley Detector (ETD) for surface imaging of the ashes. Because the ashes were nonconductive, each ash was gold sputtered on a pedestal. For imaging, a voltage of 5.00 kV and current of 0.20 nA were used.

4.3 Performance Testing

Mixtures for testing are shown in Table 4-1. All mixtures utilize a water to cementitious materials ratio of 0.5 due to the absorption of the SCMs. Agricultural ash is included in cementitious material weight. Pastes for isothermal and R^3 calorimetry were mixed with a Hamilton Beach hand mixer at low speed for 30 seconds and high speed for 90 seconds before quick placement in plastic vials in the calorimeter within 3 minutes.

All mortar was prepared according to ASTM C109 using a five-quart Hobart mixer (ASTM, 2020a).

Table 4-1: Mixture parameters.

Materials	**w/cm**	**Tests**
PLC	0.5	Isothermal calorimetry, compressive strengths, bulk electrical resistivity, mortar flow, calcium hydroxide consumption.
PLC, 10% SCM by volume		
PLC, 20% SCM by volume		
Agricultural Ash only	N/A	XRD, XRF, SEM, LOI, TGA, specific gravity, particle size

4.3.1 Compressive Strength of Mortar Cubes

Immediately after mixing, samples were compacted into 2” cube molds to cure for 24 hours in 100% relative humidity, then following demolding, were placed in a sealed limewater container at 23±2°C for 90 days. Compressive strength was tested using three cubes each at 1, 3, 7, 28, 56, and 90 days after casting using a 250-kip capacity

compression machine operated at 200 pounds/second (Instron, Forney). The Forney compression machine was set to a 75 psi/second ramp rate and to a 75% break percentage.

4.3.2 Flow of Mortar

Flow is the defined as the increase in base diameter of a mortar after a series of 25 drops of the flow table. Mortar for flow testing was prepared using ASTM C109, and flow was evaluated using ASTM C1437 (ASTM, 2013). The flow table and measuring device used meets ASTM C230-21 requirements.

4.3.3 Bulk Electrical Resistivity of Mortar Cubes

Bulk electrical resistivity of mortar cubes were measured in accordance with ASTM C1876 with the goal of relating electrical resistance to specimen porosity changes over time (ASTM, 2012) (Christensen et al., 1994). A Proceq Resipod resistivity meter with bulk resistivity accessories measuring resistance between two circular parallel metal plates with moist sponges on the surfaces of contact was used. For all measurements, three cubes were dried to a saturated surface dry state. A constant weight was applied to the top plate in the form of a concrete cylinder, and the measurement was taken within 10 seconds of the reading stabilizing. Four measurements were taken per cube, per break.

4.3.4 Isothermal Calorimetry

Isothermal calorimetry was used to study the kinetics of the agricultural residue ash in cementitious systems. Isothermal calorimetry indicates how the ashes may affect set time and microstructural development of the cementitious system by tracking the heat production rate in a small sample using heat flow sensors in a thermoregulated environment. An eight-channel isothermal TAM AIR (TAM AIR) instrument was used at a temperature of 25°C. Experimental procedure mirrored ASTM C1679 using 25-gram pastes (ASTM, 2014).

4.3.5 R^3 Calorimetry

A wide range of SCMs can be tested using the R^3 method (Snellings et al., 2019a). This method is based on testing by RILEM TC 267 RTM. Using the TAM AIR calorimeter, data was measured at 40 °C for 14 days. The mixture proportions are shown in Table 4-1 and are in accordance with proportioning guidelines in ASTM C1897-20 (ASTM, 2020c).

Table 4-2: R^3 mixture design.

	SCM	$Ca(OH)_2$	$CaCO_3$	Potassium Solution
Mass (grams)	5.00	15.00	2.50	27.00

Chapter 5: Results

5.1 Effect of preparation procedure

This section describes the process used to develop an ash for testing. Although many preparation methods were considered, the final ash produced was selected based on a balance of ideal chemistry, predicted performance from early trials, energy cost, and time required for production.

5.1.1 Pretreatments

Previous literature suggests that soak length and solution molarity are significant factors in pretreatment testing (Ataie et al., 2013; Kuglarz et al., 2016). In this study, soaking time, acid type, and acid strength were investigated. The XRD scan presented in Figure 5-1 shows a reduction in the height of the amorphous hump between 5 and 30 degrees, which could suggest that longer soak times in pretreatment in conjunction with a longer calcination are effective at removing amorphous content and creating accessibility to crystalline phases in the material.

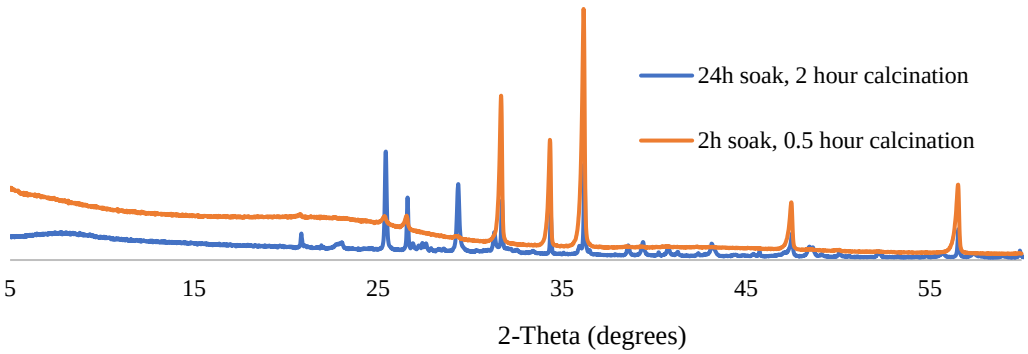

Figure 5-1: XRD scans on H-F material treated with a 0.1M sulfuric acid pretreatment and variable soak time.

Further experimentation was done with various solutions at a constant 24-hour soak time and molarity. The thermal decomposition curves for ashes calcined to 500 °C for 2.5 hours are shown in Figure 5-2 show that pretreatment solutions have an effect on thermal stability at temperatures over 500 °C. Thermal mass loss of an SCM can be used to determine total volatile material available in a sample, and is often correlated to overall carbon content. Changes in mass loss relative to temperature may indicate the presence of different plant components (primarily cellulose, hemicellulose and lignin components) (Guo et al., 2020; Yang et al., 2007b). In this study, untreated H-F has an LOI of 33%. In each case, a 24-hour pretreatment reduced LOI, for example, the 0.1M sulfuric acid-treated H-F has an LOI of 10.1%. Pretreatment testing is known to significantly alter the crystalline structure of the materials, including changing the surface area of the particle in

order to remove carbon in the form of lignin, hemicellulose, and cellulose (Ataie et al., 2013).

To assess structural changes caused by pretreatment, XRD spectra of ashes with and without pretreatments are compared in Figure 5-3. QRXD Rietveld refinement results of the XRD spectrums are presented in Table 5-1. All acid treatments increased the amount of silica in the samples. The NaOH treatment decreased the amount of quartz (an unreactive mineral) and increased the amount of amorphous material present in the ash by 16.4%.

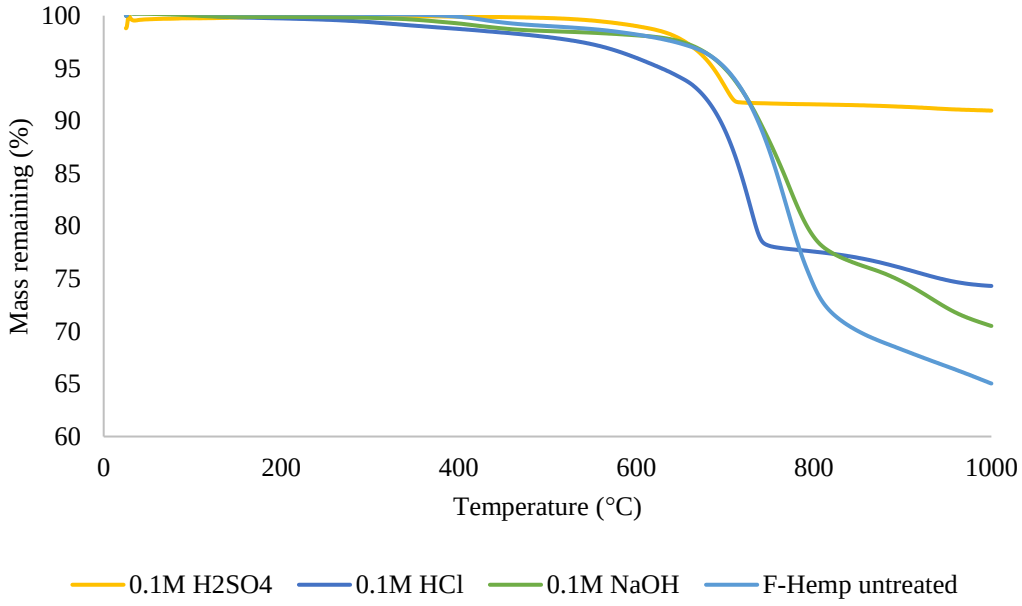

Figure 5-2: Thermal decomposition curves for pretreated H-F ashes. Ashes were calcined to 500°C for 2.5 hours.

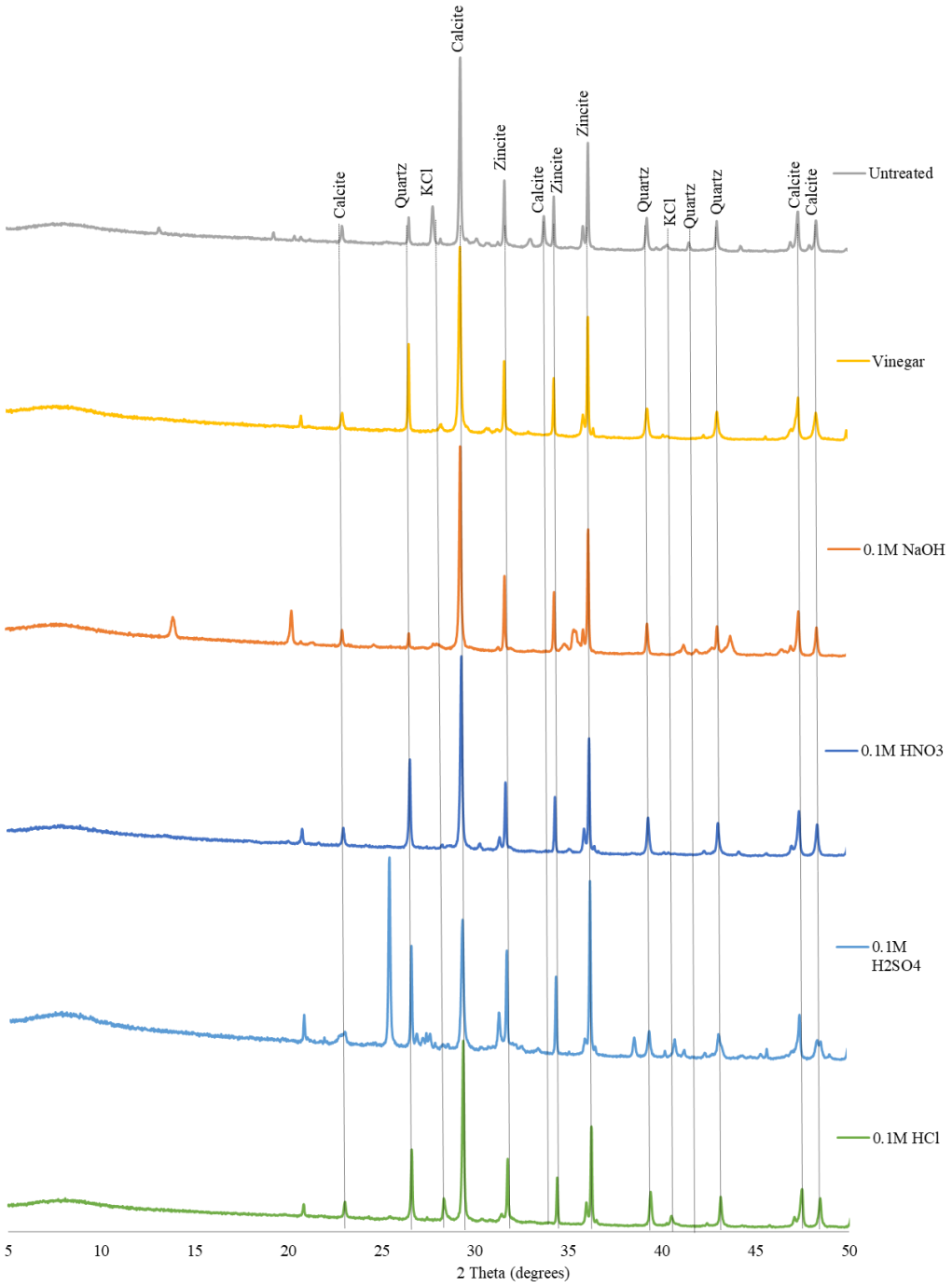

Figure 5-3: XRD spectra of pretreated H-F ashes. Pretreatments were 24 hours in length at 70 °C, calcined to 500 °C for 2.5 hours.

Table 5-1: Phase quantities from XRD refinement, H-F material, expressed in percent.

	Amorphous	Calcite	Potassium Chloride	Quartz	Albite	Sodium Phosphate
		$CaCO_3$	KCl	SiO_2	$NaAlSi_3O_8$	NaH_2PO_4
Untreated	47.7	36	0.15	2.04	9.02	5.08
Vinegar	44.1	42.26	0.5	5.9	3.51	3.73
0.1M H_2SO_4	59.4	23.89	0.73	6.92	1.49	6.9
0.1M HNO_3	46.8	39.57	0.17	10.59	2.12	0.73
0.1M HCl	42.5	39.21	2.21	10.37	4.07	1.65
0.1M NaOH	64.1	27.57	0	1.33	6.31	0

To further investigate the impact of pretreatments on extraction of chemical species from the agricultural fibers, a larger selection of the agricultural materials were exposed to the pretreatment solutions, and the soak effluent was filtered and analyzed using inductively coupled plasma (ICP) spectroscopy. The results of ICP testing are displayed in Figures 5-4 through 5-6. The goal of pretreating the agricultural products was to remove potential contaminants including sugars, alkalis, and heavy metals, which can negatively affect the timing of early hydration reactions and/or long-term durability of the hardened binder matrix.

Unlike the 3 strong acids tested, vinegar's active ingredient (acetic acid) consists only of carbon, hydrogen, and oxygen. Soaking H-F in vinegar removed more aluminum and magnesium from the material than the strong acid treatments (Figure 5-5). The DI water soak is the simplest and cheapest treatment, but was the least effective at removing

potassium (Figure 5-4) and aluminum (Figure 5-5). Potassium can reduce the specific surface area of the biomass particle, making its removal beneficial to the cement system (Ataie & Riding, 2014a, 2014b). The strong acid treatments removed more potassium than the DI water treatment for all samples except W-OH. Sulfuric acid pretreatment is known to penetrate sulfate into the material, and degrade sugar products, potentially reducing the likelihood of set retardation (Larsson et al., 1999; Palmqvist & Hahn-Hägerdal, 2000). Additionally, if the sulfate were to stay in the material after ashing, it could enhance C_3S hydration and delay the C_3A reaction (Andrade Neto et al., 2021). Sulfuric acid treatment did not remove as much potassium as the other two strong acid treatments for wheat and corn samples (Figure 5-4), nor did it remove aluminum as effectively in 5/6 samples (Figure 5-5).

The nitric acid soak was the least effective acid at removing sodium (Figure 5-6). Calcium nitrate and sodium nitrate are known accelerators that could form from a nitric acid pretreatment (Aggoun et al., 2008; Suh et al., 2019), however, Mlonka-Mędrala et al. showed that the sodium in corn stover (Na_2O), and potentially in other organic materials, is insoluble and nonreactive (Mlonka-Mędrala et al., 2020). Low removal of sodium through use of nitric acid, compared to removal in other solutions could be evidence that sodium nitrate or sodium oxide are forming and remaining in the material.

The hydrochloric acid soak removed the most magnesium in 4 out of 6 samples (Figure 5-5), which could be an indication of soluble magnesium chloride formation. Hydrochloric acid is also generally less effective at dissolving alumina when compared to sulfuric and nitric acids (Teymouri & Shakouri, 2023). After dissociating, hydrochloric

acid could leave chlorides bound in the material, producing salts like sodium or potassium chloride, which could accelerate hydration or promote the dissolution of minerals (Cao et al., 2021). Potassium chloride (KCl), a known contaminant from fertilizer usage, was detected by QXRD in greater quantities (2.21%) after hydrochloric acid pretreatment compared to 0.15% KCl on a control sample (Table 5-1). The presence of potassium chloride has been reported to increase compressive strength at 28 and 90 days in OPC (Venkateswara et al., 2011).

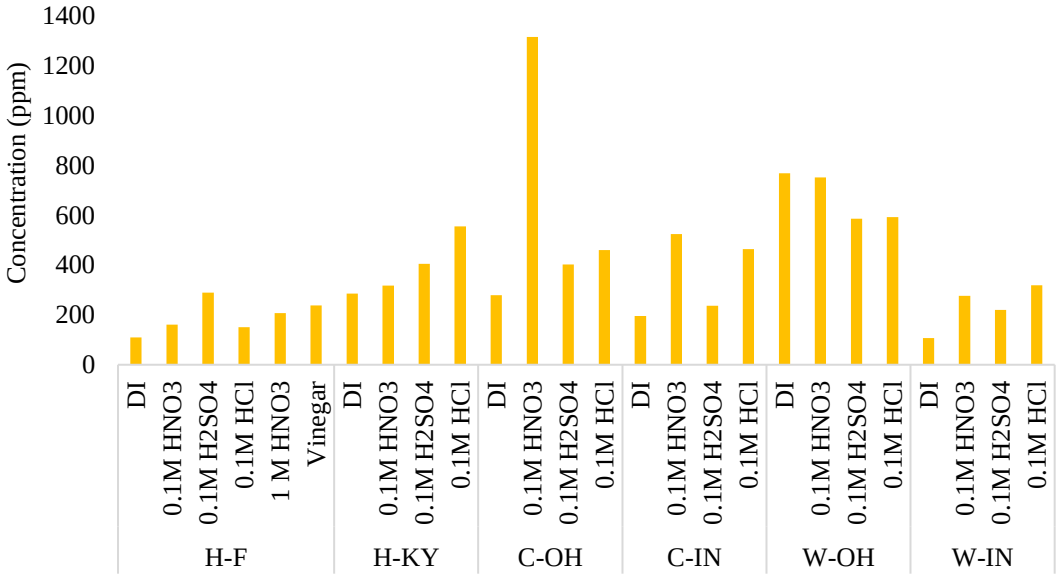

Figure 5-4: Removal of potassium due to pretreatment soak.

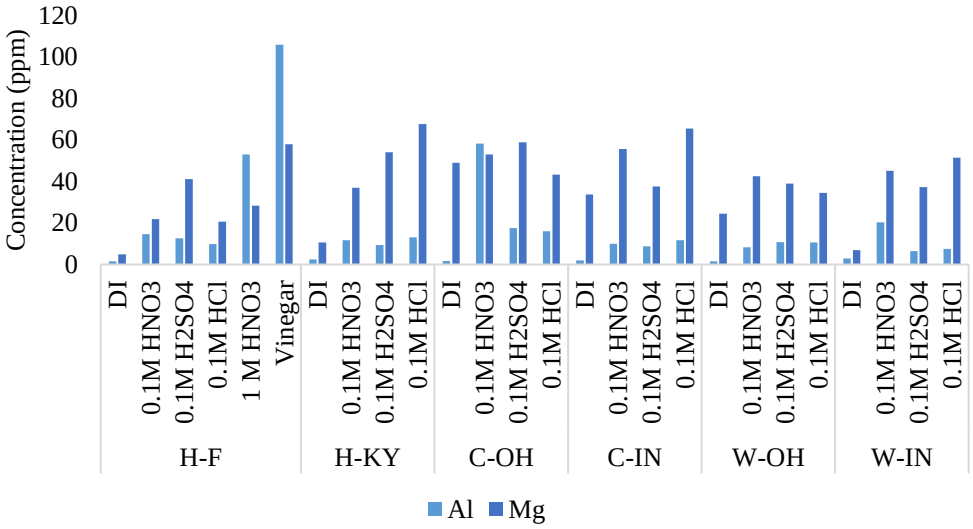

Figure 5-5: Removal of aluminum and magnesium due to pretreatment soak.

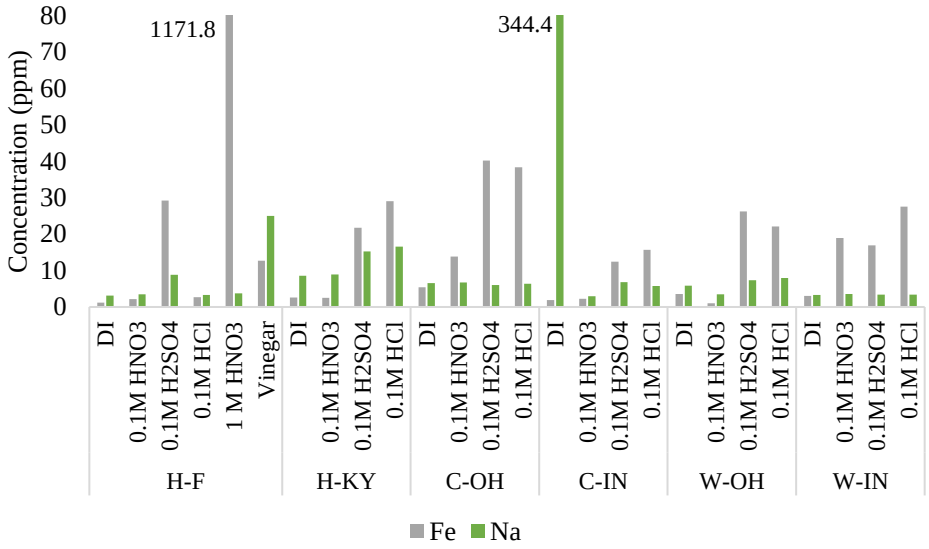

Figure 5-6: Removal of iron and sodium due to pretreatment soak.

5.1.2 Calcination

Two techniques were utilized for the production of the bioagricultural ashes – calcination in a muffle furnace and calcination in an open-burn drum. Calcination speed was found to depend partly on oven size and the layout of the material. A large oven with a thin layer of material can provide greater oxygen access to the material than a smaller oven with dense loading, resulting in faster and more even and complete burning. Based on the ovens available for this research, optimal times were established for burning. For the muffle furnace, 2.5 hours of burning brought the H-F ash to a stable mass, confirmed by TGA mass decomposition curves showing loss on ignition of only 0.7% ± 0.5% after calcination for 1 hour at 500 °C.

The temperature chosen for calcination was intentionally selected to facilitate the removal of hemicellulose and cellulose, which decompose at the temperature ranges labeled in Figure 5-7 (Yang et al., 2007a). A secondary consideration is to select a temperature at which mass loss has stabilized. However, Biricik et al. reported crystalline silica forming in wheat straw ash near 700 °C, so care must be taken to prevent crystallization (Biricik et al., 1999). A burning temperature of 500 °C was selected based on those criteria.

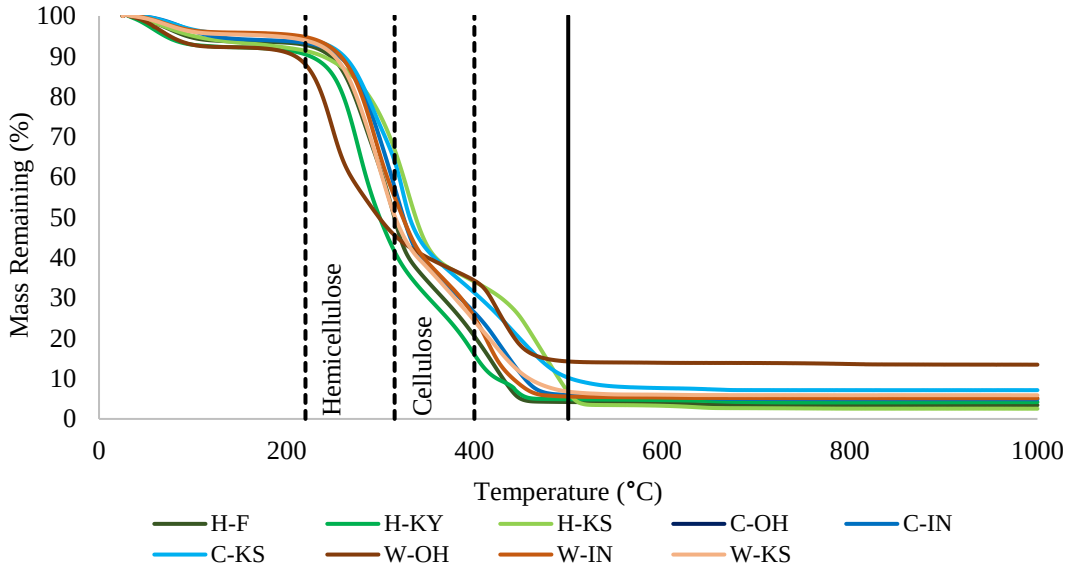

Figure 5-7: Thermal decomposition of untreated agricultural materials in air, using TGA.

Figure 5-8 shows the changes in crystallinity of the sample between a 0.5-hour calcination and 2.5 hour calcination at 500 °C. More distinct XRD peaks are visible in Figure 5-8 due to a longer calcination of the material. The flattened hump between 5 and 30 degrees could be evidence that a 2.5-hour calcination time at 500 °C removes a large amount of the residual amorphous carbon content of the material. Experimentation with 600 °C calcination of H-KY and H-F showed less than half a percent difference in in mass from materials calcined to 500 °C, and no formation of new compounds, further suggesting the sufficiency of use of a 500 °C calcination temperature (Biricik et al., 1999).

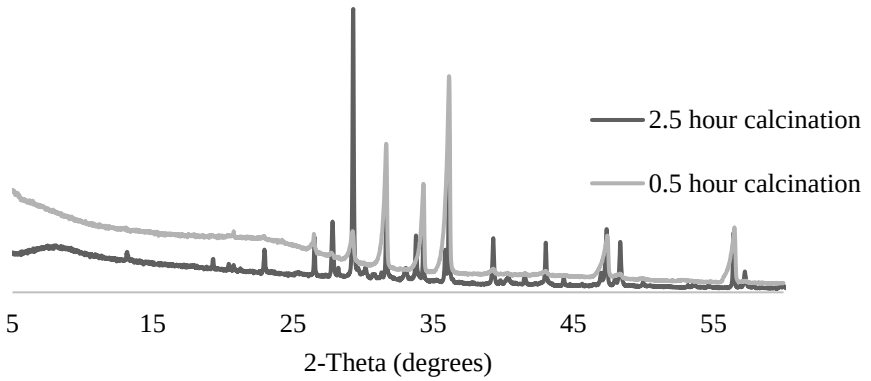

Figure 5-8: XRD scans of H-F ash, calcined at 500 °C, variable time.

In order to increase ash production capacity to enable production of ashes for mortar cubes, XRF, and calorimetry, corn and wheat materials were pre-calcined using an open burn procedure. Open burning was completed in a 30-gallon metal drum loaded to nearly half of its capacity. Initial ignition temperatures were detected around 550 °C -600 °C for the first minute of burning, but the flame was smoldering and under 400 °C within 2-3 minutes. Characterization tests were performed to ensure that the open burn technique did not burn the material above the original 500 °C calcination target temperature, and did not significantly alter the crystal structure of the material by increasing quantities of crystalline silica. X-ray diffraction and thermogravimetric analysis confirmed that open burnt material did not exhibit any trace of cristobalite, nor did it introduce any new crystal peaks relative to muffle furnace-processed samples (Figure 5-9). Thermogravimetric analysis confirmed that the material lost nearly 30% of its mass at 500 °C, indicating that further muffle furnace burning would be required to

create a uniform ash, with shorter (one hour) residence time and increased loading potential, due to most of the structural mass being decomposed in open burning.

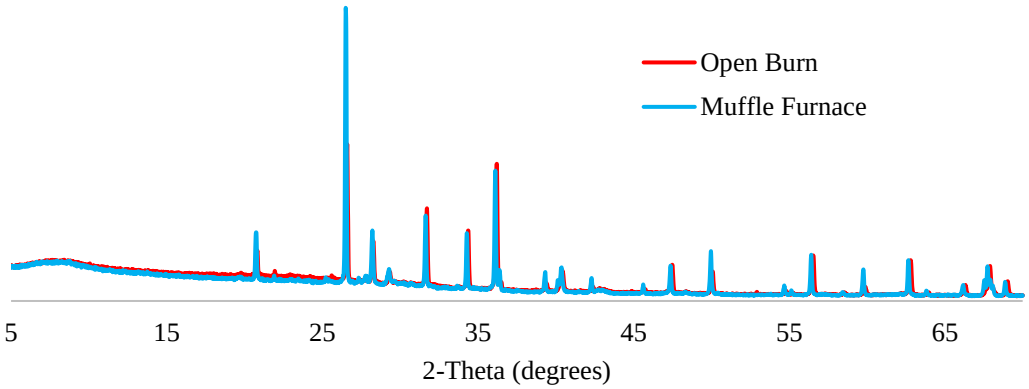

Figure 5-9: XRD scans of C-OH ash, muffle furnace vs. open burn.

5.1.3 Milling

Milling efficiency was found to depend mostly on length of milling time and sample loading size. For this research, sample loading size was controlled by sample mass. Using a consistent sample mass of 30 grams, milling time was investigated with the French hemp (H-F) material and compared to the particle size of ordinary portland cement. It was determined that a 5-hour milling time would be sufficient to lower the median particle diameter to 5.54 micrometers, comparable to OPC's median diameter of 9.35 micrometers, a reduction of 40% from post-calcination particle size. The D_{90} particle diameter was reduced from 84.87 micrometers at one hour to 24.48 micrometers at five hours of milling, 25% finer than the D_{90} particle diameter of OPC (32.43 micrometers).

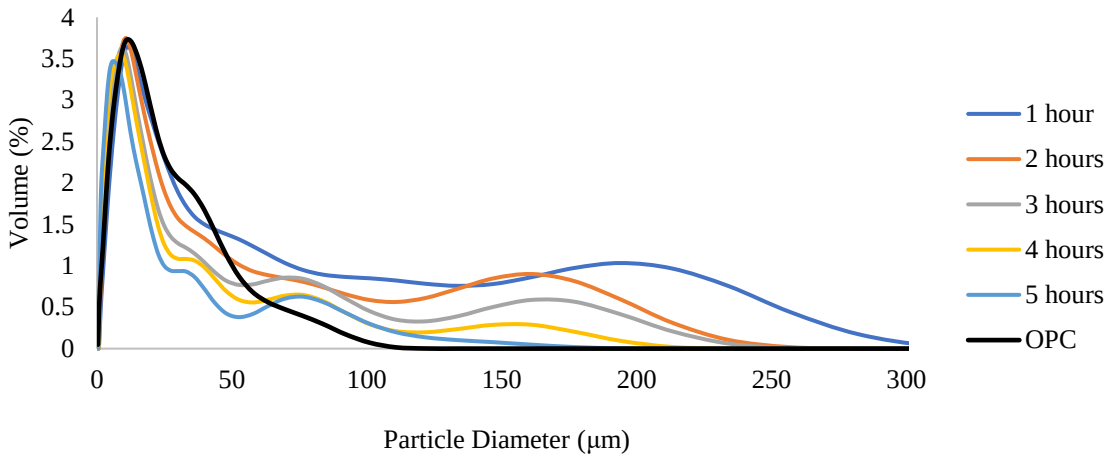

Figure 5-10: Particle size analysis for H-F ash, for various ball milling times.

Two hemp varieties (H-F and H-KY) were tested using a preliminary procedure for calcination and pretreatment. Untreated French hemp material calcined for 30 minutes is shown in Figure 5-10. Using the same calcination time, various calcination temperatures (indicated by 315, 500, and 600 °C) and 2-hour pretreatments (indicated by R = Raw, HW = Hot Water, H_2SO_4 = 1M Sulfuric Acid, NaOH = 0.1M Sodium Hydroxide) were tested and their particle size distributions are shown in Figure 5-11. The five-hour milling procedure consistency was assessed using this plot, with most samples milled sufficiently after five hours.

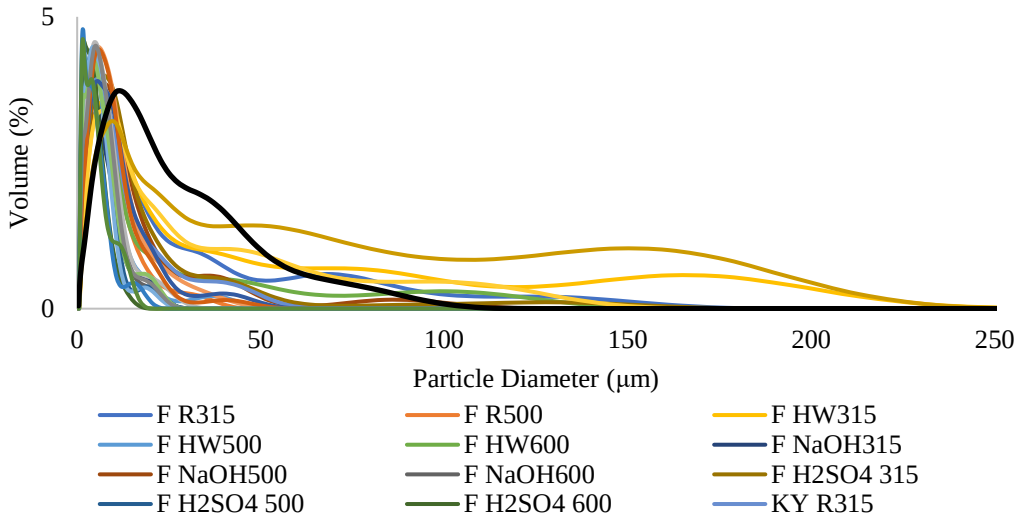

Figure 5-11: Particle size analysis for H-F and H-KY ash, for various pretreatments.

The final ashes of all agricultural materials used for testing were subject to the same five hour milling procedure. With consistent loading and a five-hour mill time, ash could be processed at reasonable speed for testing. The particle size results are consistent with PLC for particle diameters smaller than the median diameter. Two-thirds of the final ashes had a finer median diameter than the portland limestone cement, but an increased number of particles with diameters between 100 and 250 micrometers were present. Caking in the mill or the difference in bulk density of the materials during loading could be responsible for this inconsistency.

Table 5-2: Final ash particle size distribution data.

Final Ash Particle Distribution Sizes										
	PLC	**H-F**	**H-KY**	**H-KS**	**C-OH**	**C-IN**	**C-KS**	**W-OH**	**W-IN**	**W-KS**
D10	1.49	1.35	0.68	1.13	1.24	1.46	0.84	1.27	1.76	1.26
D25	4.41	3.73	1.63	3.39	3.58	4.23	3.37	3.68	4.85	3.39
D50 (median)	10.79	9.59	9.77	9.80	9.12	10.06	11.17	8.94	11.51	8.63
D75	21.36	18.73	45.89	24.91	18.55	22.97	38.63	18.45	27.42	17.86
D90	34.61	43.85	119.13	69.54	48.88	66.69	100.60	50.22	76.22	44.70

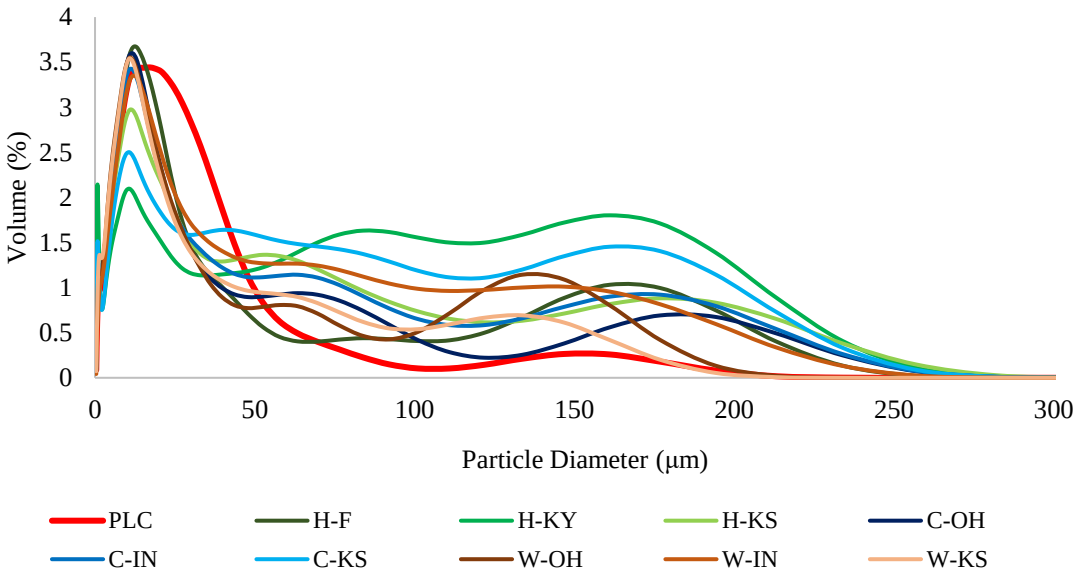

Figure 5-12: Particle size analysis for final agricultural ashes.

In summary, final processing procedures were as follows: unpretreated agricultural materials were manually broken into pieces shorter than 12 inches if

necessary for burning, calcined at 500°C for two and a half hours, then ball milled for 5 hours and stored in closed containers to prevent contamination.

5.2 Performance

5.2.1 Effect of biomass ashes on cement heat evolution

Each agricultural material was substituted in a cement paste at 10% and 20% by volume. Figure 5-13 shows the heat evolution curves of the hemp samples. In all samples, the reaction reached a maximum value of heat evolution sooner than control samples, and each agricultural ash paste produced a higher value of maximum heat evolution than control. The accelerated reaction and higher max heat release value indicate that the cement reaction is occurring faster with overall increased numbers of reaction, possibly due to increased nucleation sites associated with finer particle sizes (K. L. Scrivener et al., 2015). Increased hemp dosage further increased the reaction rate and total rate of heat release. Hemp substitution, on average, decreased the time to maximum heat evolution by 1.32 hours at 10% substitution, and by 2.93 hours at 20% substitution.

Past research has shown corn stover ash to cause retardation in cementitious systems due to its high levels of phosphorous (Shakouri et al., 2020). Figure 5-14 shows the results of heat evolution tracked for corn stover samples in this study, normalized per gram of cementitious material. All corn stover samples delayed the time to maximum heat evolution except C-KS, which behaved more like the hemp samples, with an accelerated reaction. On average, the corn stover samples took longer to reach the

maximum value of heat evolution than PLC. At 10% substitution, the average delay was 1.09 hours, and doubling the amount of corn stover caused a delay of 1.56 hours, on average.

Wheat straw ashes showed the largest amount of hydration retardation of the three types of agricultural products tested in this study. At 10% substitution, the average time to maximum heat evolution was 5.59 hours later than the control sample. At 20%, the delay was 6.95 hours (Figure 5-15), indicating that increasing wheat straw ash amount leads to increasing retardation (Figure 5-15). Heat release from cementitious samples using the industrial lignin material are shown in Figure 5-16. Increasing lignin addition reduced total heat evolution and the maximum rate of heat evolution.

Among the agricultural ash samples the second peak (C_3A hydration peak) typically observed in OPC cements, is not visible, appearing only in the control and quartz samples. This peak is referred to as the "sulfate depletion peak." In the cases where the sulfate depletion peak is not visible, the aluminate peak likely occurred in conjunction with or before the tricalcium silicate (C_3S) peak due to the surface area addition of the supplementary cementitious material or interactions with system sulfate. Additionally, a faster rate of C-S-H precipitation during the early stages of hydration will deplete the sulfate from the cement through absorption as well. Changes in the sulfate depletion peak in the agricultural samples suggests they may be subject to similar sulfate imbalance issues as other pozzolans when used in high substitution rates.

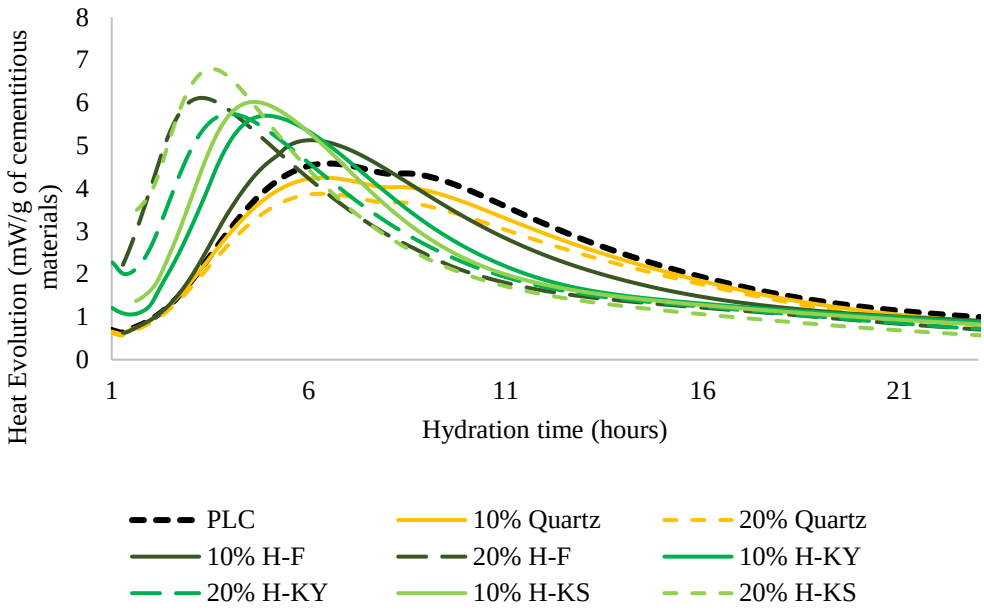

Figure 5-13: Heat evolution for hemp samples.

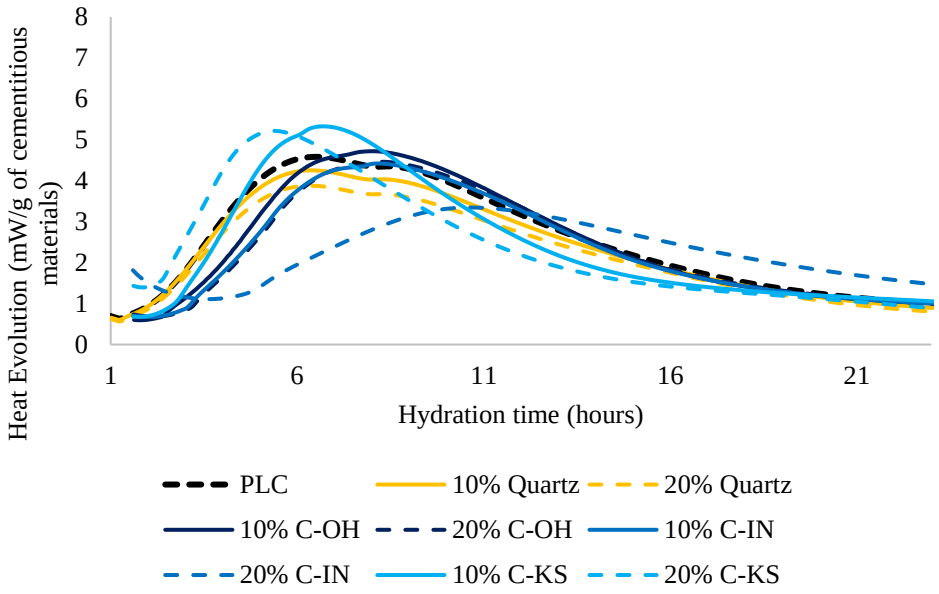

Figure 5-14: Heat evolution for corn stover samples.

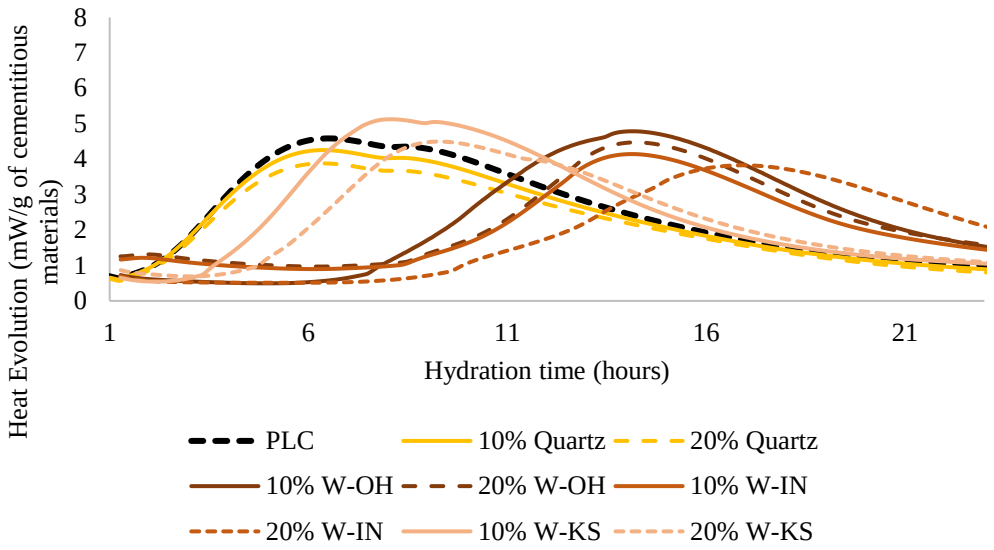

Figure 5-15: Heat evolution for wheat straw samples.

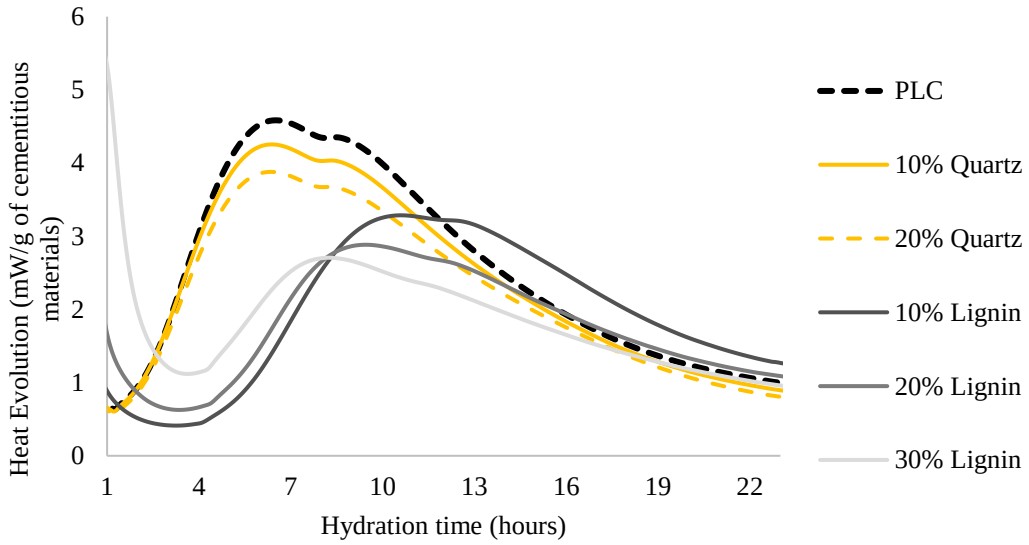

Figure 5-16: Heat evolution for lignin samples.

Cumulative heat evolved at 160 hours is shown in Figure 5-17 for all paste samples, compared to the PLC control. Hemp ash specimens evolved significantly less heat than control, 85.4% and 82.6% of control for 10% and 20% substitution respectfully suggesting that overall, less cement reaction has occurred. Corn ash specimens on average evolved the most cumulative heat at 92.3% and 91.7% of control for respective substitution percentages. Wheat ash specimens evolved 89.8% and 87.8% of PLC's heat cumulative heat evolution at 10% and 20% substitution respectively. In all samples except C-IN, adding more agricultural ash decreased total heat evolved.

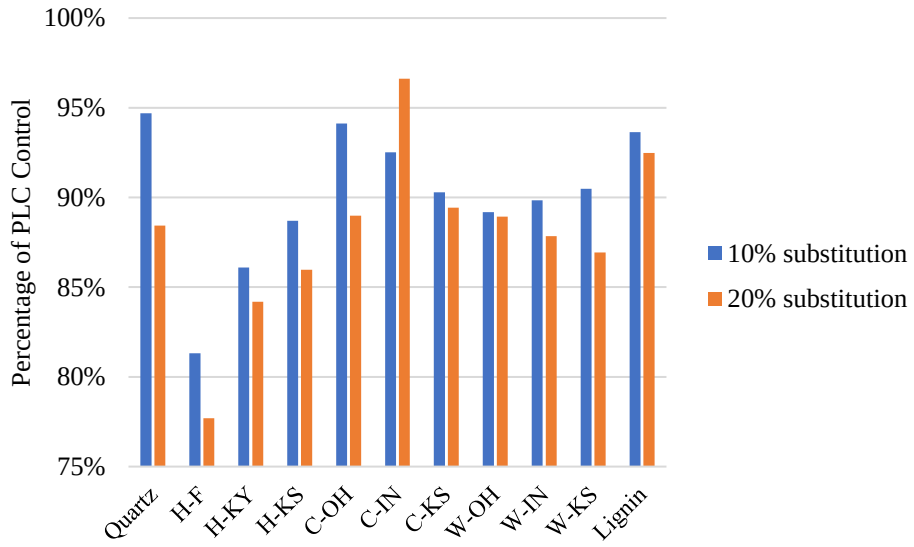

Figure 5-17: Relative cumulative heat evolved from cementitious paste samples at 160 hours.

Quartz powder was used as an inert filler to distinguish agricultural ash performance from filler effect behavior. Due to a phenomenon related to particle size known as the filler effect, increases in heat release during isothermal calorimetry may result from extra nucleation sites that can increase or quicken the cement reactions,

making differentiation of reactions caused by chemical interactions with cement and those resulting from surface nucleation, difficult. However, a new approach to calorimetry, the R^3 method has been shown to provide a strong indication of the hydraulic or pozzolanic reactivity of pozzolans, and some correlation to strength gain (Snellings et al., 2019b). This method separates the pozzolanic reaction from the cement reaction through the use of calcium carbonate, calcium hydroxide, and a potassium solution, mimicking pore solution.

Reactivity, tracked using the heat of hydration of agricultural samples in the R^3 test (ASTM C1897, 2020) was tracked for a 14 day period using a temperature of 40 °C and shown in Figure 5-18. Two hemp varieties showed reactivity similar to that of quartz, while H-F began increasing reactivity faster after four days and ended up with almost three times more heat release than the other two hemp samples at fourteen days. The corn samples showed greater variability, with C-OH being less reactive than quartz at 14 days and C-IN showing over three times more heat evolution at 14 days. Wheat ash samples had the highest cumulative heat release on average, with W-IN evolving the most heat with 470 J/g SCM at 14 days.

The performance of the agricultural ashes was also compared to the class C and class F fly ash shown in Figure 5-18. The only sample to outperform the fly ashes in heat evolution was W-IN.

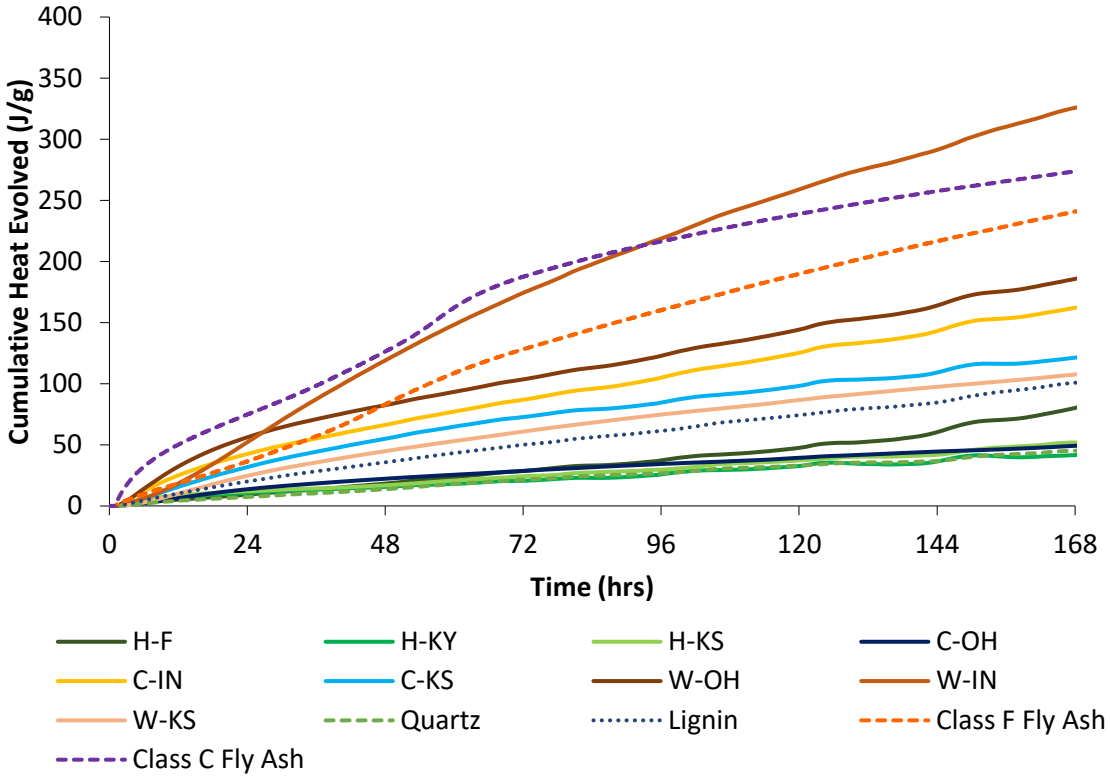

Figure 5-18: Heat of hydration using R^3 calorimetry.

5.2.2 Pozzolanic Reaction

Calcium hydroxide consumption can be used to assess the extent of the pozzolanic reaction. Calcium hydroxide forms through the primary cement hydration reaction. Calcium hydroxide contents lower than that of the quartz inert filler sample indicate reduction through reaction of the included pozzolan. Over time, if the calcium hydroxide amount decreases, this can indicate additional consumption through reaction with silica or alumina to produce calcium silicate hydrate (C-S-H) or calcium aluminum

silicate hydrate (C-A-S-H) (Mindess & Young, 1981). Initial testing over 135 days indicated that calcium hydroxide consumption tracked for a H-F and H-KY paste showed similar results. Calcium hydroxide content is reported for 10% volumetric substitution in Figures 5-19 through 5-21, and for 20% volumetric substitution in Figures 5-22 through 5-24. All samples show decreased calcium hydroxide content relative to that of the quartz sample, with many samples reaching their maximum value by 56 days, indicating that consumption of CH now exceeds production through continuing cement hydration. All hemp samples except H-F 20% show this trend. In all 20% substitution corn and wheat pastes, W-OH 20% is the only one to not show this trend. Through 90 days, the control sample is still increasing in CH content, while C-OH pastes are each decreasing and contain 3.6% and 5.2% less CH respectively.

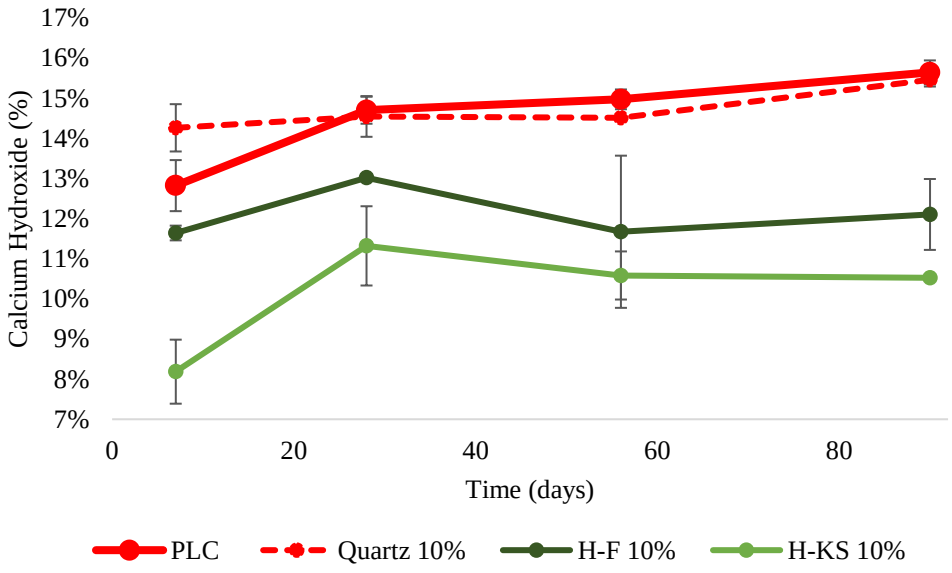

Figure 5-19: Calcium hydroxide content, Hemp, 10% substitution.

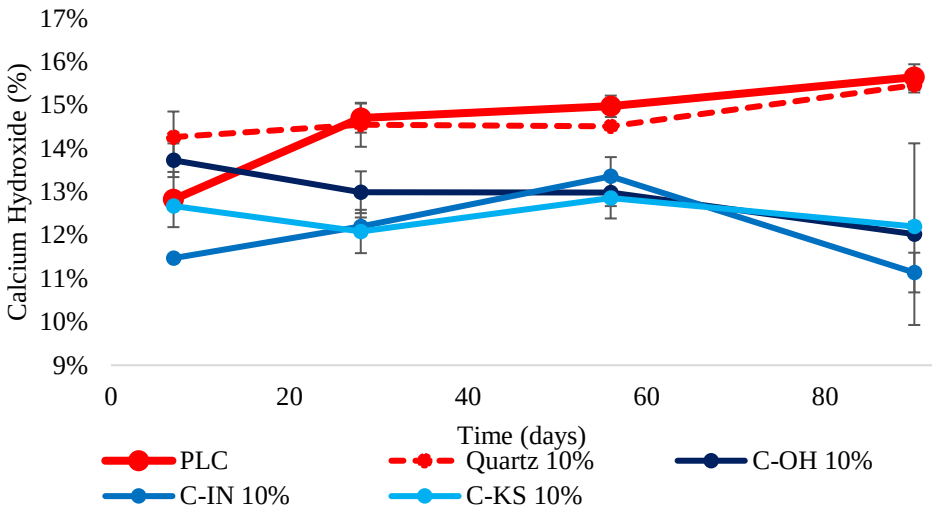

Figure 5-20: Calcium hydroxide content, Corn, 10% substitution.

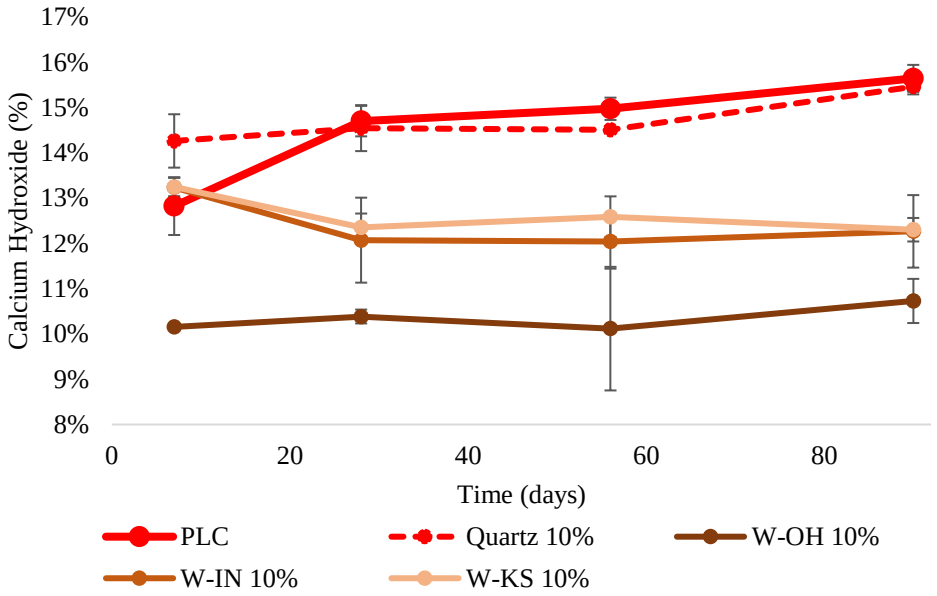

Figure 5-21: Calcium hydroxide content, Wheat, 10% substitution.

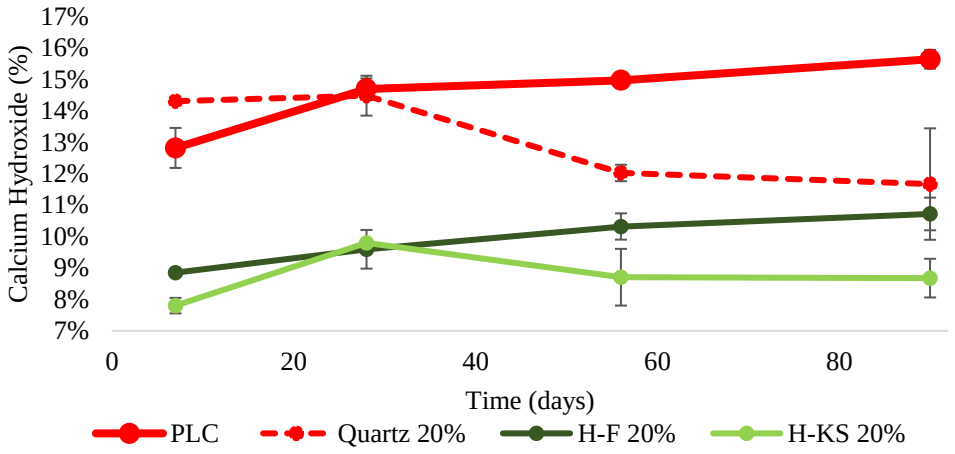

Figure 5-22: Calcium hydroxide content, Hemp, 20% substitution.

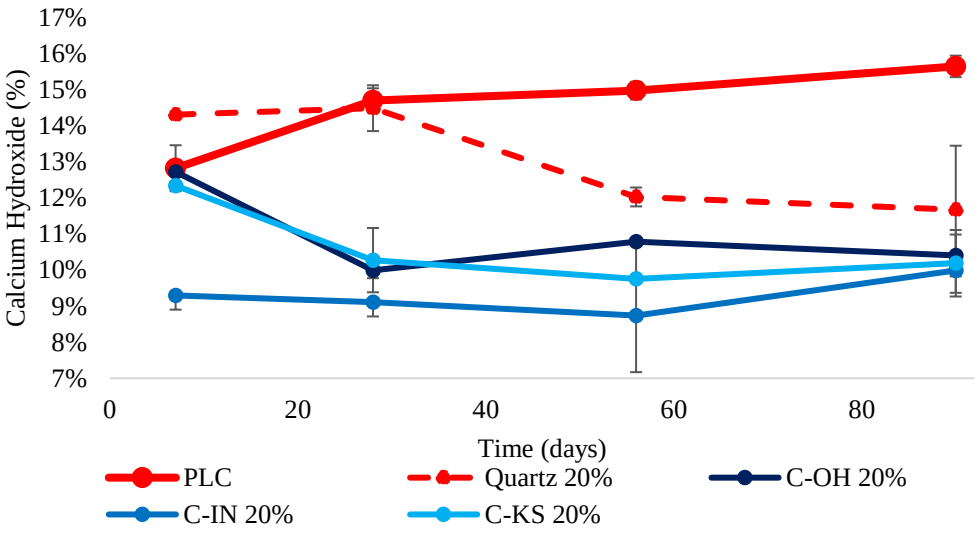

Figure 5-23: Calcium hydroxide content, Corn, 20% substitution.

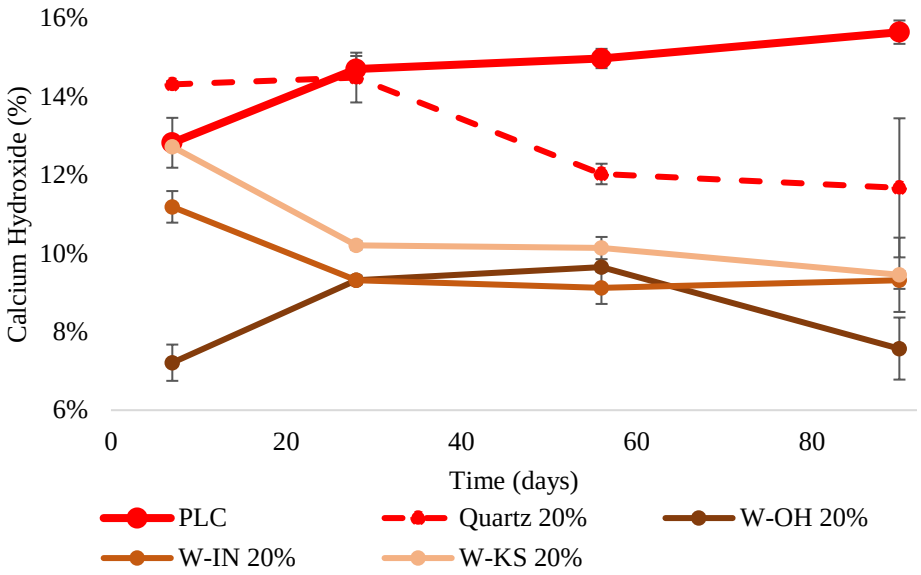

Figure 5-24: Calcium hydroxide content, Wheat, 20% substitution.

5.2.3 Mortar Testing

5.2.3.1 Compressive strength

Compressive strength development is shown in Figures 5-25 and 5-26. Compressive strength development was tested using the agricultural materials substituted for PLC at 10% and 20% volume. Both H-KS samples showed the weakest strengths at 7 days. Samples with 10% substitution all show greater strengths than the PLC control at 28 days, except for the C-IN and H-KS samples. At 56 days, the C-OH10% and C-KS10% outperform all other wheat or hemp samples at 10% substitution. At 90 days, C-OH10% displayed a 10.5% increase in compressive strength relative to the control sample.

Comparatively, at 20% substitution, all samples except W-OH are weaker than PLC control at 28 days and 56 days. The 20% wheat substitution samples on average are higher strength than the corn at 56 days. Doubling the amount agricultural ash decreased the average strength of the cube by 13% and 21% for corn and wheat, respectively, at 28 days. At 56 days, doubling the amount of agricultural ash decreased the average strength by 24% and 13% for corn and wheat respectively.

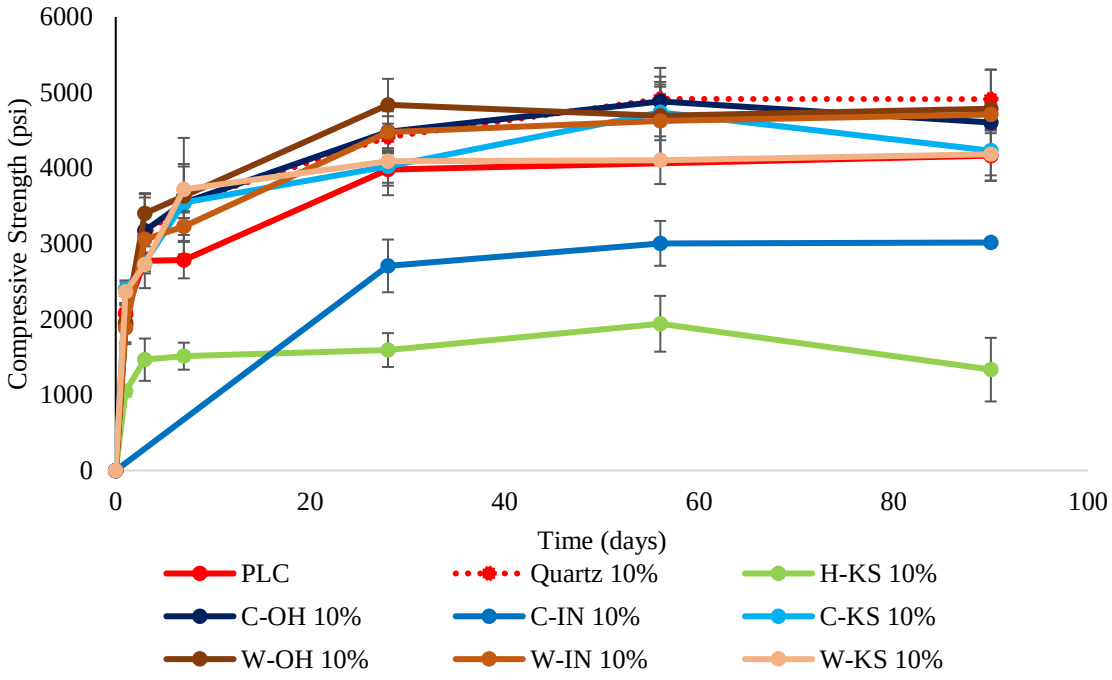

Figure 5-25: Compressive strength development of mortar cubes, 10% substitution.

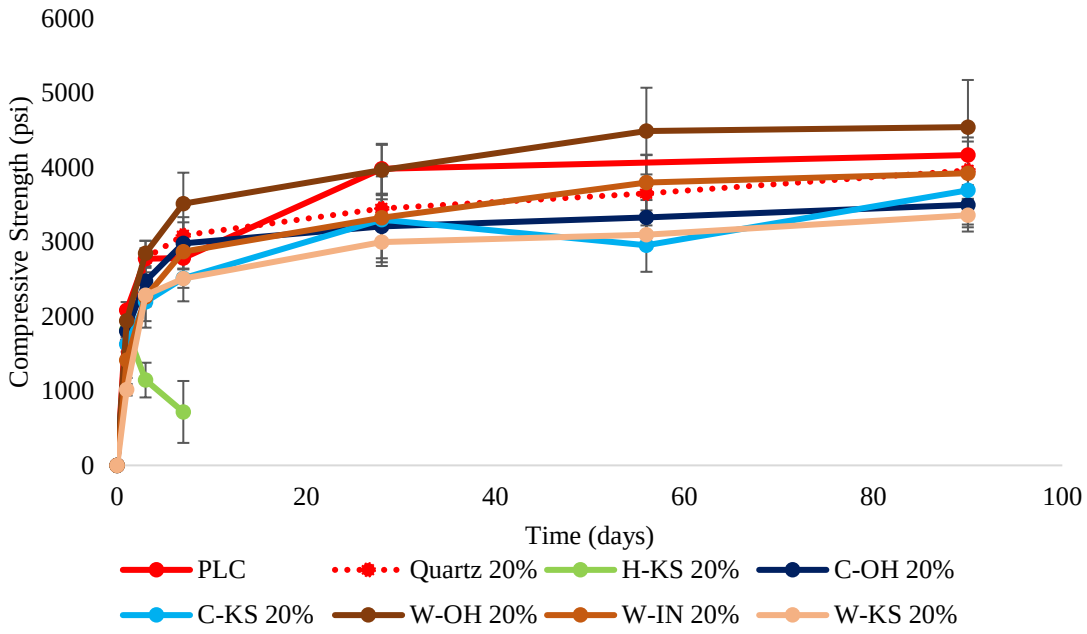

Figure 5-26: Compressive strength development of mortar cubes, 20% substitution.

5.2.3.2 Electrical bulk resistivity

Figure 5-27 through Figure 5-30 show bulk electrical resistivity of 2" mortar cubes up to 90 days after casting. Bulk resistivity is an indication of the densification of the pore structure of the cube, although it can also be affected by differences in system chemistry (Nadelman & Kurtis, 2014). Resistivity data increased fastest in wheat straw ash samples, consistent with their reported pozzolanic reactivity, suggesting that increased resistivity correlates with a denser microstructure (M. Amin et al., 2019; Katman et al., 2022). Hemp samples densified slower than the wheat and corn samples, and H-KS 20% showed decreasing electrical resistivity through 7 days (Figures 5-27 and 5-29). Corn ash samples C-KS 10% and both C-OH sets showed higher resistivity than control at 56 days (Figures 5-27 and 5-29). Wheat straw samples densified fastest. By 28

days, all wheat samples averaged higher resistivity than control. For W-OH and W-IN, doubling the amount of wheat straw ash increased resistivity at 56 days by 31% and 52% respectively (Figures 5-28 and 5-30). The only other sample with an increased 56-day resistivity caused by doubling the ash content was C-OH (17% increase).

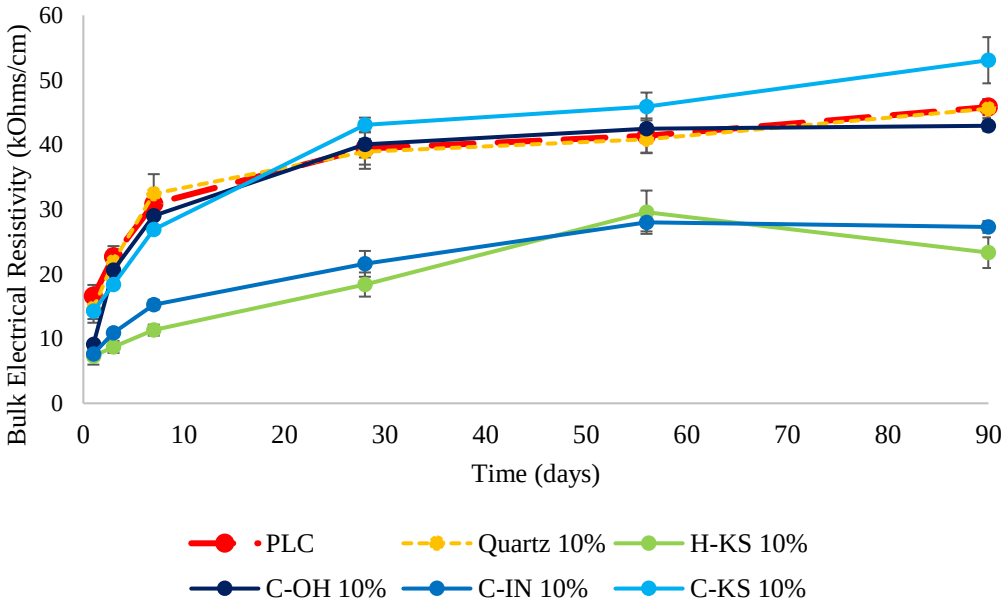

Figure 5-27: Electrical bulk resistivity of mortar cubes, Hemp and Corn, 10% substitution.

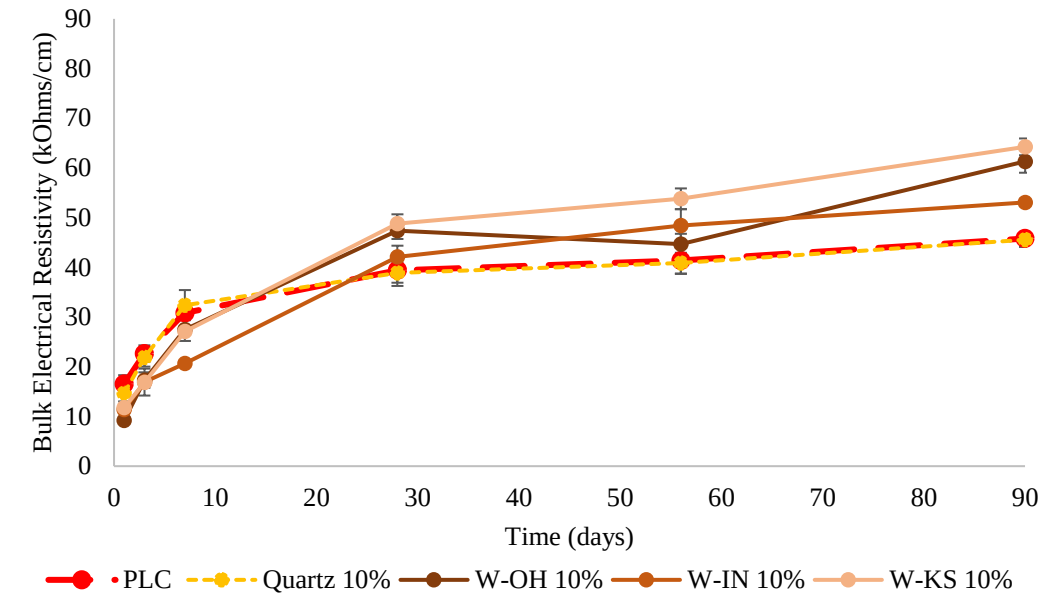

Figure 5-28: Electrical bulk resistivity of mortar cubes, Wheat, 10% substitution.

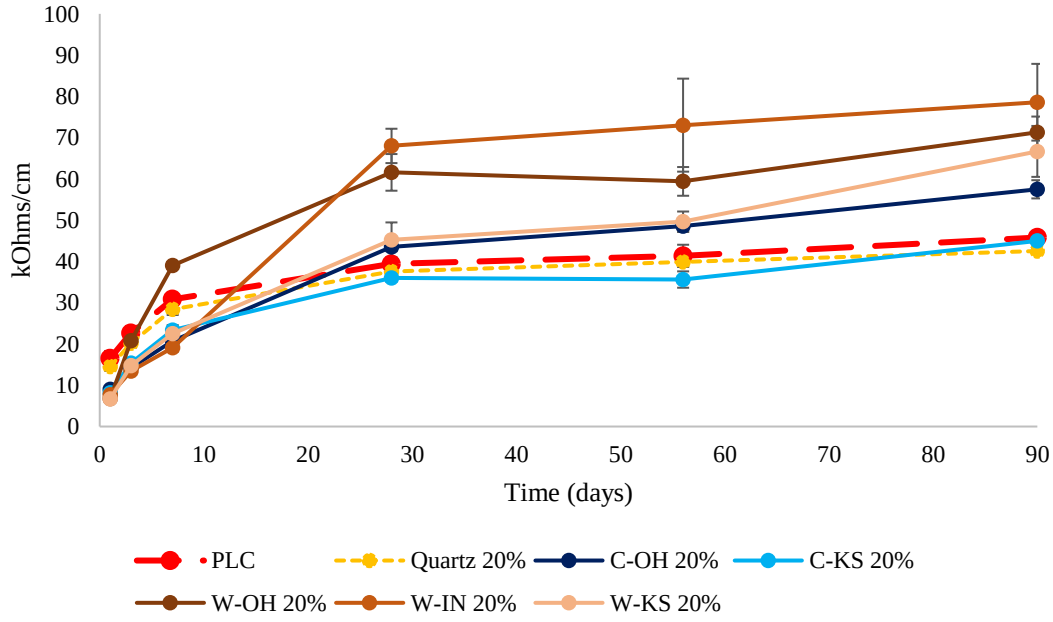

Figure 5-29: Electrical bulk resistivity of mortar cubes, Hemp and Corn, 20% substitution.

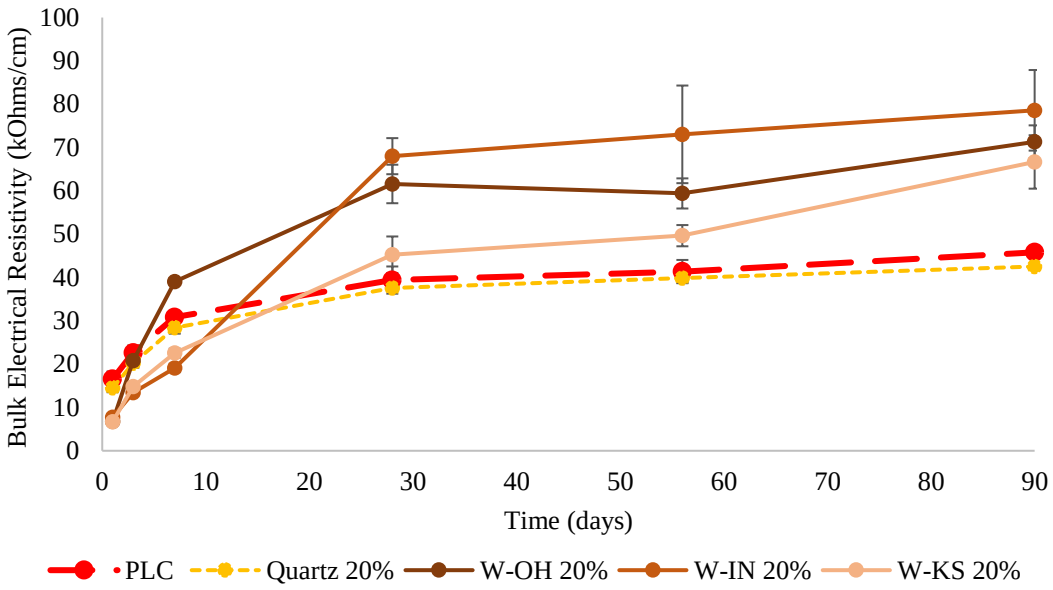

Figure 5-30: Electrical bulk resistivity of mortar cubes, Wheat, 20% substitution.

5.2.3.3 Flow data

Figure 5-31 shows the mortar flow data of each mix. The agricultural ashes decreased flow in every case. Additionally, with the exception of the W-KS, the higher 20% substitution rate led to a significantly lower flow, particularly in the case in W-IN, where adding 10% more SCM decreased the flow by 84%. The specific surface area and absorption of the particle itself plays a role in water uptake and mixture stiffening. These results indicate that workability could be a concern with higher additions of agricultural ash. Pargar et al. used superplasticizer to improve the workability for concrete specimens utilizing hemp ash (Pargar et al., 2021). Noticeably reduced workability with the H-KS10% mortar prompted the decision to use Sika ViscoCrete

2100 superplasticizer at the manufacture's maximum suggested dosage (6 fluid ounces per 100 lb cementitious materials) in the H-KS20% mortar.

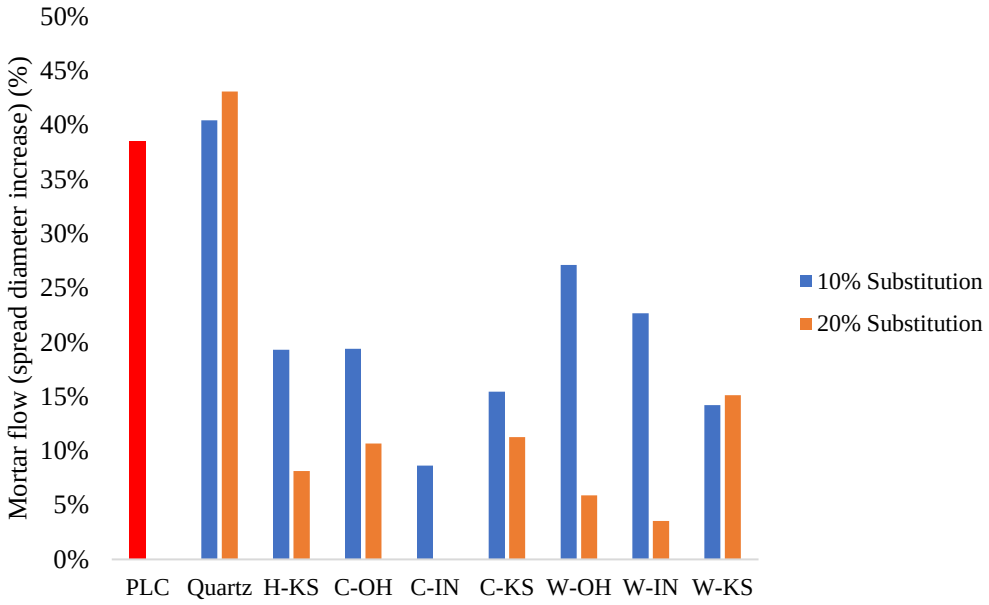

Figure 5-31: Mortar flow data, given in percent increase in diameter.

5.2.4 Ash Absorption

The foam index test was created to assess AEA dosage requirements for mixtures with fly ashes (Tyler Ley et al., 2008). It provides a relative standard by which to assess the absorptive capacity of the agricultural ashes. Results of foam index testing are presented in Table 5-3. Hemp, corn, and wheat ashes on average absorbed 213%, 80%, and 5% more AEA than a standard Class C or F fly ash.

Table 5-3: Results of foam index testing.

Sample	µL AEA absorbed/gram ash
Class C Fly Ash	0.04
Class F Fly Ash	0.04
H-F	0.12
H-KY	0.03
H-KS	0.23
C-OH	0.04
C-IN	0.05
C-KS	0.14
W-OH	0.03
W-IN	0.04
W-KS	0.06

5.2.5 SEM Imaging

Scanning electron microscopy images are provided for each ash type in Figures 5-27 through 5-35. The hemp particles appear to have a more porous surface, with some irregular plate-like shapes dispersed among large porous masses. In the H-KY and H-KS varieties, thin fibers can be seen coated with extremely small particles stuck to them. These thin fibers are occasionally used like steel fibers in concrete mixtures to prevent cracking and increase tensile strength and flexibility of composite materials (Placet, 2009). Wheat particles have similar fibers visible, however they have a much smoother surface. This could cause these fiber-like particles to have less frictional capability to resist strain compared to the hemp fibers. Wheat straw ash is known more for its chemical properties rather than its fiber strength (Biricik et al., 1999). Most of the wheat

fiber hydrogen bonds and cellulose chains are destroyed in the calcination and milling process, leaving other smooth irregular particles as well as some amorphous masses near them. Corn stover particles show significant variability, due to the nature of the stover consisting of notably different parts of the plant, including husk, stalk, leaves, and cob in C-OH and C-KS. Some of these particles are extremely smooth and have jagged edges, while some are round, and some are porous.

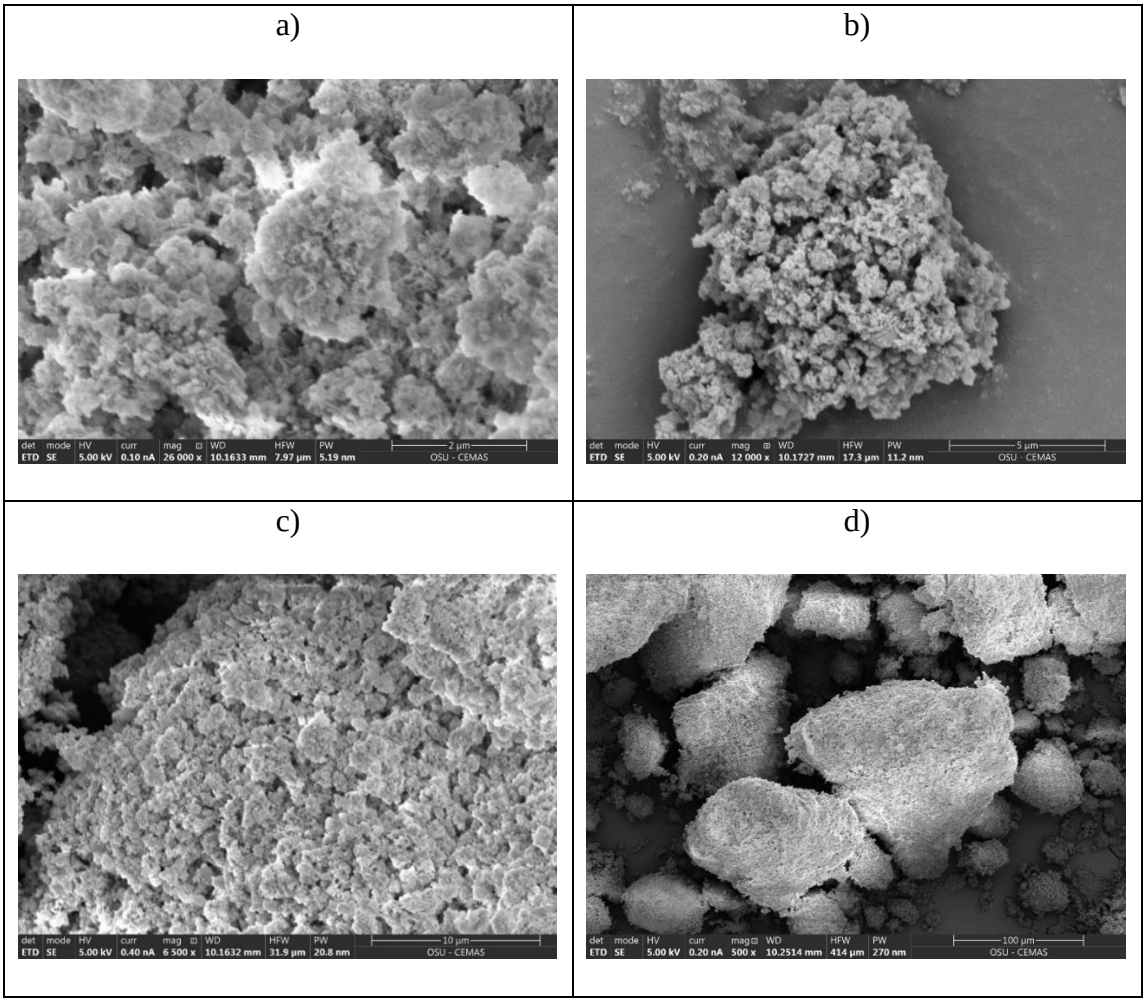

Figure 5-32: SEM Images of H-F particles: magnifications of magnifications of: a) 26,000 X, b) 12,000 X, c) 6,500 X, d) 500 X.

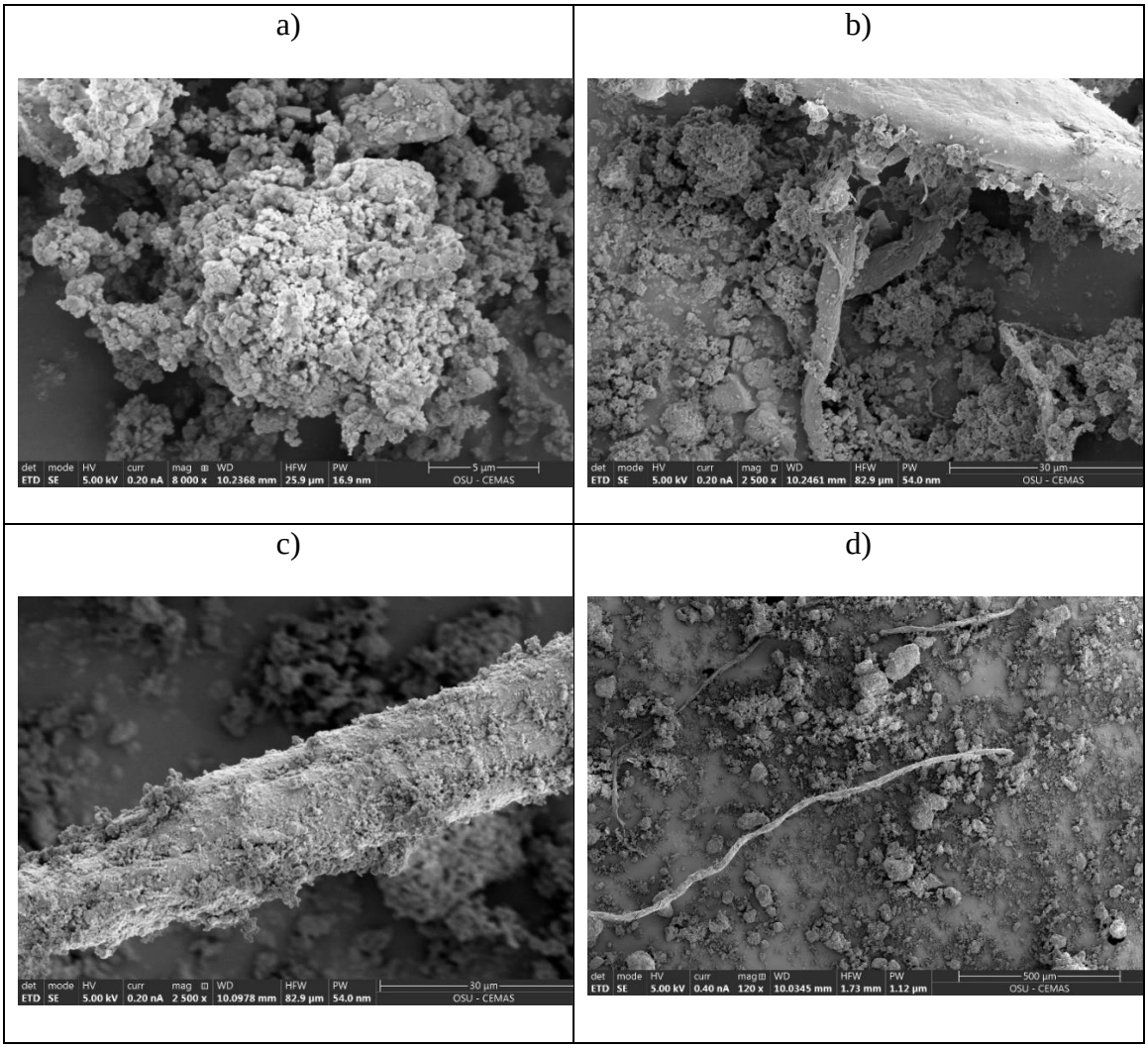

Figure 5-33: SEM Images of H-KY particles: magnifications of: a) 8,000 X, b) 2,500 X, c) 2,500 X, d) 120 X.

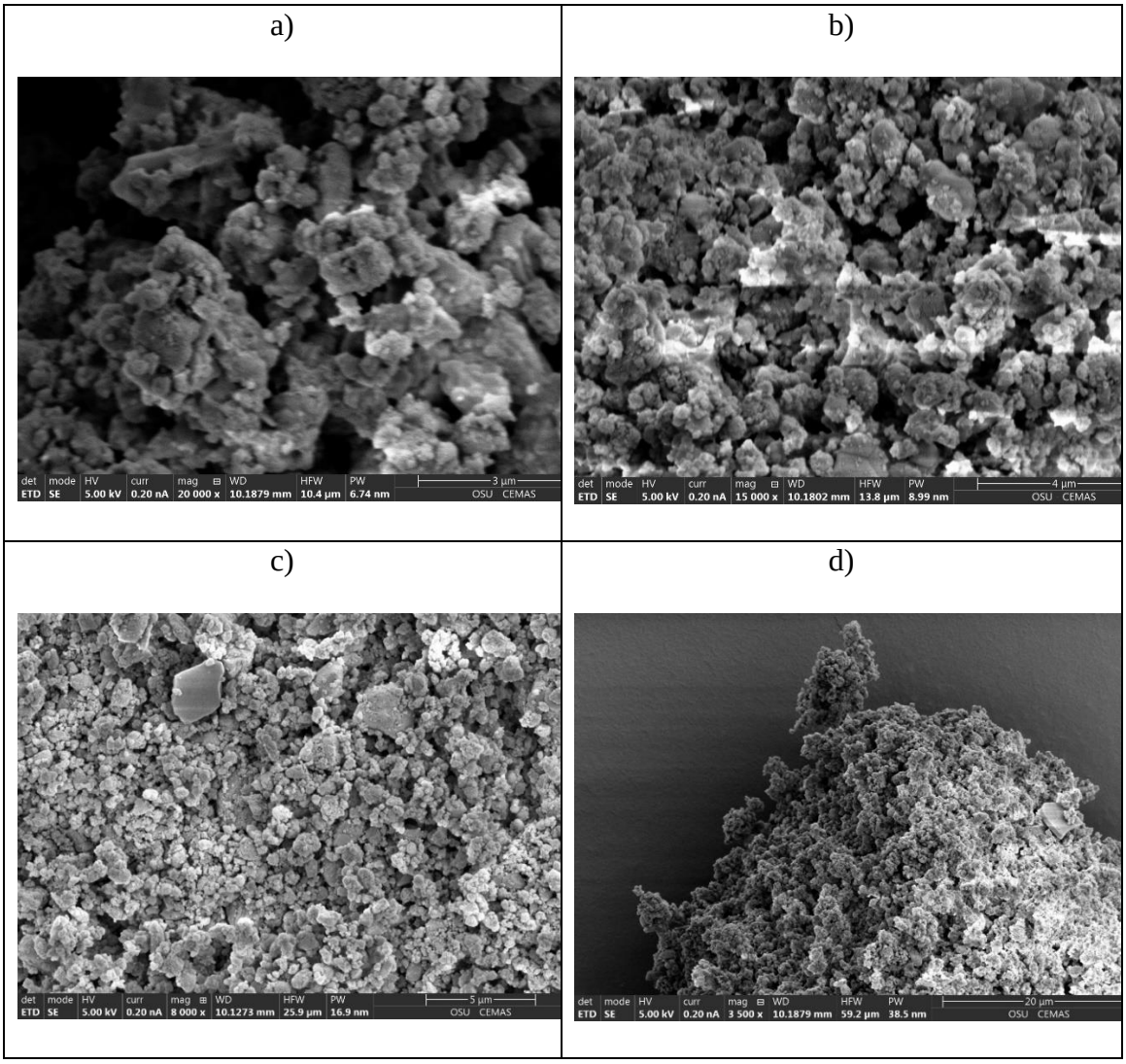

Figure 5-34: SEM Images of H-KS particles. magnifications of: a) 20,000 X, b) 15,000 X, c) 8,000 X, d) 3,500 X.

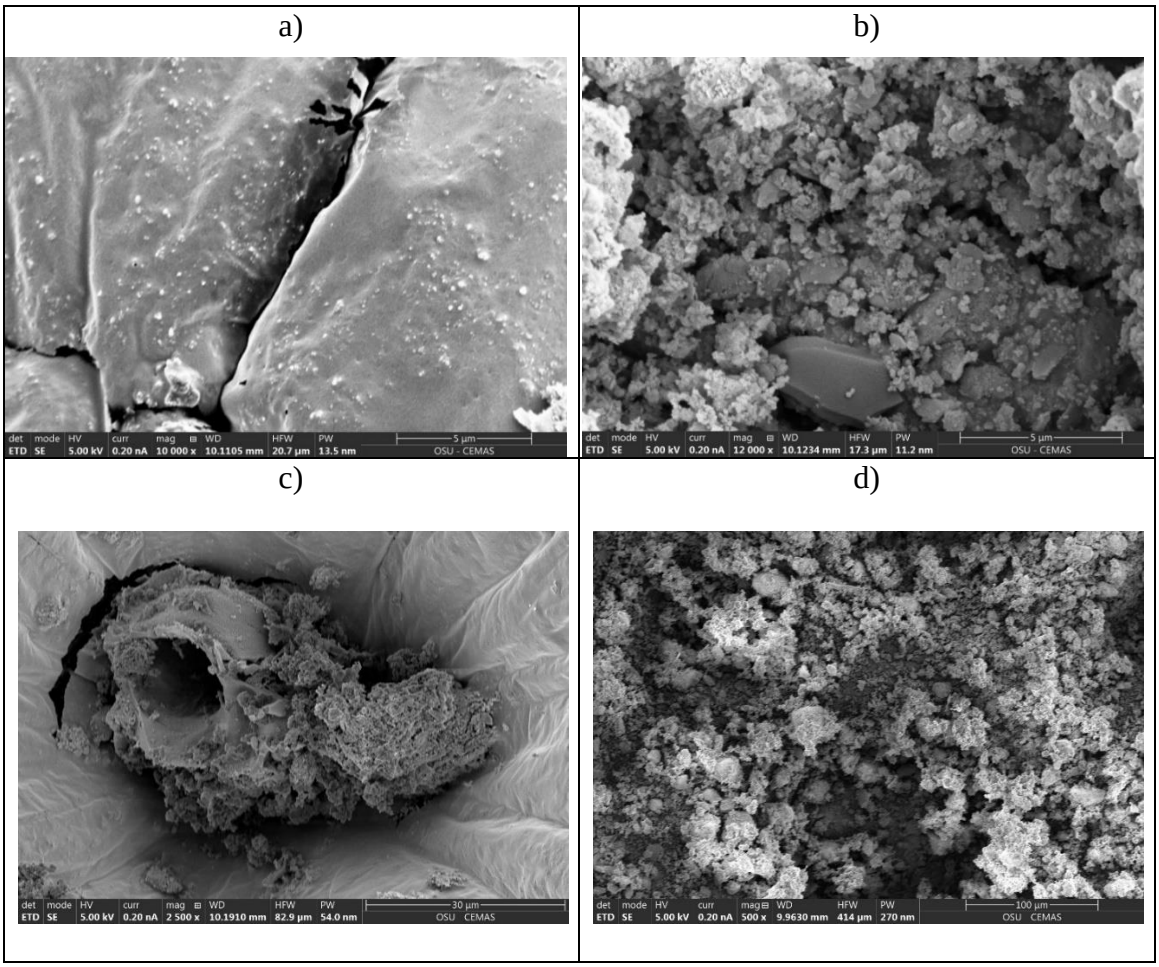

Figure 5-35: SEM Images of C-OH particles. magnifications of: a) 10,000 X, b) 12,000 X, c) 2,500 X, d) 500 X.

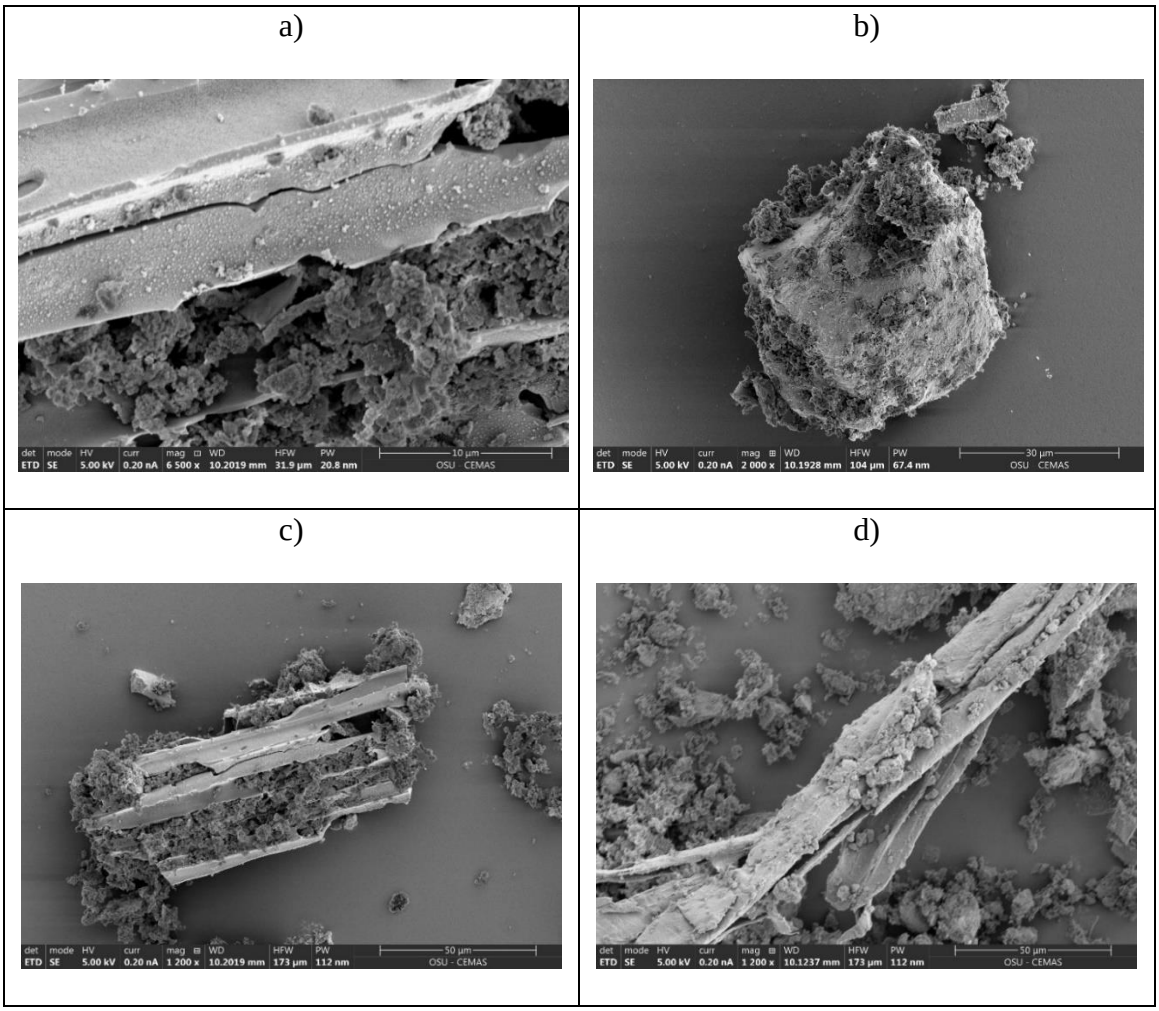

Figure 5-36: SEM Images of C-IN particles. magnifications of: a) 6,500 X, b) 2,000 X, c) 1,200 X, d) 1,200 X.

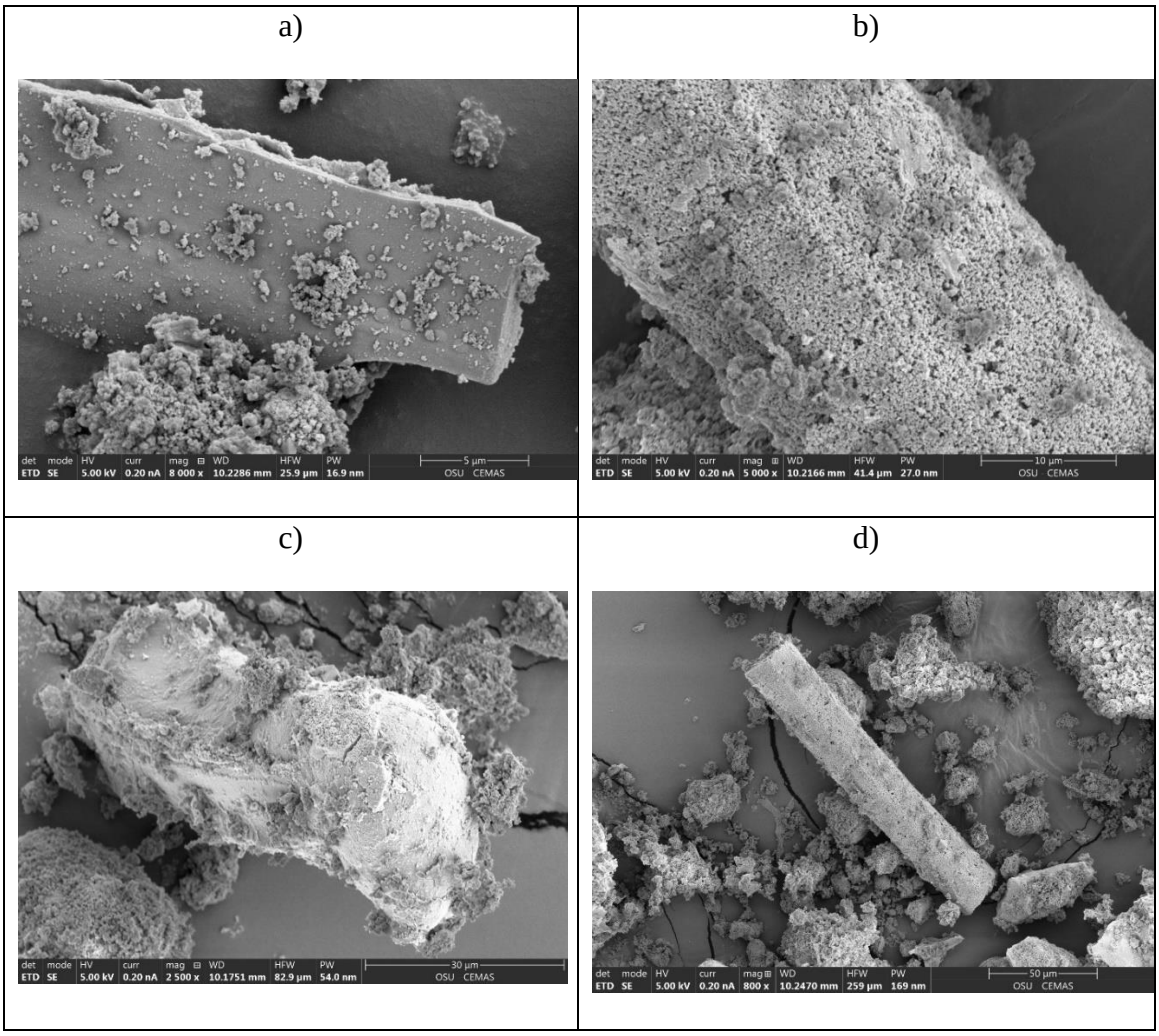

Figure 5-37: SEM Images of C-KS particles. magnifications of: a) 8,000 X, b) 5,000 X, c) 2,500 X, d) 800 X.

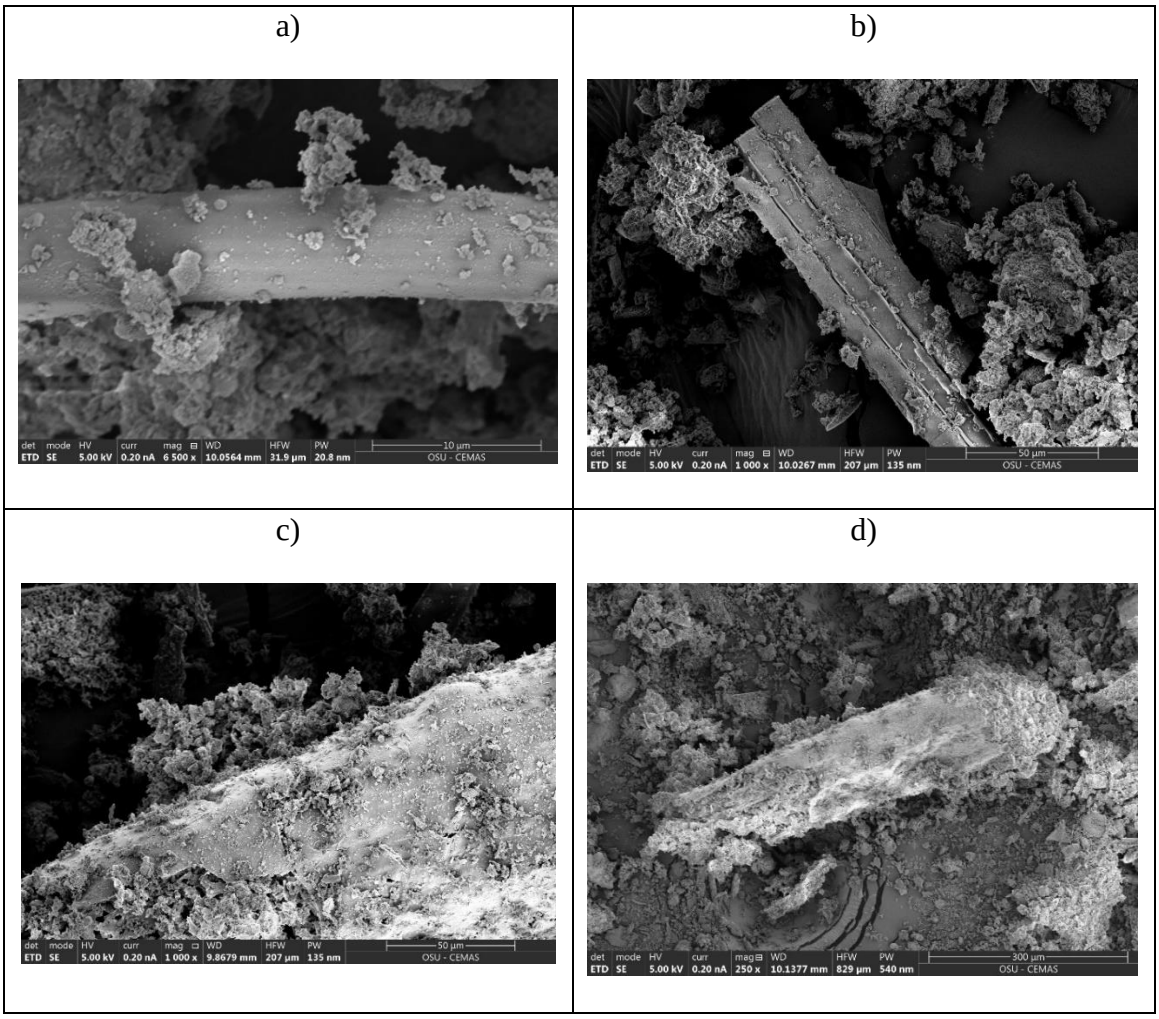

Figure 5-38: SEM Images of W-OH particles. magnifications of: a) 6,500 X, b) 1,000 X, c) 1,000 X, d) 250 X.

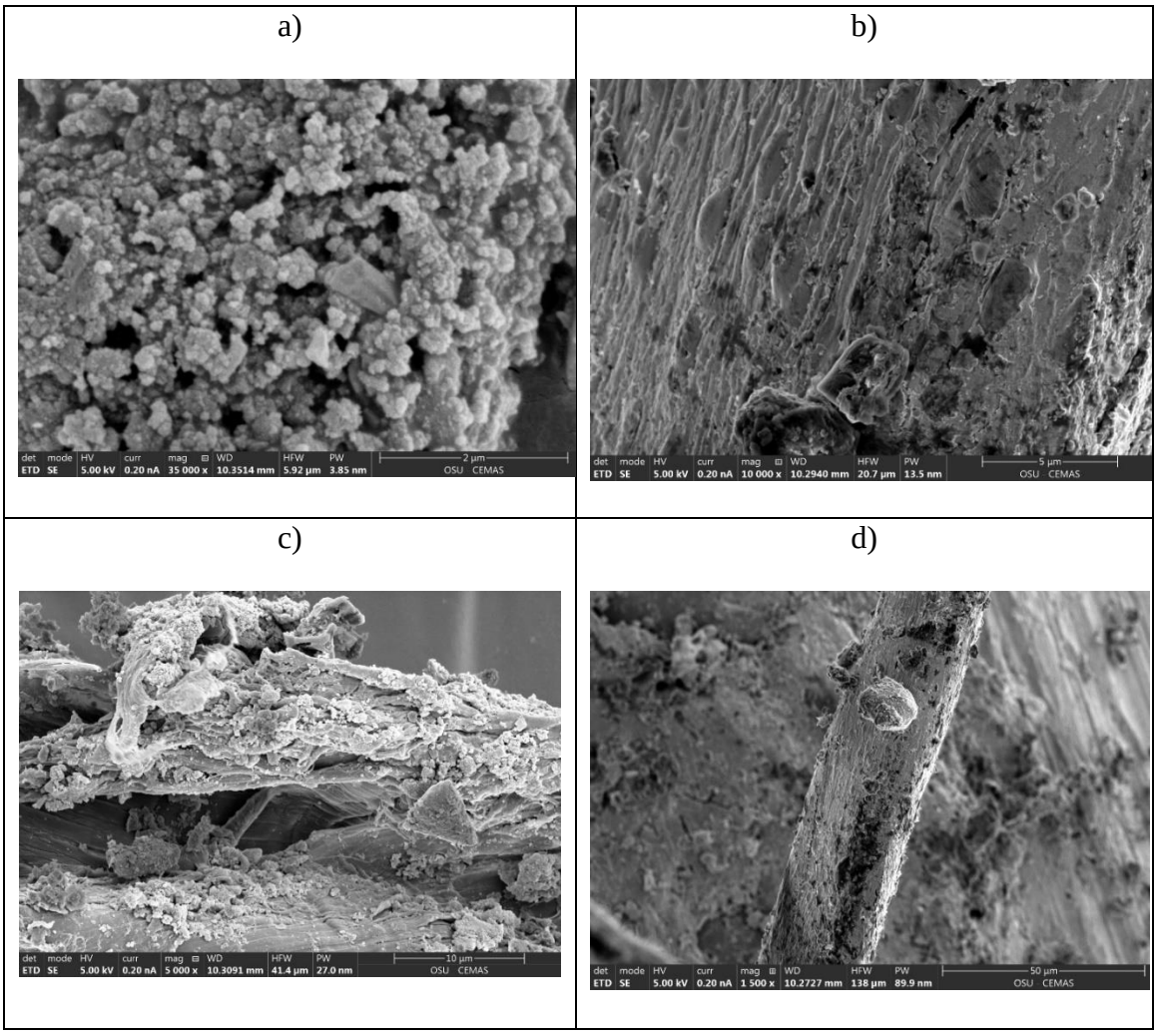

Figure 5-39: SEM Images of W-IN particles. magnifications of: a) 35,000 X, b) 10,000 X, c) 5,000 X, d)1,500 X.

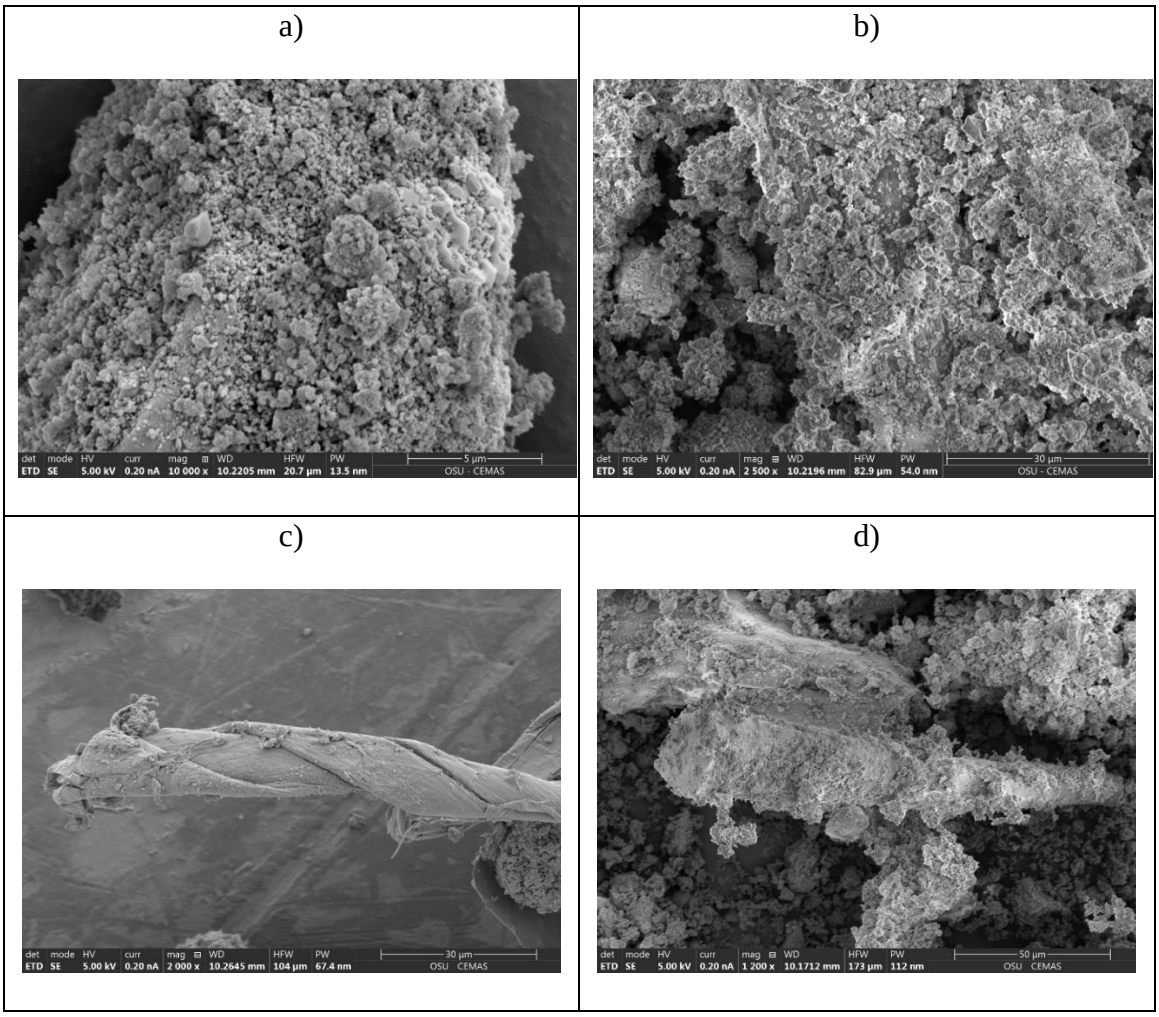

Figure 5-40: SEM Images of W-KS particles. magnifications of: a) 10,000 X, b) 2,500 X, c) 2,000 X, d) 1,200 X.

Chapter 6: Discussion

6.1 Optimizing Preparation Methods

6.1.1 Pretreatment

Preparation methods are the primary variables a producer can control to optimize the reactivity of the material, and so were investigated in this study to attempt to understand what conditions provide optimal performance of the ashes in cementitious mixtures. Some materials like rice husk ash, are naturally highly reactive, and do not require any treatment other than calcination and grinding. However, most agricultural materials are not as naturally reactive as rice husk, and could benefit from chemical pretreatment to remove impurities such as chlorides, phosphates, and heavy metals. In this study multiple preparation variables, including a variety of pretreatment soak solutions, calcination temperatures, and milling times, were investigated to identify optimum preparation procedures.

Chemical pretreatments should be considered realistically as a balance between simplicity and safety for processors, and effectiveness or necessity for the material. For these materials to be attractive to industry, the amount of energy and effort required for ash production should be as minimal for a desired performance level. A variety of

treatments were selected to assess potential performance improvements relative to cost, safety, and simplicity. Both acid treatments and DI water soaking showed reductions in impurities (Table 5-1), as well as lower LOI of the ash material (Figure 5-2), suggesting the treatments degraded initial product structure before calcination. DI water pretreatment removed less aluminum and iron from the materials than the acid soaks. As alumina, in particular, is desirable for driving the pozzolanic reaction, choice of DI water soaking over use of acidic solutions may lead to overall greater pozzolanic reactivity, in addition to assisting the material in meeting the chemical composition requirements of a Class N natural pozzolan (ASTM, 2022a). However, aluminum sulfate is known to accelerate cement hydration, and this could be a concern from using sulfuric acid for pretreatment (X. Liu et al., 2020).

Based on the ICP data and previous literature, a DI water soak could be enough to improve the material significantly, without requiring acidic solutions. In some materials, the DI water soak removed more potassium and sodium from biomass than the acid soak. However, acid treatments are more effective. Literature suggests that pretreatments can increase amorphous silica and available surface area of the particles, and decrease material LOI (Ataie et al., 2013; Kabir et al., 2013; Vo & Navard, 2016). Ataie et al. suggest that chemical pretreatments reduce the ash sensitivity to burning temperature (Ataie et al., 2013). Thermogravimetric analysis results from this study also confirm that LOI was reduced for pretreated H-F ashes by as much as 25% as shown in Figure 5-2, and quantitative XRD showed that acid soaks were effective at removing impurities like albite and sodium phosphate (Figure 5-3). Because chemical pretreatments were effective

at removing potassium, sodium, and magnesium from the material, and lowered the LOI of the ash, material pretreatment is recommended. Further study should be done to analyze the effect of pretreated materials on hydration kinetics and particle morphology.

6.1.2 Calcination

Other steps in material processing include calcination and milling. Variability in material LOI is evidence that calcination temperatures vary between products and should be selected uniquely for each material (Table 6-1). Materials should be considered individually to minimize ash LOI and crystalline silica. However, higher calcination temperatures induce carbon combustion, if the material is burned completely (Wang et al., 2021). If the calcination temperature is above 620 °C, the potassium released from K_2O decomposition will cause the silica particles to melt and wrap around the carbon particles, which can be seen in the black particles particularly in wheat straw ash and rice husk ash (Krishnarao et al., 2001). Memon et al. shows a wheat straw ash remaining dark in color at temperatures as high as 800 °C (Memon et al., 2018), suggesting that visual perception is a poor indicator of calcination completeness.

Table 6-1: Average LOI of agricultural ash based on material, calcined to 500 °C.

Hemp hurd ash	26.7%
Corn stover ash	9.1%
Wheat straw ash	8.7%

Carbon combustion is related to the accessibility of air to the materials (Wang et al., 2021), therefore ideal burning length is related to the size of the oven and loading used. With the ovens used for this study, 2.5-hour calcination produced an evenly combusted ash. The LOI of corn stover ash produced was similar to the untreated ash produced by Shakouri et al. at 550 °C with an LOI of 9.04% (Shakouri, Exstrom, Ramanathan, Suraneni, et al., 2020). Similarly, an untreated wheat straw ash burnt to 575 °C for 5 hours produced an ash with an LOI of 8.6% in a study by Biricik et al. (Biricik et al., 1999). The Shakouri et al. study showed that an HNO_3 pretreatment reduced the LOI to 0.16%, and a DI treatment reduced LOI to 4.01%, providing evidence that pretreatment is more effective at lowering LOI than raising the calcination temperature by 50 °C – 75 °C (Shakouri, Exstrom, Ramanathan, Suraneni, et al., 2020). Measured values of LOI for untreated corn ash and wheat straw are consistent with published values. However, the hemp hurd LOI values measured are above the 10% minimum set by ASTM C618 for a natural pozzolan (ASTM, 2022a). The typical range of a class C fly ash LOI is between 0.3 - 11.7%, compared to the 26.7% average from the three hemp samples tested in this study (G. Li et al., 2022). The results of foam index testing indicate that hemp hurd ash mixtures will require increased admixture dosages due in part to their high LOI. The high LOI of hemp hurd ash may be responsible for the 56-day compressive strength of H-KS 10% to be 53% and 57% lower than the average 10% corn and wheat cubes respectively.

In conclusion, a calcination temperature of 500 °C is adequate for corn and wheat materials, however, a higher calcination temperature potentially in conjunction with

chemical pretreatment is likely required to reduce hemp ash's LOI to below 10%. Strong experimental evidence and literature suggest that chemical pretreatment would be a more effective way to reduce LOI.

6.1.3 Ball Milling

Agricultural ashes are made up of particles with varying shapes and morphologies. As a result, milling or grinding of the ash to develop a uniform material is important. Milling can collapse crystalline structures to decrease the size of the particles, and create a more uniform ash (Bokhari et al., 2021). Initial experimentation achieved reductions in particle size, nearly matching the distribution of the cement particles. However, in the final ashes, a larger percentage of particles with diameters between 100 and 250 μm remained following the standard 5 hour milling time. Decreased amounts of larger particles size material likely increased overall ash early age reactivity in cementitious pastes by introducing additional sites for C-S-H growth through higher available surface area (Figure 5-32 – Figure 5-40). Longer grinding could also lead to an increase in extent of pozzolanic activity (Suraneni, 2021; Yao et al., 2020). However, using multiple methods for calcination and milling, Kevern & Wang reported that with corn stover ash, no significant improvement to reactivity was observed from increased processing (Kevern & Wang, 2010). Based on the results of particle size analysis, longer milling time is recommended to achieve particle size distributions similar to that of the PLC (Figure 5-12). Five hours of milling was enough to lower the median particle

diameter below that of PLC for all samples except C-KS and W-IN, however, the D_{90} particle diameter on average was 99% larger than that of PLC (Table 5-3). Increased milling time, or removal of the largest particles through sieving, is recommended for further study.

6.2 Effect of Agricultural Ashes on Cement Hydration and Pozzolanic Reactivity

Results of the strength, resistivity testing, and CH content measurements suggest that up to a 20% volumetric replacement of cement for corn stover ash or wheat straw ash can improve the long-term performance and durability of cementitious systems. However, use of hemp hurd ash did not provide the same benefits as traditional SCMs. The performances of agricultural ashes used as partial replacements in cementitious systems are assessed through studying hydration kinetics and fresh properties, as well as through quantified calcium hydroxide measurements and long-term studies of strength development, resistivity, and reactivity.

Results of isothermal and R^3 calorimetry indicate that material differences translate to changes in reactivity in cementitious systems. Figure 6-1 shows changes in time to maximum heat evolution compared to the PLC control for each paste with 20% substitution. Among the three samples of wheat straw tested, there is a 7.62-hour difference among most and least retarded samples, indicating variability in reaction kinetics based on source location (Figure 6-1). Similarly, a 5.27-hour spread is visible among the three corn stover samples.

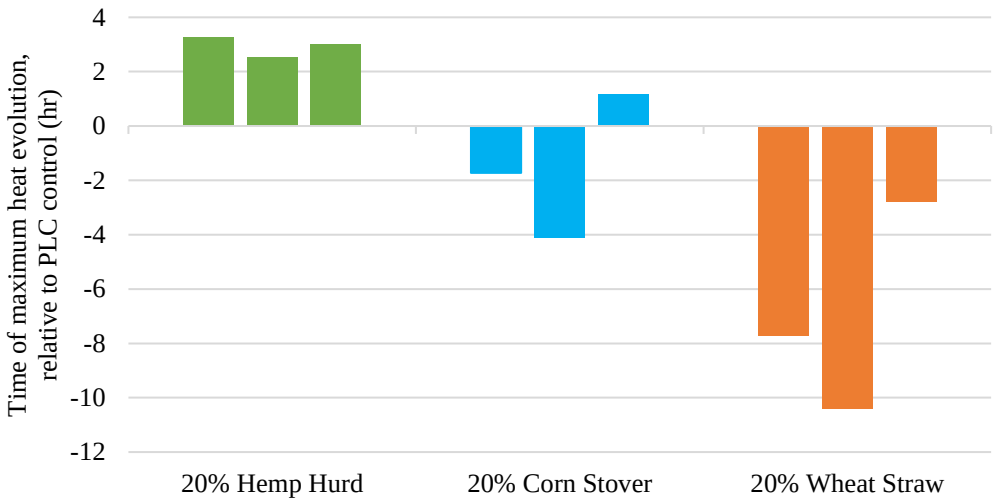

Figure 6-1 : Variability in time to maximum heat evolution relative to PLC control, by location.

Figure 6-2 and Figure 6-3 show the average delay or acceleration of the maximum heat evolution peak compared to PLC for each material. These plots show the effect of each material on the hydration reaction based on the type of material, and the substitution rate. The hemp samples on average decreased the length of the induction period and increased the average maximum heat evolution value. This is generally considered to be caused by heterogenous nucleation, a result of higher specific surface area and a more amorphous material (Cordeiro & Kurtis, 2017). SEM imaging showed a porous surface for hemp samples, supporting this conclusion, however no link was found between amorphous content and hydration speed (Figure 6-5). Hemp samples, on average, have the highest alumina content detected through XRF (39.2%) when compared to corn (12.2%) and wheat (9.5%), which could be responsible for the accelerated reactions in the hemp pastes by accelerating the hydration of the aluminate phases (X. Liu et al., 2020).

Conversely, the corn and wheat samples generally delayed hydration and reduced the maximum evolved heat value. During calcination, chelation between the calcium ions and sugar released from the plant products (Chakraborty et al., 2013; Jo & Chakraborty, 2015). Sugar components and lignin are known to delay hydration by absorbing calcium ions from the cement matrix, slowing the silicate reaction and preventing C-S-H formation (le Ngoc Huyen et al., 2011). The nature of the sugars present also helps the understanding of the delayed hydration. Sugars like glucose, lactose, cellobiose, and maltose are effective at slowing hydration (Vo & Navard, 2016). Glucose is present in cellulosic biomass and can cause retardation depending on the binder composition. Glucose will react with C_3A first, if it is plentiful, which reduces the amount of sugar remaining to retard the C_3S components (Doudart De La Grée et al., 2015). Therefore, the effects of retardation by using these materials could be controlled potentially through pretreatment to remove sugars and lignin, and choosing a cement binder carefully, as some cements, including calcium sulfoaluminate cement, are not hindered by the presence of sugar (Acarturk et al., n.d.).

Another hypothesis is that phosphorous could be causing the retardation in these samples. Shakouri et al. hypothesize that phosphorus content of 3.74% was partially responsible for a 2.3-hour retardation in untreated samples with 20% corn stover replacement for cement mass (Shakouri, Exstrom, Ramanathan, Suraneni, et al., 2020). In this work, untreated corn stover ash only showed phosphorus detected through XRF in one of the three samples, and the average retardation of 20% corn samples was 1.56 hours. Wheat straw ash was most responsible for retardation in this study with as large as

7-hour delays in peak heat release at 10% substitution by volume compared to a 4-hour retardation at 10% wheat straw ash substituted for cement mass in Ataie and Riding's work (Ataie & Riding, 2016). The hydration variability in these samples could not be correlated well to LOI or particle size, so this severe retardation is likely linked to material chemistry.

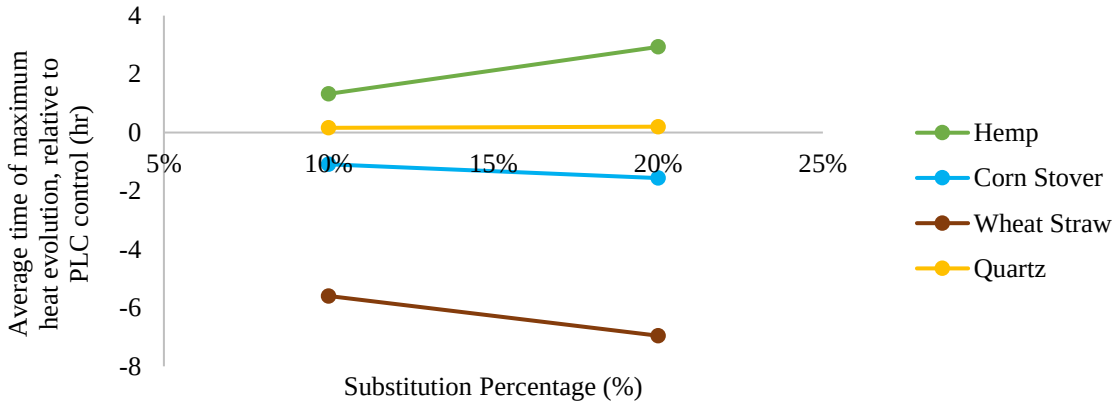

Figure 6-2: Average time of maximum heat evolution, relative to PLC, by material.

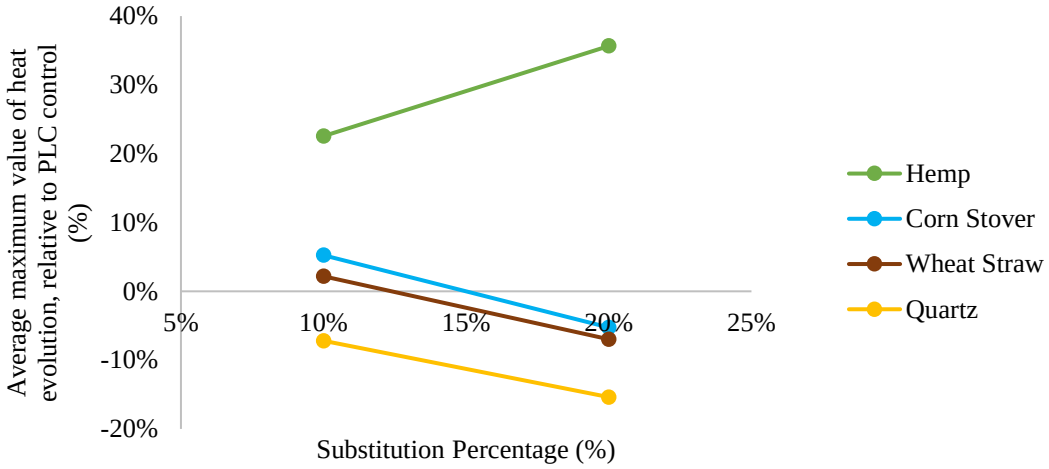

Figure 6-3: Average maximum value of heat evolution, relative to PLC, by material.

Another concern with fresh properties is workability. As confirmed with SEM imaging, these materials have inconsistent particle shapes and sizes and visible porosity (Scrivener et al., 2018). The replacement of 10% of the cement volume for agricultural ash decreased the flow of mortar by 49.9%, 62.4%, and 44.6% for the hemp, corn stover, and wheat straw mortars respectfully (Figure 6-4). With wheat straw ash, doubling the ash content nearly doubles this effect. Considering the material porosity, results of foam index testing, and reductions in flow, it can be reasonably concluded that water absorption is affecting the flowability of the mortar (Khatri et al., 1995). Pargar et al. reported that water absorption in concrete cylinders increased nearly 3% with 25% hemp ash addition, as well as reported decrease in slump from 210 mm to 0 mm for the same samples (Pargar et al., 2021).

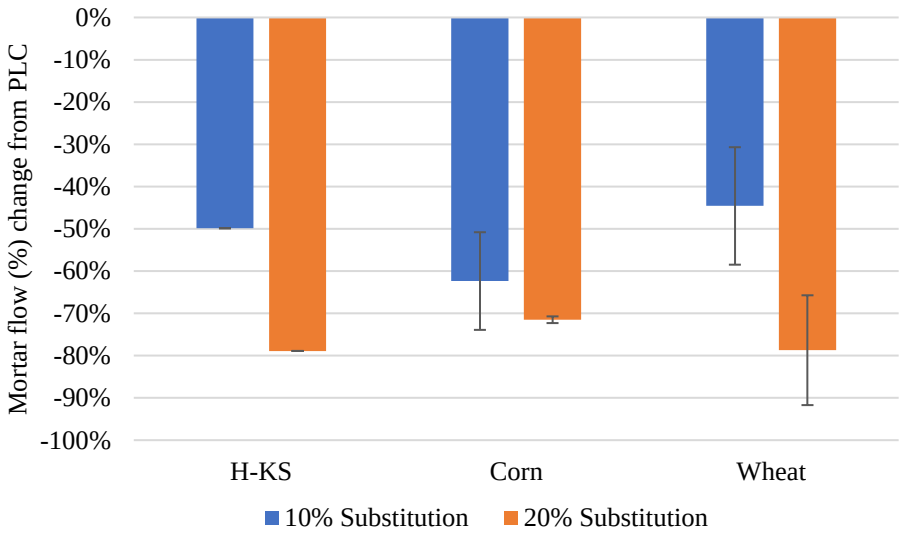

Figure 6-4: Reduction in mortar flow from addition of agricultural ash.

The effect of agricultural ashes on long term performance of cementitious systems was assessed through hardened mortar properties, and quantifying reactivity using calcium hydroxide content in pastes over time and R^3 calorimetry. Corn stover ash cubes containing 20% corn stover at 28 days displayed 81.7% of the control cube strength. All 10% corn substitution cubes were stronger than control cubes except C-IN10%, which caused the average to be a 6% reduction in strength. Shakouri et al. reported that the 28-day compressive strength of concrete specimens using 20% corn stover ash (w/cm=0.54) displayed only 68% of the control's strength (Shakouri, Exstrom, Ramanathan, Suraneni, et al., 2020). A similar study from Ataie and Riding show an untreated corn stover sample with as low as 50% of the strength of the control sample at 28 days (Ataie & Riding, 2014). The corn stover ash tested in this study did not decrease compressive strength to this extent, possibly because there was less phosphorus in the corn stover used in this study. Wheat straw ash cubes with 20% cement replacement at 28 days displayed 86.1% of the control cube strength. All 10% wheat straw substitution cubes were stronger than control cubes at 28 days, by an average of 12%. Utilizing 20% replacement of cement with wheat straw ash, Amin et al. show compressive strengths decreasing to about 90% of control (Amin et al., 2022). Using 25% replacement of cement with hemp powder, Pargar et al. showed that compressive strengths of hemp samples were about 42% lower than control samples at 28 days (Pargar et al., 2021). The H-KS 10% cubes in this study were less than half as strong as control samples at 28 days, confirming the literature's suggestion of poor strength development.

Resistivity data indicates the additions of wheat straw ash or corn stover ash on average promotes densification of the pore structure. At 28 days, agricultural cubes showed resistivity values 3% and 29% higher than control for 10% and 20% substitution respectively. At 56 days, those differences were 6% and 29%. Through 56 days, 5 of the 8 of all paste samples began to decrease in CH content for both the 10% pastes and 20% pastes. This is an indication that CH is being consumed through pozzolanic reaction, as early as 56 days in over half of the agricultural samples, which could be responsible for the densification in the pore network seen through electrical resistivity. Increased densification is thought to correlate with better durability (Thiedeitz et al., 2022).

Increases in electrical bulk resistivity are not able to identify if the reactions that are seen in densification are due to pozzolanic reactivity. Amorphous content is thought to correlate with overall reactivity, but Figure 6-5 shows the variability among amorphous contents for each material compared to its effect on time to maximum heat release (Walker & Pavía, 2011). The hypothesis that higher amorphous content would lead to faster reactivity is not consistent with this data. Figure 6-6 shows that there may be a weak connection between amorphous content and cumulative heat evolved at 160 hours, but this trend breaks down when considering materials individually.

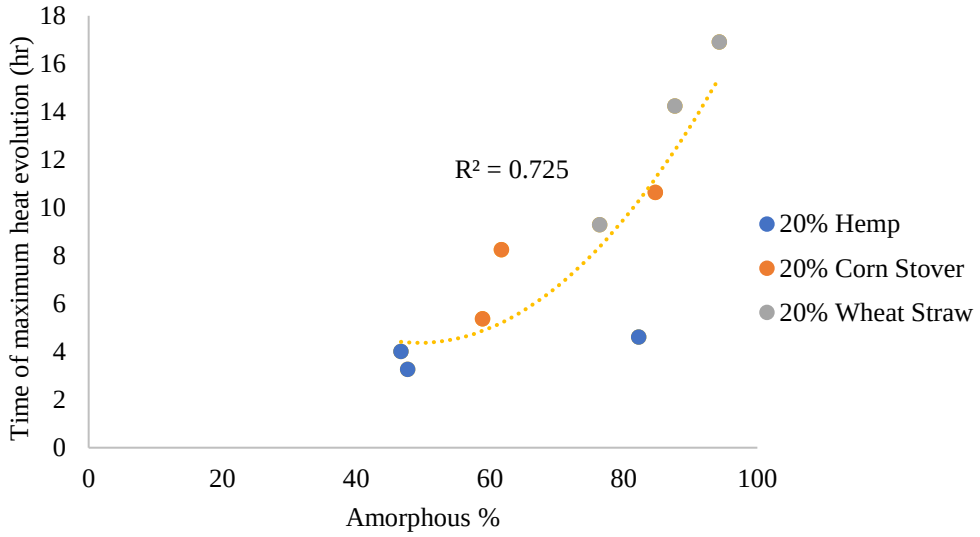

Figure 6-5: Amorphous content effect on hydration.

In theory, the amount of amorphous and reactive silica accessible in the agricultural ash is an indication of how reactive the ash will be (Skibsted & Snellings, 2019). There is a trend among all materials tested that shows silica content increasing with amorphous content, but the amount of amorphous silica present was not quantified in this study. The hemp samples' silica contents are similar, yet the cumulative heat released at 160 hours varied more than it did in other samples, suggesting the reaction must be governed by another variable.

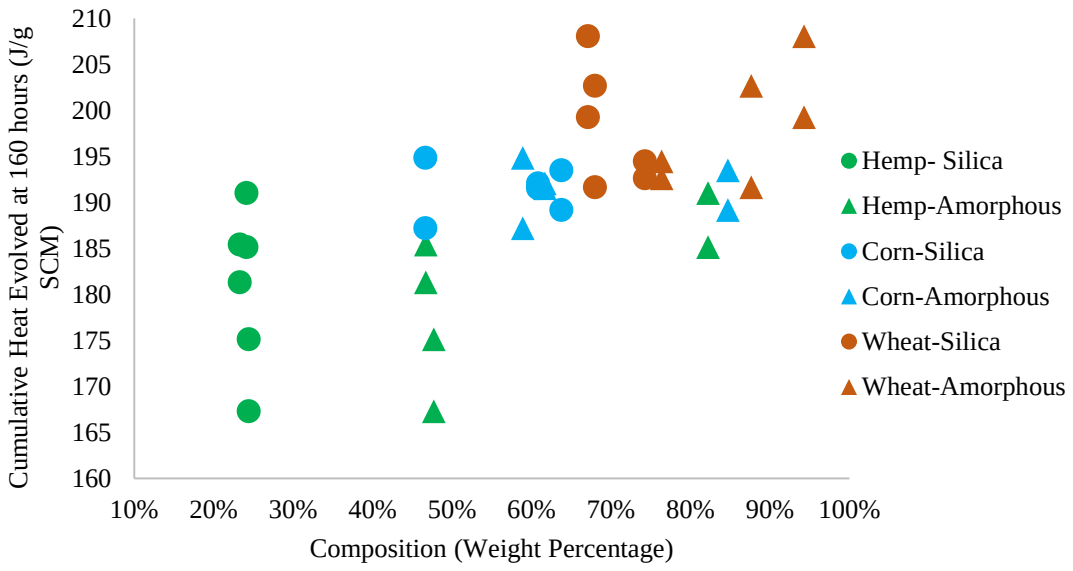

Figure 6-6: Silica composition (%) vs. cumulative heat evolved (J/g) for samples at 10% and 20% substitution.

RILEM Testing committee 267 has investigated the use of the R^3 test to characterize the pozzolanic reactivity of materials (X. Li et al., 2018).The test makes use of isothermal calorimetry at 40 °C using an SCM, calcium hydroxide, and a potassium solution to mimic the pozzolanic reaction in a shorter time and predict the performance of SCMs in cementitious systems (Snellings et al., 2019). The cumulative heat release values using this rapid test are indications of the relative extent of pozzolanic reactivity, and are expected to correlate with compressive strength development (Skibsted & Snellings, 2019). RILEM TC267 has investigated this test method with a wide range of materials, and has set thresholds for reactivity at 7 days using cumulative heat release

values: 98 J/g SCM for 66% confidence and 160 J/g SCM for 90% confidence. The performance of agricultural materials in this system are shown in Table 6-2. Wheat samples show reactivity as early as 3 days, and 2/3 wheat samples show reactivity with 90% confidence at 7 days. Corn samples showed lower heat release values at 7 days on average, but 2/3 met the 60% confidence threshold for reactivity. Hemp samples showed the least amount of reactivity, with only one sample releasing over 100 J/g SCM of heat after 14 days. Hemp samples evolved heat similar to quartz, which is known to be inert, and this suggests that increases in maximum heat release seen in Figure 5-13 could be due to the filler effect, which can extend the hydration reaction (Berodier & Scrivener, 2014; Gutteridge & Dalziel, 1990). Although early work by the RILEM committee suggested reasonable links between R^3 total heat evolution and strengths, heat release results from the agricultural products were not found to correlate well to compressive strength at any time (X. Li et al., 2018).

Table 6-2: Cumulative heat release values for R3 testing (J/g SCM).

	3 days	**7 days**	**14 days**
Quartz	22	45	89
Lignin	50	101	185
Class C Fly Ash	188	274	-
Class F Fly Ash	128	241	-
H-F	29	80	221
H-KY	21	42	77
H-KS	24	52	98
C-OH	29	49	81
C-IN	87	162	291
C-KS	73	121	188
W-OH	104	186	319
W-IN	174	326	470
W-KS	61	108	159

Green cells meet the threshold for pozzolanic reactivity per RILEM 267. (90% confidence (160 J/g SCM) =dark green, 66% confidence (98 J/g SCM) =light green) (X. Li et al., 2018).

Based on results from R^3 testing and calcium hydroxide content measurements, it can be concluded that wheat straw ash shows strong evidence of pozzolanic reactivity, which is partially responsible for the rapid densification in mortar cube pore structure, and its heat evolution from the R^3 test. Though it increased retardation significantly, its long-term properties outperform the other two materials. Corn stover ash also evidences pozzolanic reactivity, though not to the same extent as wheat straw. Though corn stover ash on average evolved only 59% of the cumulative heat evolved of wheat straw ash at 14 days, it still performs pozzolanically on average with 60% confidence at 7 days (111 J/g SCM). Corn stover ash did not significantly change hydration reaction timing or reduce flowability at 20% substitution as much as the other two materials. Hemp hurd ash did

not meet either standard for pozzolanic reactivity at 7 days set by RILEM TC 267, and this was consistent with its poor compressive strength and resistivity development. Hemp hurd ash chemistry's makes it unlikely to function as a pozzolan, which is consistent with the limited studies done on this material (Guo et al., 2020; Pargar et al., 2021).

6.3 Geographic Variability

6.3.1 Variability in soil chemistry

The variability of the chemistry of the plant depends on factors like soil, climate, crop rotation, fertilizer, and other factors. Most of these factors are outside of the scope and knowledge of this study, however, using available data from the USGS geochemical survey, chemical compositions of soils were contrasted based on five sampling locations near each corn stover source and are displayed in Figure 6-7 (Smith et al., 2013). The phosphorous and sulfur content of KS soils are lower on average than OH and IN soils, but the sodium content is higher. The variability of sodium, potassium, phosphorous, and sulfur between sources is potentially enough to result in differences in ash properties.

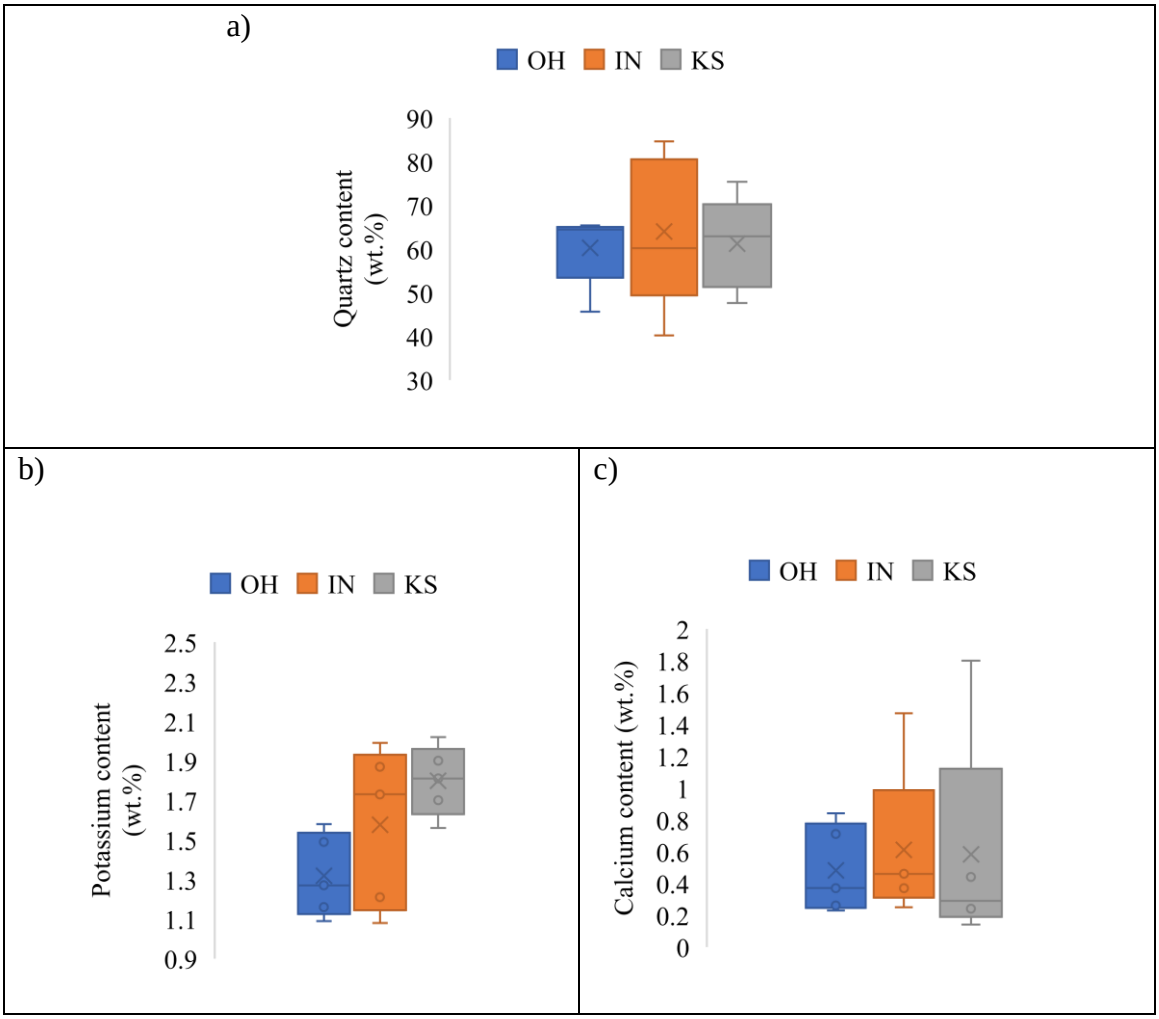

Continued

Figure 6-7: Chemical variability in soils, averaged from 5 locations around each corn sampling area accessed through USGS geochemical survey. Figure shows contents of: a) quartz, b) potassium, c) calcium, d) aluminum, e) sulfur, f) sodium, g) phosphorous (Smith et al., 2013)

Figure 6-7 Continued

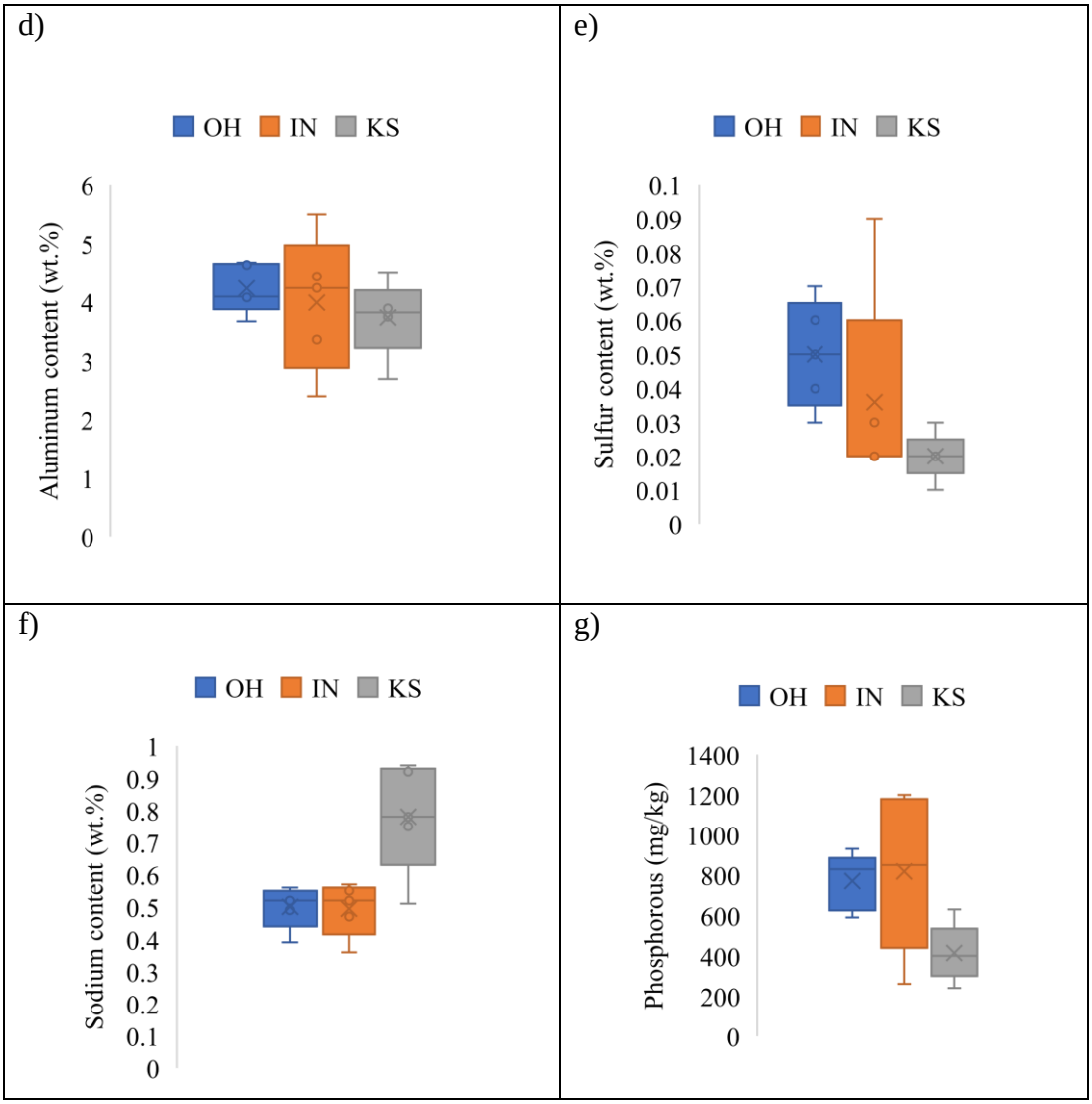

6.3.2 Variability in properties of agricultural ashes

Variability can also be assessed by considering physical characterization properties of the ashes. Four crystalline phase quantities are contrasted in Figure 6-8. The error bars represent variability among the 3 source locations for each material. A majority of each ash's weight is amorphous due to the organic nature of the materials. Hemp hurd ashes show average amorphous contents 9.6% and 27.2% lower than corn and wheat respectively. The variability of hemp amorphous contents is over 30%, which could be significant. Limited information has been published regarding the quantitative crystallinity of hemp hurd ash. The amorphous content of wheat straw ash varies by 17.9%, but of the three materials it has the highest average (86.1%) amorphous content value. The amorphous content of wheat straw ash calcined to 650 °C has been reported at 99.3% (Ataie & Riding, 2016). A notable difference can be seen in reported impurity content of corn stover ash for example, where Kevern and Wang report significant XRD peaks matching sylvite and periclase (Kevern & Wang, 2010). Similarly, two forms of crystalline phosphates were identified in the current study's ashes in lower quantities than were seen in previous work using untreated corn stover ash (Shakouri, Exstrom, Ramanathan, Suraneni, et al., 2020). Inconsistency in impurity content is one of the reasons many researchers have recommended chemical pretreatments (Bokhari et al., 2021; Galbe & Zacchi, 2012).

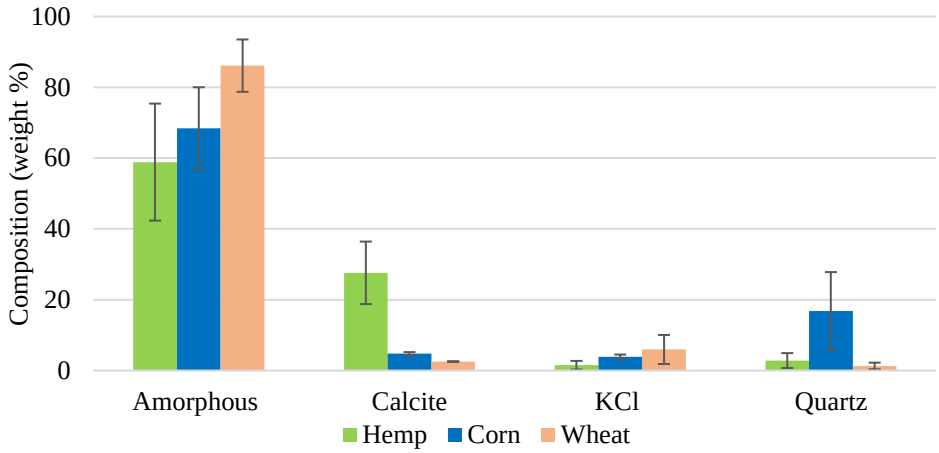

Figure 6-8: Average crystalline phase quantities of agricultural materials, expressed in percent weight.

Oxide analysis is another way to examine the composition of the ashes. The content of SiO_2 ,Al_2O_3, plus Fe_2O_3 should be above 70% to be considered a Class N pozzolan per ASTM C618 (ASTM, 2022a). Oxide contents are averaged for each material, and compared to the results of similar studies in Table 6-3. Each material, on average, meets the ASTM C618 requirement for SiO_2, Al_2O_3, and Fe_2O_3 content. Corn stover and hemp hurd had significantly different oxide composition than reported in previous studies, but wheat straw is consistent particularly with Ataie & Riding's study (Ataie & Riding, 2016). Hemp ash had lessened silica content (24 ± 0.5%) than wheat (69.8 ± 3.2) or corn ash (57.1 ± 7.5%), which would make it less likely to react pozzolanically, in comparison with the other materials tested.

Table 6-3: Average oxide content of ashes, compared to published literature.

Oxide weight (%)	**Si**	**Fe**	**Al**	**Si+ Fe + Al**	**S**	**K**	**Na**	**Calcination Temperature**
Hemp Hurd								
Avg. Measured data	24	13.6	39.2	76.8	14.6			
(Pargar et al., 2021)	*1.17*	*0.18*	*0*	*1.35*	*0.82*	*22.94*		*500°C*
Corn Stover								
Avg. Measured data	57.1	22.2	12.2	91.5	3.3			
(Teymouri & Shakouri, 2023)	*57.7*	*1.6*	*5*	*64.3*	*0.4*	*10.8*	*0.6*	*550°C*
(Kevern & Wang, 2010)	*38.33*	*0.47*	*0.22*	*39.02*	*1.72*	*27.58*		*500°C*
(Shakouri, Exstrom, Ramanathan, Suraneni, et al., 2020)	*49*	*1.07*	*3.27*	*53.34*	*0.63*	*22.7*	*0.41*	*600°C - 700°C*
Wheat Straw								
Avg. Measured data	69.8	10.7	9.5	90	5.4			
(Ataie & Riding, 2016)	*86.5*	*1.13*	*0.28*	*87.91*		*1.54*	*0.1*	*650°C*
(Al-Akhras & Abu-Alfoul, 2002)	*50.7*	*0*	*0.48*	*51.18*	*6.13*	*11.4*	*5.41*	*650°C*
(Amin et al., 2022)	*65.1*	*2.67*	*9.1*	*76.87*	*1.13*	*10.5*	*0.4*	*550°C*

A high alkali content can negatively impact concrete properties by making the mixture susceptible to alkali-silica reaction (ASR), accelerating hydration with an above optimal Al/Si ratio, and reducing compressive strength (Abbas et al., 2017; Kasaniya & Thomas, 2022; Z. Li et al., 2016). Sodium and potassium were undetectable with the XRF device used, but Table 6-3 lists alkali contents from tests where they were measured. These studies show high amounts of potassium in corn and wheat ash samples, which can negatively affect the performance of concrete specimens if not removed through pretreatment (Ataie et al., 2013; Teymouri & Shakouri, 2023). Additionally, the presence of alkalis can reduce pore solution resistivity, suggesting that mixtures may appear less durable through electrical resistivity testing than they actually are (Bu & Weiss, 2014). The presence of impurities like chlorides and sulphates can also decrease electrical resistivity (Saleem et al., 1996).

6.3.2 Variability in mortar strength and densification

The variability among materials is additionally seen in compressive strength data, presented in Figures 6-9 and 6-10. For reference, the 28-day compressive strength of PLC control samples was 3982 ± 335 psi. The box and whisker plots are helpful to showing the variability within a sample set. For example, the largest variability is in 10% corn ash cubes where strengths ranged from 2745 psi to 4777 psi, as seen by the whiskers in Figure 6-9. A 42.5% spread in 28-day compressive strength based on source location is occurred in 20% corn ash cubes (Figures 6-9 and 6-10). The same trend is not observed for wheat ash cubes. The smallest spread of data is seen in the 28-day compressive

strengths of 20% corn cubes at 23.5% (Figure 6-9). An inner quartile range of 623 psi (20% corn 28-day strengths) likely is not significant, but a range of 1933 psi (10% corn 56-day strengths) could be.

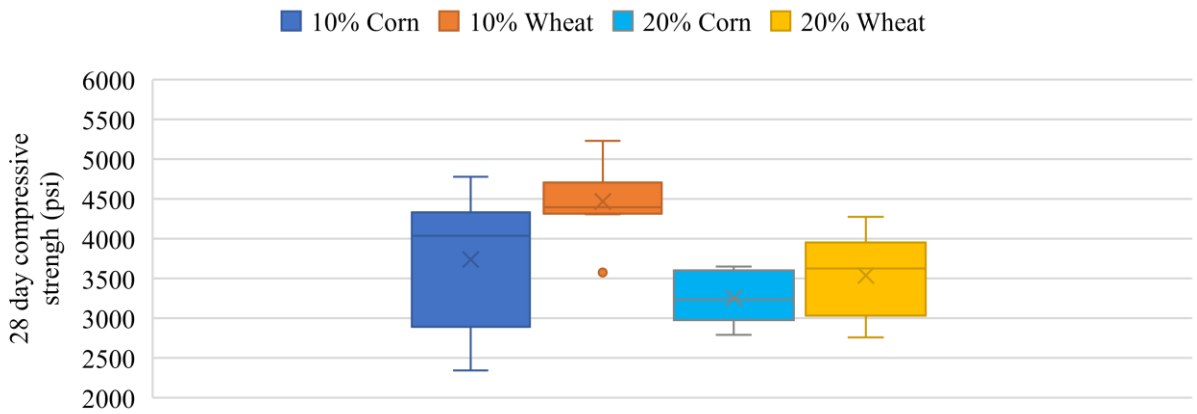

Figure 6-9: 28-day compressive strength variability of cubes containing 10% or 20% replacements of PLC with wheat or corn ash, by volume. Box and whisker plots show the mean (shown by the x), minimum, first quartile, median, third quartile, and maximum value of strength values across samples from the three different locations.

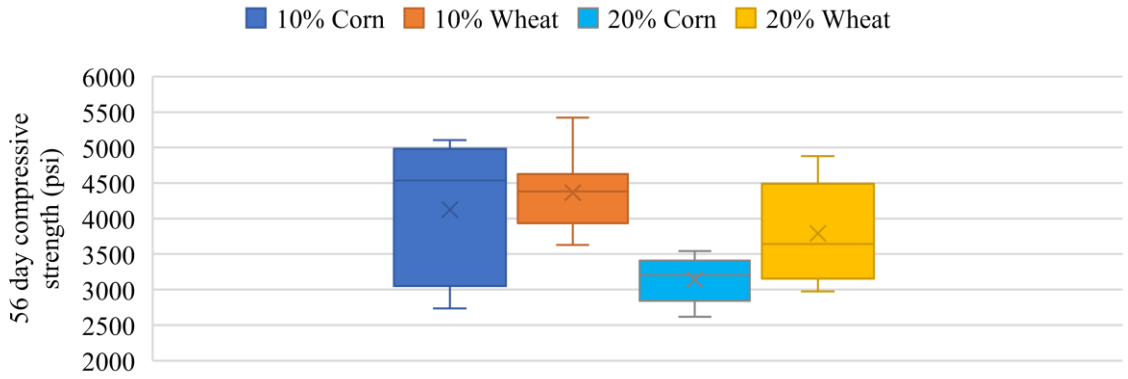

Figure 6-10: 56-day compressive strength variability of cubes containing 10% or 20% replacements of PLC with wheat or corn ash, by volume. Box and whisker plots show the mean (shown by the x), minimum, first quartile, median, third quartile, and maximum value of strength values across samples from the three different locations.

No correlation is found between 28-day or 56-day compressive strength and any characterization variable, for example, strength is not definitively controlled by chemical composition of the ash, particle size, or loss on ignition. At 56 days, there is a statistical difference between corn samples based on source location at 10% substitution using one way ANOVA hypothesis testing. In ANOVA hypothesis testing a p value <0.05 indicates statistical significance. The 10% corn sample p-value = 0.002, when comparing samples from the different geographical regions, suggesting that regional variability is statistically significant in this case (Table 6-4). Additionally, ANOVA hypothesis testing provides a p-value of 0.02 among 20% wheat samples, again supporting that there is statistically significant difference between the regional locations. Variability between samples produced using 10% wheat and 20% corn were not significantly different.

Electrical bulk resistivity and calcium hydroxide consumption data show variability indicating changes in the evolution of pore structure and pozzolanic reactivity associated with each material's source location (Figures 6-11 and 6-12). ANOVA hypothesis testing confirmed that there is significant variability between source locations for each type of material at 56 days at its respective substitution percentage (Table 6-4). Variability in bulk electrical resistivity values show relatively more consistent data with 10% wheat substitution and 20% corn substitution cubes. Significance in bulk electrical resistivity values are better quantified using ANOVA hypothesis testing, but there are visibly large ranges shown in the box and whisker plots for 10% corn samples and 20% wheat samples that could likely be linked to changes in other properties.

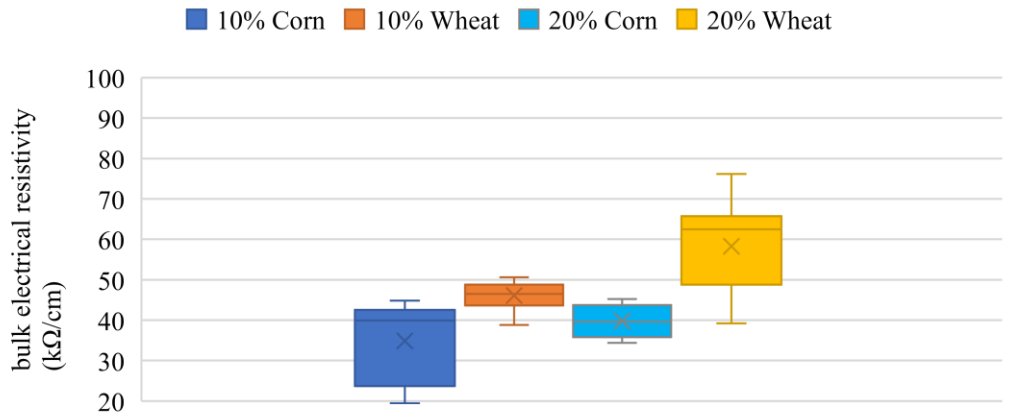

Figure 6-11: 28-day bulk electrical resistivity variability of cubes containing 10% or 20% replacements of PLC with wheat or corn ash, by volume. Box and whisker plots show the mean (shown by the x), minimum, first quartile, median, third quartile, and maximum values across samples from the three different locations.

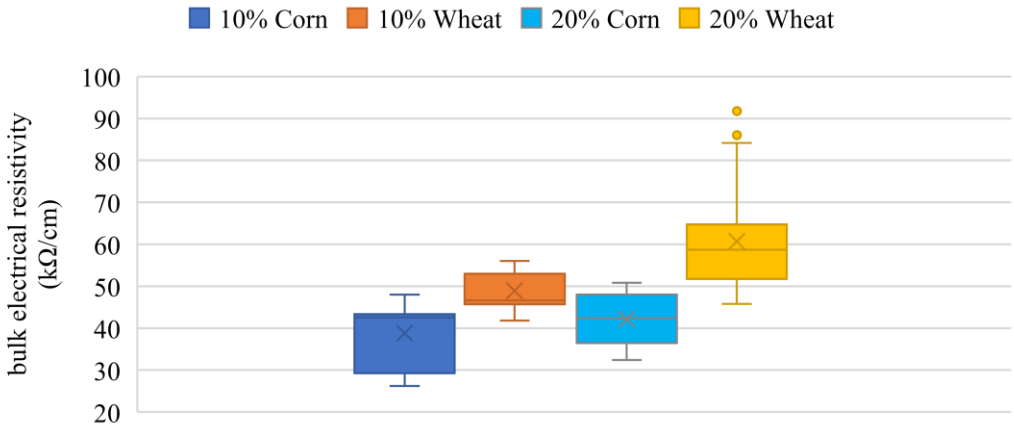

Figure 6-12: 56-day bulk electrical resistivity variability of cubes containing 10% or 20% replacements of PLC with wheat or corn ash, by volume. Box and whisker plots show the mean (shown by the x), minimum, first quartile, median, third quartile, and maximum values across samples from the three different locations.

Electrical resistivity could be increasing due to pozzolanic reactions, creating C-S-H and therefore introducing tortuosity and changes in porosity to the pore structure.

SCMs are generally known to increase bulk resistivity for that reason (Nadelman & Kurtis, 2014; Scrivener et al., 2015). Resistivity measurements cannot fully conclude that the material is reacting pozzolanically, but only that there are changes in chemistry or microstructure. However, reductions in calcium hydroxide shown in Figures 5-19 through 5-24 also support the conclusion that the agricultural ashes are reacting pozzolanically within the cementitious mixtures.

Table 6-4: Results of one way ANOVA hypothesis testing.

Test	Comparison	P-Value (<0.05 indicates statistical significance)
56-day compressive strength	10% corn ash (3 locations)	0.02
	10% wheat ash (3 locations)	0.44
	20% corn ash (2 locations)	0.21
	20% wheat ash (3 locations)	0.02
56-day bulk electrical resistivity	10% corn ash (3 locations)	6.93E-25
	10% wheat ash (3 locations)	7.00E-15
	20% corn ash (2 locations)	2.39E-9
	20% wheat ash (3 locations)	9.00E-9
56-day CH content	Across all samples	0.00

Variability among agricultural material sources was assessed through comparing soil composition, ash composition, and selected performance results. The differences in ash chemistry varied enough to cause changes to the material's interaction in

cementitious systems. This variability has been shown to affect compressive strength development significantly in some cases. However, variability across material sources is not as great as variability between unique materials. This variability is most evident material composition differences, and it indicates that some materials may have better performance in strength and durability measures than others.

6.4 Recommendations for Code Implementation

The requirements for a calcined natural pozzolan listed in ASTM C618-22 are general enough to allow calcined agricultural materials to be considered a Class N pozzolan. The composition requirements for a Class N pozzolan require that it must be at least 70.0% silicon dioxide plus aluminum oxide plus iron oxide. For Class F and Class C fly ashes, this requirement is 50.0%, making the standard 20% higher for Class N. Additionally, the composition cannot contain more than 4.0% sulfur trioxide. The moisture content must be less than 3.0%, and the LOI must be less than 10.0%. The physical requirements are not as restrictive to these materials since these can be easily controlled in the preparation process. The chemical requirements could be a challenge for materials like hemp that are not naturally high in silica and its use as filler may not be of great interest to producers or industry who would prefer an SCM with reactivity. However, simple pretreatments including water soaking can help to remove impurities and improve the chemistry of the material, if producers or suppliers are willing take the extra step. The advantage of agricultural and natural SCMs is that fly ash and industrial

SCM supplies are not as plentiful as they once were. To ensure specific code updates are implemented for various types of natural SCMs, there must be a better understanding of long-term performance of these materials, durability testing, and a stronger connection between industries that currently do not interact frequently.

Chapter 7: Conclusions

7.1 Conclusion

This study focused on the viability of three agricultural materials to serve as low-cost supplementary cementitious materials to supplement the fly ash supply. In-depth characterization testing and performance testing were conducted to assess the potential and reactivity of these materials in cementitious systems.

Ash preparation components included pretreatment of the material, calcination, and milling. Chemical pretreatments were effective at removing impurities and reducing material LOI. Of the acids tested, there was no conclusive optimal choice. Further analysis of acid-treated ash on cement hydration and strength development are required to make that decision. Acid pretreatment will introduce energy cost and safety considerations to the preparation procedure, therefore it is advised only when necessary. Calcination allows the producer to reduce the volume of the material into a reactive ash. The challenge is to balance removing as much cellulose and hemicellulose (and other polysaccharides) as possible while not crystalizing the silica in the material. A calcination temperature of 500 °C is sufficient for corn and wheat materials, but a higher temperature is recommended for hemp hurd due to its high LOI remaining after calcination at 500 °C.

A two-hour calcination length is adequate so long as the material has ample airflow. Ball milling is necessary to reducing the particle size of the material to near that of cement.

Hemp hurd has naturally poor chemistry for reactivity due to its low silica content, making it unlikely to meet the chemical requirements of ASTM C618 without chemical pretreatment. The market for hemp in the United States is growing, yet small relative to wheat and corn. The use of hemp as substitute for cement is cautiously recommended at 5% substitution due to its low reactivity and high absorption. Wheat straw and corn stover naturally have high amounts of silica, and are more likely to meet the chemical requirements for ASTM C618 without chemical pretreatment. They have well-established markets in the United States. Corn stover and wheat straw ash are recommended to partially replace up to 10% of the cement volume for strength improvements, and up to 20% substitution for durability improvements. However, significant retardation in wheat straw samples may necessitate the use of an accelerator. Due to the porous nature of the ash microstructure, agricultural ashes tended to absorb water and reduce workability of mortar and will require superplasticizer use. Variability in material chemistry and performance across source locations is significant in some measures, including reactivity. However, due to the environmental impact of reducing cement content and using another industry's waste, the use of agricultural materials as SCMs is beneficial and sustainable.

7.2 Future Work

Implementation remains a challenge for agricultural biomass ashes to be desirable to industry. Acceptance of a new material takes time and familiarity, as well as an established understanding of the performance of the materials in cementitious systems. Of the three materials tested, wheat straw has the most published literature on use in cementitious systems, with only limited studies on the use hemp hurd in cementitious systems. However, these materials require further investigation on durability and standardization of treatment techniques to reduce variability for industry comfort to grow. A relevant durability concern for natural pozzolans with high alkali content is susceptibility to alkali silica reaction. Additionally, large-scale testing would provide further insight into the workability, constructability, and consistency of freshly mixed concrete using agricultural biomass ashes. Substantial investigation should continue to validate and further the results of this study.

Bibliography

A. Sluiter, B. H. R. R. C. S. J. S. D. T. and D. C. (n.d.). *Determination of Structural Carbohydrates and Lignin in Biomass. Laboratory Analytical Procedure (LAP)* .

Abbas, S., Kazmi, S. M. S., & Munir, M. J. (2017). Potential of rice husk ash for mitigating the alkali-silica reaction in mortar bars incorporating reactive aggregates. *Construction and Building Materials*, *132*, 61–70. https://doi.org/10.1016/j.conbuildmat.2016.11.126

Acarturk, B. C., Sandalci, I., Hull, N., Bundur, Z. B., & Burris, L. (n.d.). Calcium Sulfoaluminate Cement and Supplementary Cementitious Materials-Containing Binders in Self-Healing Systems. *Cement and Concrete Composites: In Review*.

Aggoun, S., Cheikh-Zouaoui, M., Chikh, N., & Duval, R. (2008). Effect of some admixtures on the setting time and strength evolution of cement pastes at early ages. *Construction and Building Materials*, *22*(2), 106–110. https://doi.org/10.1016/j.conbuildmat.2006.05.043

Air Resources Board 1998. (1999). *The 1997 Biennial Report to the Legislature—Progress Report on the Phase Down of Rice Straw Burning in the Sacramento Valley.*

Al-Akhras, N. M., & Abu-Alfoul, B. A. (2002). *Effect of wheat straw ash on mechanical properties of autoclaved mortar*.

Alloway, B. J. (2013). *Heavy Metals in Soils*. http://www.springer.com/series/5929

Álvarez, C., Mullen, A. M., Pojić, M., Hadnađev, T. D., & Papageorgiou, M. (2021). Classification and target compounds. *Food Waste Recovery: Processing Technologies, Industrial Techniques, and Applications*, 21–49. https://doi.org/10.1016/B978-0-12-820563-1.00024-X

American Concrete Institute, & ACI Committee 232. (n.d.). *Report on the Use of Raw or Processed Natural Pozzolans in Concrete*.

Amin, M., Murtaza, T., Shahzada, K., Khan, K., & Adil, M. (2019). Pozzolanic Potential and Mechanical Performance of Wheat Straw Ash Incorporated Sustainable Concrete. *Sustainability*, *11*(2), 519. https://doi.org/10.3390/su11020519

Amin, M. N., Siffat, M. A., Shahzada, K., & Khan, K. (2022). Influence of Fineness of Wheat Straw Ash on Autogenous Shrinkage and Mechanical Properties of Green Concrete. *Crystals*, *12*(5), 588. https://doi.org/10.3390/cryst12050588

Andrade Neto, J. da S., De la Torre, A. G., & Kirchheim, A. P. (2021). Effects of sulfates on the hydration of Portland cement – A review. *Construction and Building Materials*, *279*, 122428. https://doi.org/10.1016/j.conbuildmat.2021.122428

Andrew, R. M. (2019). Global CO2 emissions from cement production, 1928–2018. *Earth System Science Data*, *11*(4), 1675–1710. https://doi.org/10.5194/essd-11-1675-2019

Angelova, V., Ivanova, R., Delibaltova, V., & Ivanov, K. (2004). Bio-accumulation and distribution of heavy metals in fibre crops (flax, cotton and hemp). *Industrial Crops and Products*, *19*(3), 197–205. https://doi.org/10.1016/j.indcrop.2003.10.001

Aprianti, E., Shafigh, P., Bahri, S., & Farahani, J. N. (2015). Supplementary cementitious materials origin from agricultural wastes - A review. In *Construction and Building Materials* (Vol. 74, pp. 176–187). Elsevier Ltd. https://doi.org/10.1016/j.conbuildmat.2014.10.010

Arunrat, N., Pumijumnong, N., & Sereenonchai, S. (2018). Air-Pollutant Emissions from Agricultural Burning in Mae Chaem Basin, Chiang Mai Province, Thailand. *Atmosphere*, *9*(4), 145. https://doi.org/10.3390/atmos9040145

ASTM. (2012). Standard Test Method for Bulk Electrical Resistivity or Bulk Conductivity of Concrete. In *ASTM International: Vol. i* (Issue c).

ASTM. (2013). ASTM C1437 - Standard test method for flow of hydraulic cement mortar. In *ASTM International*.

ASTM. (2014). ASTM C1679-14 Standard Practice for Measuring Hydration Kinetics of Hydraulic Cementitious Mixtures Using Isothermal Calorimetry. In *ASTM International*.

ASTM. (2015). Standard Test Method for Specific Gravity and Absorption of Fine Aggregate, ASTM C128. *ASTM International*, *15*.

ASTM. (2017). ASTM C778 Standard Specification for Standard Sand. *ASTM International*, *C*.

ASTM. (2019a). ASTM C150 / C150M-19a Standard Specification for Portland Cement. *ASTM International*.

ASTM. (2019b). ASTM C595/C595M-Standard Specification for Blended Hydraulic Cements. In *ASTM International*.

ASTM. (2020a). ASTM C109 / C109M - 20b. Standard Test Method for Compressive Strength of Hydraulic Cement Mortars (Using 2-in. or [50 mm] Cube Specimens). In *ASTM International* (Vol. 04).

ASTM. (2020b). *ASTM C1827-20: Standard Test Method for Determination of the Air-Entraining Admixture Demand of a Cementitious Mixture*.

ASTM. (2020c). Standard Test Methods for Measuring the Reactivity of Supplementary Cementitious Materials by Isothermal Calorimetry and Bound Water Measurements. *ASTM International*, *04*.

ASTM. (2022). ASTM C618 − 22 Standard Specification for Coal Fly Ash and Raw or Calcined Natural Pozzolan for Use in Concrete 1. *ASTM International*. https://doi.org/10.1520/C0618-22

Ataie, F. F., Asce, A. M., Riding, K. A., & Asce, M. (2013). *Thermochemical Pretreatments for Agricultural Residue Ash Production for Concrete*. https://doi.org/10.1061/(ASCE)MT

Ataie, F. F., & Riding, K. A. (2014a). Use of bioethanol byproduct for supplementary cementitious material production. *Construction and Building Materials*, *51*, 89–96. https://doi.org/10.1016/J.CONBUILDMAT.2013.10.092

Ataie, F. F., & Riding, K. A. (2014b). Impact of pretreatments and enzymatic hydrolysis on agricultural residue ash suitability for concrete. *Construction and Building Materials*, *58*, 25–30. https://doi.org/10.1016/J.CONBUILDMAT.2014.01.099

Ataie, F. F., & Riding, K. A. (2016). Influence of agricultural residue ash on early cement hydration and chemical admixtures adsorption. *Construction and Building Materials*, *106*, 274–281. https://doi.org/10.1016/j.conbuildmat.2015.12.091

B., S., Patil, N., Jaiswal, K. K., Gowrishankar, T. P., Selvakumar, K. K., Jyothi, M. S., Jyothilakshmi, R., & Kumar, S. (2023). Development of sustainable alternative materials for the construction of green buildings using agricultural residues: A review. *Construction and Building Materials*, *368*, 130457. https://doi.org/10.1016/j.conbuildmat.2023.130457

Balat, M., Balat, H., & Öz, C. (2008). Progress in bioethanol processing. *Progress in Energy and Combustion Science*, *34*(5), 551–573. https://doi.org/10.1016/j.pecs.2007.11.001

Bermudez, G. M. A., Jasan, R., Plá, R., & Pignata, M. L. (2011). Heavy metal and trace element concentrations in wheat grains: Assessment of potential non-carcinogenic health hazard through their consumption. *Journal of Hazardous Materials*, *193*, 264–271. https://doi.org/10.1016/J.JHAZMAT.2011.07.058

Berodier, E., & Scrivener, K. (2014). Understanding the Filler Effect on the Nucleation and Growth of C-S-H. *Journal of the American Ceramic Society*, *97*(12), 3764–3773. https://doi.org/10.1111/jace.13177

Bheel, N., Sohu, S., Awoyera, P., Kumar, A., Abbasi, S. A., & Olalusi, O. B. (2021). Effect of Wheat Straw Ash on Fresh and Hardened Concrete Reinforced with Jute Fiber. *Advances in Civil Engineering*, *2021*, 1–11. https://doi.org/10.1155/2021/6659125

Binici, H., Yucegok, ; Faruk, Orhan Aksogan, ;, & Kaplan, H. (2008). Effect of Corncob, Wheat Straw, and Plane Leaf Ashes as Mineral Admixtures on Concrete Durability. *ASCE*. https://doi.org/10.1061/ASCE0899-1561200820:7478

Biricik, H., Aköz, F., Berktay, L., & Tulgar, A. N. (1999). Study of pozzolanic properties of wheat straw ash. In *Cement and Concrete Research* (Vol. 29).

Bish, D. L., & Howard, S. A. (1988). Quantitative phase analysis using the Rietveld method. *Journal of Applied Crystallography*, *21*(2), 86–91. https://doi.org/10.1107/S0021889887009415

Bish, D. L., & Reynolds, R. C. (1989). 4. SAMPLE PREPARATION FOR X-RAY DIFFRACTION. In *Reviews in Mineralogy* (pp. 73–99). https://doi.org/10.1515/9781501509018-007

Bokhari, S. M. Q., Chi, K., & Catchmark, J. M. (2021). Structural and physico-chemical characterization of industrial hemp hurd: Impacts of chemical pretreatments and mechanical refining. *Industrial Crops and Products*, *171*, 113818. https://doi.org/10.1016/J.INDCROP.2021.113818

Bonifacio, A. L., & Archbold, P. (2022). The effect of calcination conditions on oat husk ash pozzolanic activity. *Materials Today: Proceedings*, *65*, 622–628. https://doi.org/10.1016/j.matpr.2022.03.197

Bruun, S., Jensen, J. W., Magid, J., Lindedam, J., & Engelsen, S. B. (2010). Prediction of the degradability and ash content of wheat straw from different cultivars using near

infrared spectroscopy. *Industrial Crops and Products*, *31*(2), 321–326. https://doi.org/10.1016/j.indcrop.2009.11.011

Bu, Y., & Weiss, J. (2014). The influence of alkali content on the electrical resistivity and transport properties of cementitious materials. *Cement and Concrete Composites*, *51*, 49–58. https://doi.org/10.1016/j.cemconcomp.2014.02.008

Cao, Y., Guo, L., Chen, B., & Wu, J. (2021). Effect of pre-introduced sodium chloride on cement hydration process. *Advances in Cement Research*, *33*(12), 526–539. https://doi.org/10.1680/jadcr.19.00159

CemNet.com. (2023, February 8). *US production and consumption increased in 2022*. CemNet.

Chakraborty, S., Kundu, S. P., Roy, A., Adhikari, B., & Majumder, S. B. (2013). Effect of Jute as Fiber Reinforcement Controlling the Hydration Characteristics of Cement Matrix. *Industrial & Engineering Chemistry Research*, *52*(3), 1252–1260. https://doi.org/10.1021/ie300607r

Chandrasekhar, S., Pramada, P. N., & Majeed, J. (2006). Effect of calcination temperature and heating rate on the optical properties and reactivity of rice husk ash. *Journal of Materials Science*, *41*(23), 7926–7933. https://doi.org/10.1007/s10853-006-0859-0

Charai, M., Sghiouri, H., Mezrhab, A., & Karkri, M. (2021). Thermal insulation potential of non-industrial hemp (Moroccan cannabis sativa L.) fibers for green plaster-based building materials. *Journal of Cleaner Production*, *292*. https://doi.org/10.1016/j.jclepro.2021.126064

Chen, Z., Xu, Y., & Shivkumar, S. (2018). Microstructure and tensile properties of various varieties of rice husk. *Journal of the Science of Food and Agriculture*, *98*(3), 1061–1070. https://doi.org/10.1002/jsfa.8556

Chindaprasirt, P., Kanchanda, P., Sathonsaowaphak, A., & Cao, H. T. (2007). Sulfate resistance of blended cements containing fly ash and rice husk ash. *Construction and Building Materials*, *21*(6), 1356–1361. https://doi.org/10.1016/j.conbuildmat.2005.10.005

Christensen, B. J., Coverdale, T., Olson, R. A., Ford, S. J., Garboczi, E. J., Jennings, H. M., & Mason, T. O. (1994). Impedance Spectroscopy of Hydrating Cement-Based Materials: Measurement, Interpretation, and Application. *Journal of the American Ceramic Society*, *77*(11), 2789–2804. https://doi.org/10.1111/j.1151-2916.1994.tb04507.x

Chusilp, N., Jaturapitakkul, C., & Kiattikomol, K. (2009). Effects of LOI of ground bagasse ash on the compressive strength and sulfate resistance of mortars. *Construction and Building Materials*, *23*(12), 3523–3531. https://doi.org/10.1016/j.conbuildmat.2009.06.046

Cordeiro, G. C., & Kurtis, K. E. (2017). Effect of mechanical processing on sugar cane bagasse ash pozzolanicity. *Cement and Concrete Research*, *97*, 41–49. https://doi.org/10.1016/j.cemconres.2017.03.008

Custodio, M., Peñaloza, R., Cuadrado, W., Ochoa, S., Álvarez, D., & Chanamé, F. (2021). Data on the detection of essential and toxic metals in soil and corn and barley grains by atomic absorption spectrophotometry and their effect on human health. *Chemical Data Collections*, *32*, 100650. https://doi.org/10.1016/J.CDC.2021.100650

Deshmukh, P., Bhatt, J., Peshwe, D., & Pathak, S. (2012). Determination of Silica Activity Index and XRD, SEM and EDS Studies of Amorphous SiO2 Extracted from Rice Husk Ash. *Transactions of the Indian Institute of Metals*, *65*(1), 63–70. https://doi.org/10.1007/s12666-011-0071-z

Doebelin, N., & Kleeberg, R. (2015). *Profex* : a graphical user interface for the Rietveld refinement program *BGMN*. *Journal of Applied Crystallography*, *48*(5), 1573–1580. https://doi.org/10.1107/S1600576715014685

Doudart De La Grée, G. C. H., Yu, Q. L., & Brouwers, H. J. H. (2015, June). *THE EFFECT OF GLUCOSE ON THE HYDRATION KINETICS OF ORDINARY PORTLAND CEMENT*.

Eggeman, T., & Elander, R. T. (2005). Process and economic analysis of pretreatment technologies. *Bioresource Technology*, *96*(18), 2019–2025. https://doi.org/10.1016/J.BIORTECH.2005.01.017

Falah, F., Adly, M., Lubis, R., Triastuti, W., Fatriasari, F., & Puspita, S. (2020). Utilization of Lignin from the Waste of Bioethanol Production as a Mortar Additive. *Jurnal Sylva Lestari ISSN*, *8*(3), 326–339.

FAO. (2019). *Forest Products Annual Market Review*.

FAO Stat. (2020). *Emissions Totals* .

Fatma, S., Hameed, A., Noman, M., Ahmed, T., Shahid, M., Tariq, M., Sohail, I., & Tabassum, R. (2018). Lignocellulosic Biomass: A Sustainable Bioenergy Source for the Future. *Protein & Peptide Letters*, *25*(2), 148–163. https://doi.org/10.2174/0929866525666180122144504

Feng, Q., Yamamichi, H., Shoya, M., & Sugita, S. (2004). Study on the pozzolanic properties of rice husk ash by hydrochloric acid pretreatment. *Cement and Concrete Research*, *34*(3), 521–526. https://doi.org/10.1016/j.cemconres.2003.09.005

Flower, D. J. M., & Sanjayan, J. G. (2007). Green house gas emissions due to concrete manufacture. *The International Journal of Life Cycle Assessment*, *12*(5), 282–288. https://doi.org/10.1065/lca2007.05.327

Friedlingstein, P., O'Sullivan, M., Jones, M. W., Andrew, R. M., Gregor, L., Hauck, J., Le Quéré, C., Luijkx, I. T., Olsen, A., Peters, G. P., Peters, W., Pongratz, J., Schwingshackl, C., Sitch, S., Canadell, J. G., Ciais, P., Jackson, R. B., Alin, S. R., Alkama, R., … Zheng, B. (2022). Global Carbon Budget 2022. *Earth System Science Data*, *14*(11), 4811–4900. https://doi.org/10.5194/essd-14-4811-2022

FWHA. (n.d.). *User Guidelines for Waste and Byproduct Materials in Pavement Construction*.

Galbe, M., & Zacchi, G. (2012). Pretreatment: The key to efficient utilization of lignocellulosic materials. *Biomass and Bioenergy*, *46*, 70–78. https://doi.org/10.1016/J.BIOMBIOE.2012.03.026

García-Segura, T., Yepes, V., & Alcalá, J. (2014). Life cycle greenhouse gas emissions of blended cement concrete including carbonation and durability. *The International Journal of Life Cycle Assessment*, *19*(1), 3–12. https://doi.org/10.1007/s11367-013-0614-0

Gineys, N., Aouad, G., & Damidot, D. (2010). Managing trace elements in Portland cement – Part I: Interactions between cement paste and heavy metals added during mixing as soluble salts. *Cement and Concrete Composites*, *32*(8), 563–570. https://doi.org/10.1016/j.cemconcomp.2010.06.002

Gu, H. (2009). Tensile behaviours of the coir fibre and related composites after NaOH treatment. *Materials & Design*, *30*(9), 3931–3934. https://doi.org/10.1016/j.matdes.2009.01.035

Gümüşkaya, E., Usta, M., & Balaban, M. (2007). Carbohydrate components and crystalline structure of organosolv hemp (Cannabis sativa L.) bast fibers pulp. *Bioresource Technology*, *98*(3), 491–497. https://doi.org/10.1016/j.biortech.2006.02.031

Guo, A., Sun, Z., Qi, C., & Sathitsuksanoh, N. (2020). Hydration of Portland Cement Pastes Containing Untreated and Treated Hemp Powders. *Journal of Materials in Civil Engineering*, *32*(6). https://doi.org/10.1061/(ASCE)MT.1943-5533.0003209

Gusovius, H.-J., Lühr, C., Hoffmann, T., Pecenka, R., & Idler, C. (2019). An Alternative to Field Retting: Fibrous Materials Based on Wet Preserved Hemp for the Manufacture of Composites. *Agriculture*, *9*(7), 140. https://doi.org/10.3390/agriculture9070140

Gutteridge, W. A., & Dalziel, J. A. (1990). Filler cement: The effect of the secondary component on the hydration of Portland cement. *Cement and Concrete Research*, *20*(5), 778–782. https://doi.org/10.1016/0008-8846(90)90011-L

Hasparyk, N. P., Monterio, P. J. M., & Carasek, H. (2000). Effect of Silica Fume and Rice Husk Ash on Alkali-Silica Reaction. *ACI Structural Journal*, *97*(4), 486–492.

H.C. Visvesvaraya. (1986). Recycling of Agricultural Wastes with Special Emphasis on Rice Husk Ash. *Use of Vegetable Plants and Fibres as Building Materials Joint Symposium RILEM/CIB/NCCL*, 1–22.

Hendriks, C. A., Worrell, E., de Jager, D., Blok, K., & Riemer, P. (2004). *Emission Reduction of Greenhouse Gases from the Cement Industry*. http://www.ieagreen.org.uk/prghgt42.htm

Hocking, P. J., & McLaughlin, M. J. (2000). Genotypic variation in cadmium accumulation by seed of linseed, and comparison with seeds of some other crop species. *Australian Journal of Agricultural Research*, *51*(4). https://doi.org/10.1071/AR99124

Ismail, M. S., & Waliuddin, A. M. (1996). Effect of rice husk ash on high strength concrete. *Construction and Building Materials*, *10*(7), 521–526. https://doi.org/10.1016/0950-0618(96)00010-4

Jimoh, Y., & Apampa, O. (2013). An Evaluation of the Energy Consumption and Co2 Emission associated with Corn Cob Ash Compared with the Cement Clinker. *Civil and Environmental Research*, *3*(2).

Jo, B. W., & Chakraborty, S. (2015). A mild alkali treated jute fibre controlling the hydration behaviour of greener cement paste. *Scientific Reports*, *5*. https://doi.org/10.1038/srep07837

Jonathan Hilburg. (2019, January 2). Concrete production produces eight percent of the world's carbon dioxide emissions. *The Architect's Newspaper*.

Jorge, F. C., Pereira, C., & Ferreira, J. M. F. (2004). Wood-cement composites: a review. *Holz Als Roh- Und Werkstoff*, *62*(5), 370–377. https://doi.org/10.1007/s00107-004-0501-2

Kabir, M. M., Wang, H., Lau, K. T., & Cardona, F. (2013). Effects of chemical treatments on hemp fibre structure. *Applied Surface Science*, *276*, 13–23. https://doi.org/10.1016/J.APSUSC.2013.02.086

Kaiser, M. L., Williams, M. L., Basta, N., Hand, M., & Huber, S. (2015). When Vacant Lots Become Urban Gardens: Characterizing the Perceived and Actual Food Safety Concerns of Urban Agriculture in Ohio. *Journal of Food Protection, 78*(11), 2070–2080. https://doi.org/10.4315/0362-028X.JFP-15-181

Kaleli, M. J., Kamweru, P. K., Gichumbi, J. M., & Ndiritu, F. G. (2020). Characterization of rice husk ash prepared by open air burning and furnace calcination. *Journal of Chemical Engineering and Materials Science*, *11*(2), 24–30. https://doi.org/10.5897/jcems2020.0348

Karam, R., Becquart, F., Abriak, N.-E., & Khouja, H. (2021). Vapothermal curing of hemp shives: Influence on some chemical and physical properties. *Industrial Crops and Products*, *171*, 113870. https://doi.org/10.1016/j.indcrop.2021.113870

Kasaniya, M., & Thomas, M. D. A. (2022). Role of the alkalis of supplementary cementing materials in controlling pore solution chemistry and alkali-silica reaction. *Cement and Concrete Research*, *162*, 107007. https://doi.org/10.1016/j.cemconres.2022.107007

Katman, H. Y. B., Khai, W. J., Bheel, N., Kırgız, M. S., Kumar, A., Khatib, J., & Benjeddou, O. (2022). Workability, Strength, Modulus of Elasticity, and Permeability Feature of Wheat Straw Ash-Incorporated Hydraulic Cement Concrete. *Buildings*, *12*(9), 1363. https://doi.org/10.3390/buildings12091363

Kevern, J. T., & Wang, K. (2010). *Investigation of Corn Ash as a Supplementary Cementitious Material in Concrete*. http://www.claisse.info/Proceedings.htm

Khatri, R. P., Sirivivatnanon, V., & Gross, W. (1995). Effect of different supplementary cementitious materials on mechanical properties of high performance concrete. *Cement and Concrete Research*, *25*(1), 209–220. https://doi.org/10.1016/0008-8846(94)00128-L

Kiran, Bharti, R., & Sharma, R. (2022). Effect of heavy metals: An overview. *Materials Today: Proceedings*, *51*, 880–885. https://doi.org/10.1016/J.MATPR.2021.06.278

Krishnarao, R. V., Subrahmanyam, J., & Jagadish Kumar, T. (2001). Studies on the formation of black particles in rice husk silica ash. *Journal of the European Ceramic Society*, *21*(1), 99–104. https://doi.org/10.1016/S0955-2219(00)00170-9

Kuglarz, M., Alvarado-Morales, M., Karakashev, D., & Angelidaki, I. (2016). Integrated production of cellulosic bioethanol and succinic acid from industrial hemp in a

biorefinery concept. *Bioresource Technology*, *200*, 639–647. https://doi.org/10.1016/j.biortech.2015.10.081

K.V. Sarkanen, C. H. L. (1971). Lignins, Occurrence, Formation, Structure and Reactions. *Wiley-Interscience*.

Larsson, S., Palmqvist, E., Hahn-Hägerdal, B., Tengborg, C., Stenberg, K., Zacchi, G., & Nilvebrant, N.-O. (1999). The generation of fermentation inhibitors during dilute acid hydrolysis of softwood. *Enzyme and Microbial Technology*, *24*(3–4), 151–159. https://doi.org/10.1016/S0141-0229(98)00101-X

le Ngoc Huyen, T., Queneudec T'Kint, M., Remond, C., Chabbert, B., & Dheilly, R.-M. (2011). Saccharification of Miscanthus x giganteus, incorporation of lignocellulosic by-product in cementitious matrix. *Comptes Rendus Biologies*, *334*(11), 837.e1-837.e11. https://doi.org/10.1016/j.crvi.2011.07.008

Li, G., Zhou, C., Ahmad, W., Usanova, K. I., Karelina, M., Mohamed, A. M., & Khallaf, R. (2022). Fly Ash Application as Supplementary Cementitious Material: A Review. *Materials*, *15*(7), 2664. https://doi.org/10.3390/ma15072664

Li, X., Snellings, R., Antoni, M., Alderete, N. M., Ben Haha, M., Bishnoi, S., Cizer, Ö., Cyr, M., De Weerdt, K., Dhandapani, Y., Duchesne, J., Haufe, J., Hooton, D., Juenger, M., Kamali-Bernard, S., Kramar, S., Marroccoli, M., Joseph, A. M., Parashar, A., … Scrivener, K. L. (2018). Reactivity tests for supplementary cementitious materials: RILEM TC 267-TRM phase 1. *Materials and Structures/Materiaux et Constructions*, *51*(6). https://doi.org/10.1617/s11527-018-1269-x

Li, Z., Afshinnia, K., & Rangaraju, P. R. (2016). Effect of alkali content of cement on properties of high performance cementitious mortar. *Construction and Building Materials*, *102*, 631–639. https://doi.org/10.1016/j.conbuildmat.2015.10.110

Lim, J. S., Abdul Manan, Z., Wan Alwi, S. R., & Hashim, H. (2012). A review on utilisation of biomass from rice industry as a source of renewable energy. *Renewable and Sustainable Energy Reviews*, *16*(5), 3084–3094. https://doi.org/10.1016/J.RSER.2012.02.051

Liu, M., Fernando, D., Daniel, G., Madsen, B., Meyer, A. S., Ale, M. T., & Thygesen, A. (2015). Effect of harvest time and field retting duration on the chemical composition, morphology and mechanical properties of hemp fibers. *Industrial Crops and Products*, *69*, 29–39. https://doi.org/10.1016/j.indcrop.2015.02.010

Liu, X., Ma, B., Tan, H., Gu, B., Zhang, T., Chen, P., Li, H., & Mei, J. (2020). Effect of aluminum sulfate on the hydration of Portland cement, tricalcium silicate and

tricalcium aluminate. *Construction and Building Materials*, *232*, 117179. https://doi.org/10.1016/j.conbuildmat.2019.117179

Lizotte, P.-L., Savoie, P., & de Champlain, A. (2015). Ash Content and Calorific Energy of Corn Stover Components in Eastern Canada. *Energies*, *8*(6), 4827–4838. https://doi.org/10.3390/en8064827

Lu, F., & Ralph, J. (2010). Lignin. *Cereal Straw as a Resource for Sustainable Biomaterials and Biofuels: Chemistry, Extractives, Lignins, Hemicelluloses and Cellulose*, 169–207. https://doi.org/10.1016/B978-0-444-53234-3.00006-7

Marangu, J. M., Muturia M'thiruaine, C., & Bediako, M. (2020). Physicochemical Properties of Hydrated Portland Cement Blended with Rice Husk Ash. *Journal of Chemistry*, *2020*, 1–10. https://doi.org/10.1155/2020/5304745

Martirena, F., & Monzó, J. (2018). Vegetable ashes as Supplementary Cementitious Materials. In *Cement and Concrete Research* (Vol. 114, pp. 57–64). Elsevier Ltd. https://doi.org/10.1016/j.cemconres.2017.08.015

Memon, S. A., Javed, U., Haris, M., Khushnood, R. A., & Kim, J. (2021). Incorporation of Wheat Straw Ash as Partial Sand Replacement for Production of Eco-Friendly Concrete. *Materials*, *14*(8), 2078. https://doi.org/10.3390/ma14082078

Memon, S. A., & Khan, M. K. (2018). Ash blended cement composites: Eco-friendly and sustainable option for utilization of corncob ash. *Journal of Cleaner Production*, *175*, 442–455. https://doi.org/10.1016/j.jclepro.2017.12.050

Memon, S., Wahid, I., Khan, M., Tanoli, M., & Bimaganbetova, M. (2018). Environmentally Friendly Utilization of Wheat Straw Ash in Cement-Based Composites. *Sustainability*, *10*(5), 1322. https://doi.org/10.3390/su10051322

Mindess, S., & Young, J. F. (1981). *Concrete*. Prentice Hall.

Mindess, S., Young, J. F., & Darwin, D. (2003). *Concrete* (2nd ed.). Prentice-Hall.

Mlonka-Mędrala, A., Magdziarz, A., Gajek, M., Nowińska, K., & Nowak, W. (2020). Alkali metals association in biomass and their impact on ash melting behaviour. *Fuel*, *261*, 116421. https://doi.org/10.1016/j.fuel.2019.116421

Morissette, R., Savoie, P., & Villeneuve, J. (2011). Combustion of Corn Stover Bales in a Small 146-kW Boiler. *Energies*, *4*(7), 1102–1111. https://doi.org/10.3390/en4071102

Mwaikambo, L. Y., & Ansell, M. P. (2002). Chemical modification of hemp, sisal, jute, and kapok fibers by alkalization. *Journal of Applied Polymer Science*, *84*(12), 2222–2234. https://doi.org/10.1002/app.10460

Nadelman, E. I., & Kurtis, K. E. (2014). A Resistivity-Based Approach to Optimizing Concrete Performance. *Concrete International*, *36*(5), 50–54.

Nair, A., Ithnin, N. B., Sim, H. L., & Appleton, D. R. (2017). Energy Crops. *Encyclopedia of Applied Plant Sciences*, *3*, 164–176. https://doi.org/10.1016/B978-0-12-394807-6.00173-8

Nair, D. G., Fraaij, A., Klaassen, A. A. K., & Kentgens, A. P. M. (2008). A structural investigation relating to the pozzolanic activity of rice husk ashes. *Cement and Concrete Research*, *38*(6), 861–869. https://doi.org/10.1016/j.cemconres.2007.10.004

Nehdi, M., Duquette, J., & el Damatty, A. (2003). Performance of rice husk ash produced using a new technology as a mineral admixture in concrete. *Cement and Concrete Research*, *33*(8), 1203–1210. https://doi.org/10.1016/S0008-8846(03)00038-3

Niu, Y., Tan, H., & Hui, S. (2016). Ash-related issues during biomass combustion: Alkali-induced slagging, silicate melt-induced slagging (ash fusion), agglomeration, corrosion, ash utilization, and related countermeasures. *Progress in Energy and Combustion Science*, *52*, 1–61. https://doi.org/10.1016/j.pecs.2015.09.003

Pacheco-Torgal, F., & Jalali, S. (2011). Cementitious building materials reinforced with vegetable fibres: A review. *Construction and Building Materials*, *25*(2), 575–581. https://doi.org/10.1016/j.conbuildmat.2010.07.024

Palmqvist, E., & Hahn-Hägerdal, B. (2000). Fermentation of lignocellulosic hydrolysates. II: inhibitors and mechanisms of inhibition. *Bioresource Technology*, *74*(1), 25–33. https://doi.org/10.1016/S0960-8524(99)00161-3

Pan, Z., Zhang, R., & Zicari, S. (2019). *Integrated Processing Technologies for Food and Agricultural By-Products*. Academic Press.

Pandey, A., & Kumar, B. (2020). Investigation on the effects of acidic environment and accelerated carbonation on concrete admixed with rice straw ash and microsilica. *Journal of Building Engineering*, *29*, 101125. https://doi.org/10.1016/j.jobe.2019.101125

Pargar, F., Talukdar, S., Pal, K., & Zanotti, C. (2021). Hemp Waste Valorization as Biofuel and Cement Replacement in Cement and Concrete Production. *Waste and Biomass Valorization*, *12*(2), 913–923. https://doi.org/10.1007/s12649-020-01051-z

Park, B.-D., Wi, S. G., Lee, K. H., Singh, A. P., Yoon, T.-H., & Kim, Y. S. (2004). X-ray photoelectron spectroscopy of rice husk surface modified with maleated polypropylene and silane. *Biomass and Bioenergy*, *27*(4), 353–363. https://doi.org/10.1016/j.biombioe.2004.03.006

Peng, Y. S., Brown, M. A., Wu, J. P., & Liu, Z. (2010). Different oilseed supplements alter fatty acid composition of different adipose tissues of adult ewes. *Meat Science*, *85*(3), 542–549. https://doi.org/10.1016/j.meatsci.2010.03.003

Placet, V. (2009). Characterization of the thermo-mechanical behaviour of Hemp fibres intended for the manufacturing of high performance composites. *Composites Part A: Applied Science and Manufacturing*, *40*(8), 1111–1118. https://doi.org/10.1016/j.compositesa.2009.04.031

Qudoos, A., Ullah, Z., & Baloch, Z. (2019). Performance Evaluation of the Fiber-Reinforced Cement Composites Blended with Wheat Straw Ash. *Advances in Materials Science and Engineering*, *2019*, 1–8. https://doi.org/10.1155/2019/1835764

Ray, A. E., Williams, C. L., Hoover, A. N., Li, C., Sale, K. L., Emerson, R. M., Klinger, J., Oksen, E., Narani, A., Yan, J., Beavers, C. M., Tanjore, D., Yunes, M., Bose, E., Leal, J. H., Bowen, J. L., Wolfrum, E. J., Resch, M. G., Semelsberger, T. A., & Donohoe, B. S. (2020). Multiscale Characterization of Lignocellulosic Biomass Variability and Its Implications to Preprocessing and Conversion: a Case Study for Corn Stover. *ACS Sustainable Chemistry & Engineering*, *8*(8), 3218–3230. https://doi.org/10.1021/acssuschemeng.9b06763

Research and Markets. (2022). *Global Industrial Hemp Market by Type (Hemp Seed, Hemp Seed Oil, CBD Hemp Oil, Hemp Bast, Hemp Hurd), Source (Conventional, Organic), Application (Food & Beverages Pharmaceuticals, Textiles, Personal Care Products) and Region - Forecast to 2027*.

Ribeiro, D. V., & Morelli, M. R. (2014). Effect of Calcination Temperature on the Pozzolanic Activity of Brazilian Sugar Cane Bagasse Ash (SCBA). *Materials Research*, *17*(4), 974–981. https://doi.org/10.1590/S1516-14392014005000093

Saleem, M., Shameem, M., Hussain, S. E., & Maslehuddin, M. (1996). Effect of moisture, chloride and sulphate contamination on the electrical resistivity of Portland cement concrete. *Construction and Building Materials*, *10*(3), 209–214. https://doi.org/10.1016/0950-0618(95)00078-X

Salentijn, E. M. J., Zhang, Q., Amaducci, S., Yang, M., & Trindade, L. M. (2015). New developments in fiber hemp (Cannabis sativa L.) breeding. *Industrial Crops and Products*, *68*, 32–41. https://doi.org/10.1016/j.indcrop.2014.08.011

Scheller, H. V., & Ulvskov, P. (2010). Hemicelluloses. *Annual Review of Plant Biology*, *61*(1), 263–289. https://doi.org/10.1146/annurev-arplant-042809-112315

Scrivener, K. L., John, V. M., & Gartner, E. M. (2018). Eco-efficient cements: Potential economically viable solutions for a low-CO2 cement-based materials industry.

Cement and Concrete Research, *114*, 2–26. https://doi.org/10.1016/j.cemconres.2018.03.015

Scrivener, K. L., Lothenbach, B., De Belie, N., Gruyaert, E., Skibsted, J., Snellings, R., & Vollpracht, A. (2015). TC 238-SCM: hydration and microstructure of concrete with SCMs. *Materials and Structures*, *48*(4), 835–862. https://doi.org/10.1617/s11527-015-0527-4

Scrivener, K., Snellings, R., & Lothenbach, B. (2016). A Practical Guide to Microstructural Analysis of Cementitious Materials. In *A Practical Guide to Microstructural Analysis of Cementitious Materials*. https://doi.org/10.1201/b19074

Sedan, D., Pagnoux, C., Smith, A., & Chotard, T. (2008). Mechanical properties of hemp fibre reinforced cement: Influence of the fibre/matrix interaction. *Journal of the European Ceramic Society*, *28*(1), 183–192. https://doi.org/10.1016/j.jeurceramsoc.2007.05.019

Sederoff, R. R., MacKay, J. J., Ralph, J., & Hatfield, R. D. (1999). Unexpected variation in lignin. *Current Opinion in Plant Biology*, *2*(2), 145–152. https://doi.org/10.1016/S1369-5266(99)80029-6

Shaaban, M. (2021). Properties of concrete with binary binder system of calcined dolomite powder and rice husk ash. *Heliyon*, *7*(2), e06311. https://doi.org/10.1016/j.heliyon.2021.e06311

Shakouri, M., Exstrom, C. L., & Piccini, G. D. (2022). Chloride binding and desorption properties of the concrete containing corn stover ash. *Journal of Sustainable Cement-Based Materials*, *11*(1), 62–82. https://doi.org/10.1080/21650373.2021.1880982

Shakouri, M., Exstrom, C. L., Ramanathan, S., Suraneni, P., & Vaux, J. S. (2020). *Pretreatment of corn stover ash to improve its effectiveness as a supplementary cementitious material in concrete*. https://doi.org/10.1016/j.cemconcomp.2020.103658

SHINOHARA, Y., & KOHYAMA, N. (2004). Quantitative Analysis of Tridymite and Cristobalite Crystallized in Rice Husk Ash by Heating. *INDUSTRIAL HEALTH*, *42*(2), 277–285. https://doi.org/10.2486/indhealth.42.277

Skibsted, J., & Snellings, R. (2019). Reactivity of supplementary cementitious materials (SCMs) in cement blends. *Cement and Concrete Research*, *124*, 105799. https://doi.org/10.1016/j.cemconres.2019.105799

Smil, V. (1999). Crop Residues: Agriculture's Largest Harvest. *BioScience*, *49*(4), 299–308. https://doi.org/10.2307/1313613

Smith, D. B., Cannon, W. F., Woodruff, L. G., Solano, F., Kilburn, J. E., & Fey, D. L. (2013). *Geochemical and mineralogical data for soils of the conterminous United States*. https://pubs.usgs.gov/ds/801/

Snellings, R., Li, X., Avet, F., & Scrivener, K. (2019a). Rapid, Robust, and Relevant (R3) reactivity test for supplementary cementitious materials. *ACI Materials Journal*, *116*(4), 155–162. https://doi.org/10.14359/51716719

Sousa Coutinho, J. (2003). The combined benefits of CPF and RHA in improving the durability of concrete structures. *Cement and Concrete Composites*, *25*(1), 51–59. https://doi.org/10.1016/S0958-9465(01)00055-5

Stevulova, N., Cigasova, J., Estokova, A., Terpakova, E., Geffert, A., Kacik, F., Singovszka, E., & Holub, M. (2014). Properties Characterization of Chemically Modified Hemp Hurds. *Materials*, *7*(12), 8131–8150. https://doi.org/10.3390/ma7128131

Suh, J.-I., Yum, W. S., Song, H., Park, H.-G., & Oh, J. E. (2019). Influence of calcium nitrate and sodium nitrate on strength development and properties in quicklime(CaO)-activated Class F fly ash system. *Materials and Structures*, *52*(6), 115. https://doi.org/10.1617/s11527-019-1413-2

Sun, Y., & Cheng, J. J. (2005). Dilute acid pretreatment of rye straw and bermudagrass for ethanol production. *Bioresource Technology*, *96*(14), 1599–1606. https://doi.org/10.1016/J.BIORTECH.2004.12.022

Suraneni, P. (2021). Recent developments in reactivity testing of supplementary cementitious materials. *RILEM Technical Letters*, *6*, 131–139. https://doi.org/10.21809/rilemtechlett.2021.150

Swamy, R. N. (1986). *Cement Replacement Materials: Concrete Technology and Design* (Vol. 3). Surrey University Press.

Tait, M. W., & Cheung, W. M. (2016). A comparative cradle-to-gate life cycle assessment of three concrete mix designs. *The International Journal of Life Cycle Assessment*, *21*(6), 847–860. https://doi.org/10.1007/s11367-016-1045-5

Teymouri, M., & Shakouri, M. (2023). Optimum Pretreatment of Corn Stover Ash as an Alternative Supplementary Cementitious Material. *CEMENT*, 100066. https://doi.org/10.1016/j.cement.2023.100066

Thiedeitz, M., Ostermaier, B., & Kränkel, T. (2022). Rice husk ash as an additive in mortar – Contribution to microstructural, strength and durability performance. *Resources, Conservation and Recycling*, *184*, 106389. https://doi.org/10.1016/j.resconrec.2022.106389

Tyler Ley, M., Harris, N. J., Folliard, K. J., & Hover, K. C. (2008). Investigation of air-entraining admixture dosage in fly ash concrete. *ACI Materials Journal*, *105*(5). https://doi.org/10.14359/19979

USDA. (2021a). *Rice: Production per Harvested Acre by County*.

USDA. (2021b). *National Hemp Report*.

USDA. (2023a). *Grain: World Markets and Trade*.

USDA. (2023b). *World Agricultural Supply and Demand Estimates*.

Vassilev, S. v., Vassileva, C. G., & Vassilev, V. S. (2015). Advantages and disadvantages of composition and properties of biomass in comparison with coal: An overview. *Fuel*, *158*, 330–350. https://doi.org/10.1016/j.fuel.2015.05.050

Venkateswara, R. V., Kontham, G., Nelluru Venkata, R., & Chundupalli, S. (2011). Effect of Potassium Chloride (KCl) on Ordinary Portland Cement (OPC) Concrete. *Research Journal of Chemical Sciences*, *1*(2).

Vo, L. T. T., & Navard, P. (2016). Treatments of plant biomass for cementitious building materials – A review. In *Construction and Building Materials* (Vol. 121, pp. 161–176). Elsevier Ltd. https://doi.org/10.1016/j.conbuildmat.2016.05.125

Walker, R., & Pavía, S. (2011). Physical properties and reactivity of pozzolans, and their influence on the properties of lime–pozzolan pastes. *Materials and Structures*, *44*(6), 1139–1150. https://doi.org/10.1617/s11527-010-9689-2

Wallace, D. R., & Buha Djordjevic, A. (2020). Heavy metal and pesticide exposure: A mixture of potential toxicity and carcinogenicity. *Current Opinion in Toxicology*, *19*, 72–79. https://doi.org/10.1016/J.COTOX.2020.01.001

Wang, J., Xiao, J., Zhang, Z., Han, K., Hu, X., & Jiang, F. (2021). Action mechanism of rice husk ash and the effect on main performances of cement-based materials: A review. *Construction and Building Materials*, *288*, 123068. https://doi.org/10.1016/j.conbuildmat.2021.123068

Weaver, D. E., Coppock, C. E., Lake, G. B., & Everett, R. W. (1978). Effect of Maturation on Composition and In Vitro Dry Matter Digestibility of Corn Plant Parts. *Journal of Dairy Science*, *61*(12), 1782–1788. https://doi.org/10.3168/jds.S0022-0302(78)83803-X

Weeks, C., Hand, R. J., & Sharp, J. H. (2008). Retardation of cement hydration caused by heavy metals present in ISF slag used as aggregate. *Cement and Concrete Composites*, *30*(10), 970–978. https://doi.org/10.1016/j.cemconcomp.2008.07.005

Wei, H., Yingting, Y., Jingjing, G., Wenshi, Y., & Junhong, T. (2017). Lignocellulosic Biomass Valorization: Production of Ethanol. In *Encyclopedia of Sustainable Technologies* (pp. 601–604). Elsevier. https://doi.org/10.1016/B978-0-12-409548-9.10239-8

William T. Choate. (2003). Energy and Emission Reduction Opportunities for the Cement Industry . *U.S. Department of Energy*.

Wyman, C., Viikari, L., Decker, S., Himmel, M., Brady, J., & Skopec, C. (n.d.). Hydrolysis of Cellulose and Hemicellulose. *2004, Structural Diversity and Functional Versatility, Second Edition*.

Yang, H., Yan, R., Chen, H., Lee, D. H., & Zheng, C. (2007). Characteristics of hemicellulose, cellulose and lignin pyrolysis. *Fuel*, *86*(12–13), 1781–1788. https://doi.org/10.1016/j.fuel.2006.12.013

Yao, G., Cui, T., Zhang, J., Wang, J., & Lyu, X. (2020). Effects of mechanical grinding on pozzolanic activity and hydration properties of quartz. *Advanced Powder Technology*, *31*(11), 4500–4509. https://doi.org/10.1016/j.apt.2020.09.028

Zampori, L., Dotelli, G., & Vernelli, V. (2013). Life Cycle Assessment of Hemp Cultivation and Use of Hemp-Based Thermal Insulator Materials in Buildings. *Environmental Science & Technology*, *47*(13), 7413–7420. https://doi.org/10.1021/es401326a

Zhang, L., Zhang, C., Du, B., Lu, B., Zhou, D., Zhou, J., & Zhou, J. (2020). Effects of node restriction on cadmium accumulation in eight Chinese wheat (Triticum turgidum) cultivars. *Science of The Total Environment*, *725*, 138358. https://doi.org/10.1016/J.SCITOTENV.2020.138358

Zhao, J., Xu, Y., Wang, W., Griffin, J., Roozeboom, K., & Wang, D. (2020). Bioconversion of industrial hemp biomass for bioethanol production: A review. *Fuel*, *281*, 118725. https://doi.org/10.1016/J.FUEL.2020.118725

Appendix A. Material Availability

Wheat and corn are both established markets particularly in the midwestern United States. Hemp is a newer market, but is growing quickly, particularly in the Midwest. During the material searching phase of this project, it was found that hemp farmers were more than willing to sell or donate material to this project. In general, farmers encountered were unfamiliar with the potential for use of these products in concrete. In Ohio, many farmers were contacted for corn and wheat, and most of them responded positively particularly during harvest time (late summer to early fall). Because the nature of this project required samples from a larger geographic range than just Ohio, only one wheat source and one corn source were selected from Ohio.

Hemp sources were more difficult to find, but farmers were happy to see their material used in this research. The French hemp was donated by a local entrepreneur who had interest in both the hemp and concrete industries. The H-KY was donated through Kentucky Hemp Works, which is a company that exists to provide a farm-to-table connection for hemp farmers and product sellers in Kentucky. There is a smaller market for hemp because the industry is still strictly regulated in most states, and most growers have smaller scale operations since the market is so new. However, organizations like the Midwest Hemp Council are working to mediate between the producers and curious

industries. The Executive Director of the Midwest Hemp Council indicated on a phone call that universities have approached them eager for collaboration for use of various parts of the plant for a variety of academic pursuits.

High lignin residue from bioethanol refinery waste was also sought after, but was difficult to find. Many refineries are no longer producing hydrolysis lignin as a waste source. The product obtained was from an agricultural residue feedstock from NREL, which is the only organization that responded positively to the request for material. A quality manager from a local company said that they were not aware of any commercial scale cellulosic facilities in production that they knew of that would produce lignin cake. There is some potential for using humus, which is a high lignin residual from anaerobic digestion, but this was not investigated.